CONCENTRATION OF BLACK LIQUOR TO HIGH SOLIDS

by

Pritham Ramamurthy

A thesis submitted to the Faculty of Graduate Studies and Research in partial fulfillment of the requirements for the degree of Doctor of Philosophy

Department of Chemical Engineering

McGill University

Montreal, Canada.

July 1991.

RESUME

L'évaporation d'eau d'une couche mince (film) de la liqueur noire a été etudiée en utilisant l'injection par jet; d'air chaud ou de la vapeur. L'épaisseur du film est variée entre 0.8 et 1.2 mm et la temperature du sechage est échelonneé de 180 à 250°C. Autres paramètres ont été étudiés; le pourcentage du solide dans la liqueur noire (60-74%) et le debit du fluide du sechage (0.8 - 1.0 kg/s m^2)

Les caractéristiques du transfert du système de sechage ont été déterminées en utilisant la téchnique de sublimation du naphthalène. Les procédures et les téchniques experimentales ont été verifiées par le sechage d'une pâte d'oxyde d'aluminium avec l'air chaud et avec la vapeur. Pour ce système la temperature d'inversion obtenue est entre 210 et 230°C

Le taux de sechage de la liqueur noire avec la vapeur était plus élevé que celui avec l'air pour une temperature d'injection superieure à 200°C. Le sechage par la vapeur presente des caractéristiques differentes du sechage par l'air :a] une condersation initiale de la vapeur ,b] une courte période de croissance,c] un retour graduel ;par conséquent ,le taux de sechage le plus élevé est atteint quand la liqueur renferme le minimum d'eau,d] une augmentation rapide de la temperature du film pour atteindre la temperature d'ebullition.Les faibles taux de sechage avec l'air peuvent être expliqués par la formation d'une peau flexible sur la surface exposée du film alors q'avec la vapeur ,la peau est absente.Le sechage par la vapeur à temperatures élevées est caracterisé par une ébullition à la surface du film alors que le séchage par l'air provoque un enflement extensif.La liqueur noire oxydee presente des taux élevés de séchage par la vapeur et des taux faibles de séchage par l'air.

Une analyse numérique du problème de sechage avec la vapeur est presentée. Une bonne correlation est obtenue avec les resultats experimentaux pour les conditions où le taux de sechage est limité par la diffusion de l'eau dans le film de la liqueur noire. Des nouvelles téchniques sont utilisées pour mesurer la viscosité et la conductivité thermique de la liqueur noir pour des taux elevés de solide .

TABLE OF CONTENTS

CHAPTER III : RESULTS AND DISCUSSION - BLACK LIQUOR DRYING/

CHAPTER IV : MATHEMATICAL MODEL FOR SUPERHEATED STEAM DRYING

CHAPTER V : VISCOSITY AND THERMAL CONDUCTIVITY OF BLACK LIQUOR

List of figures

Tables

CHAPTER I

INTRODUCTION AND BACKGROUND

1.1 INTRODUCTION

The chemical recovery cycle plays an important role in the economy of the pulping process to recover the chemicals used in the pulping of wood. The pulping effluent which contains the recoverable chemicals is called "Black Liquor". Black liquor is the liquid recovered by washing the pulp. The name black liquor is based on its appearance. Black liquor contains complex organic/inorganic components in an alkaline aqueous medium.

The spent liquor is burnt in a recovery furnace/boiler and the inorganic chemicals are recovered The conventional recovery process is both capital and energy intensive, and pulp mills are very often striving for additional liquor firing capacity in existing recovery boilers Incentives therefore exist for improving the recovery process in terms of reduced energy consumption, increased throughput, and lower capital investment The recovery furnace is the single most expensive unit in a pulp and paper mill

One of the consistent patterns in recovery boiler technology is a gradual rise in the solids content of the black liquor being fired in the boiler (Grace 1987) as depicted in Fig. 1 Black liquor concentration is measured by drying a liquid sample under specified conditions and is expressed as percent solids. The liquor obtained from the pulp washing stage (weak black liquor) has about 15 % solids. Typically, in evaporation plants, black liquor is concentrated to about 50 % solids in multiple effect evaporators. This is followed by concentrating black liquor to 65 % solids in a concentrator (falling film evaporator) The liquor is then burnt in a recovery furnace to

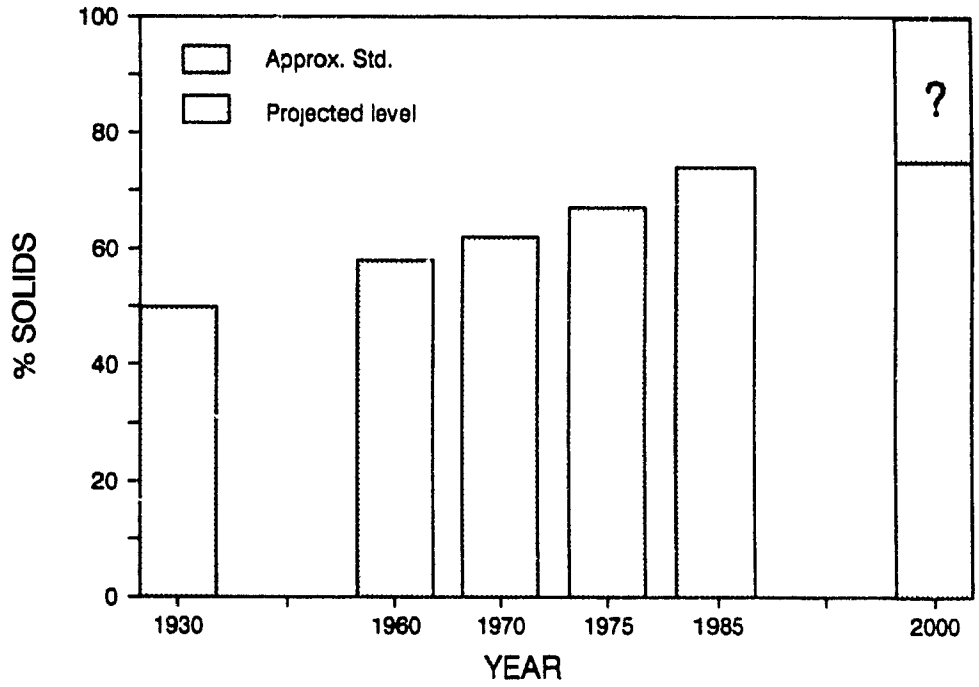

Fig. 1.1 : Trend of black liquor solids level to recovery furnace.

dispose the organics and recover most of the inorganics.

Even at 70 % solids a significant amount of water enters the furnace and exits with the flue gas. "The latent heat of water in the flue gas represents the largest potentially recoverable energy from the recovery boiler" (Avedesian et al. 1988).

Concentration to high solids is attractive for three reasons (Avedesian et al. 1988) :

First, over 40% of the total energy consumed for water removal from weak black liquor is used in the recovery furnace to evaporate the remaining water at a low efficiency, compared to about that in the multiple effect evaporators. Thus, the concentration to higher solids prior to the furnace will save a considerable amount of energy. It is estimated by firing 100 % dry solids instead of 63 %, the generated energy would increase by about 12% or 900 MJ/ton of pulp (Delin and Wennberg, 1983)

Second, a higher solids concentration allows an increase in recovery furnace capacity if fireside pluggage is limiting increased black liquor throughput (Harrison et al. 1988). Fireside pluggage of the generator bank and economized represents the most common limiting condition in the industry. The economic impact of increased capacity can be appreciated from a calculation by Barde and Patel (1983), that a one percent increase in pulp production for a 800 tpd pulp mill is worth $800,000 per year in terms of additional pulp and steam.

The third reason is operating cost reductions due to recovery boiler operational impacts. Burning dry liquor solids can fulfill at the extreme the current operating trend of maximizing the temperature in the char bed and its vicinity as well as lowering the zone at which maximum temperature occurs in the furnace (Blackwell, 1986). This change will have the following impacts :

i) The smelt reduction efficiency and rate of char burning will increase, while the emission of TRS and SO_2 will decrease due to increased lower furnace temperatures.

ii) The safety and stability of the recovery furnace operation can be expected to improve due to the absence of moisture in the liquor.

For the conventional recovery, the burning of liquors at high solids concentration is an operational and economic incentive. However, for some new alternative recovery systems such as the Weyerhauser dry pyrolysis process (Hurley, 1980), the fluidized bed gasifier (Krogh, 1985), and fluidized bed pyrolysis and combustions system (Avedesian et al, 1988), the successful production and handling of black liquor dry solids is a requirement for operation.

The traditional concentrators can not be used to evaporate black liquor to solids level above 70-72%. The limiting factor is the rapid increase in viscosity with increase in solids content It has been observed that the viscosity of black liquor increases exponentially with solids content (Sandquist 1981). The black liquor becomes unpumpable (when the high shear viscosity increases above 200 mPa s) at a certain solids level and temperature. On further increasing the solids level the black liquor becomes sticky and tarry (when the extrapolated low shear viscosity on a logarithmic plot reaches 20,000 mPa s) When the liquor reaches above a certain solids level, it becomes "friable" (this boundary has not been defined quantitatively and hence the question mark). These physical states of black liquor are shown in Fig 1 2

Recent attempts (Wennberg 1991, Rasanen and Alajärvi 1991) have been made to increase the solids level to 80% in falling film evaporators. This has primarily been possible due to the discovery that storing black liquor at high temperatures (>100°C) for a period of time (1-2 days) causes the viscosity to decrease due to lignin degradation.

Practically, the only two physical states in which black liquor can

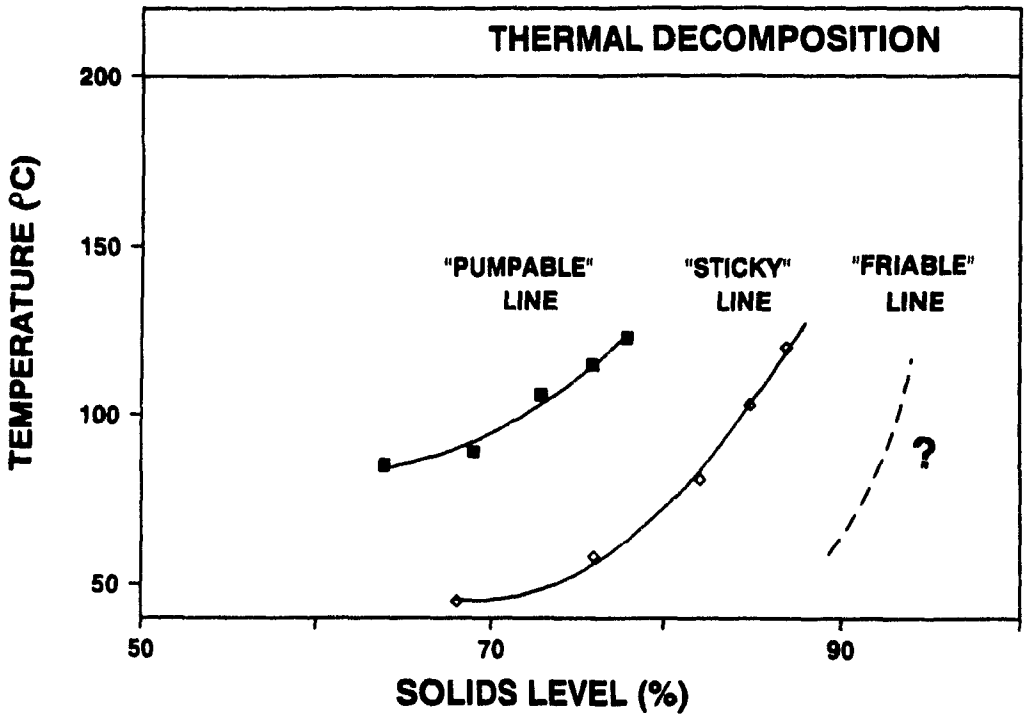

Fig. 1.2 : The physical states of black liquor.

be handled are a pumpable liquid and a dry friable solid. A number of processes were proposed in literature which can potentially produce dry black liquor solids. Each of these has the unique ability to carry black liquor solids across the stick-tarry region and produce a solid-like material. The processes can be divided into five broad categories based on the method of handling :

a) Methods which allow sticking of black liquor, followed by removal of dried solids by mechanical action An example is drying of liquor on a heated surface such as a steam heated drum or torous disc, followed by scraping the dried solids from the surface Another possibility is spraying of black liquor on inert particles in a fluid bed followed by separation of the fine black liquor solids particles produced by attrition in a cyclone after the fluid bed. There is concern about trouble free operation when air or steam are used in fluid bed drying because of particle stickiness and also about steam cleanliness for possible reuse. The drum dryer seems to be the most feasible system from an operational view but the capital cost of the equipment might be very high.

b) Methods which allow sticking of black liquor on solid particles and use dry, coated particles in a recovery process. Examples are spraying of black liquor in a fluid bed consisting of Na_2CO_3 and Na_2SO_4 seed particles or of inert particles such as Al_2O_3. Clay (1987) was concerned about the swelling of black liquor during drying to high solids with superheated steam.

c) Methods which prevent sticking of black liquor by dispersion into small droplets An example is spray-drying of black liquor with superheated steam (Delin and Wennberg, 1983) or hot air The drying of black liquor droplets with hot oil was used in the Carver-Greenfield oil-flash evaporation process (Clay and Karnofski, 1981). This process was tried in a 100 kg/hr pilot plant. However major economical and operational problems were foreseen with oil losses due to incomplete

separation of the solids for commercial scale operation.

d) Methods which prevent sticking of liquor by adding another material. Krogh (1985) and Nelson et al. (1982) found that heavy black liquor could be handled as a solid after mixing with a sufficient amount of sawdust.

e) Methods which prevent sticking of black liquor by using a non-stick heat transfer surface. Plastic coated metal or sintered metal surfaces have been proposed for drying black liquor (Harrison et al, 1988).

After a critical review of all the above processes Avedesian et al (1988) proposed a system which was based on drying a thin film of liquor on the outside surface of a drum by direct contact with impinging jets of superheated steam. In order to increase the heat transfer and have additional control of the film temperature, it was proposed that the drum be heated inside with saturated steam. The drum was to be covered with a steam hood similar to the Yankee dryer as shown in Fig. 1.3.

1.2 OBJECTIVES

This research project is a part of a large project proposed by Avedesian et al. (1988) (Fig. 1.4). The objective of the entire project was to oxidize black liquor, evaporate it to ultra-high solids (> 93 %) using a drum type dryer, and gasify / combust the black liquor solids in fluidized beds. This thesis concentrates on laying the foundations for the design of a superheated steam drying equipment for black liquor concentration.

The primary objective of the thesis was to :

Study the concentration characteristics of black liquor subjected to impinging jets of hot air and superheated steam.

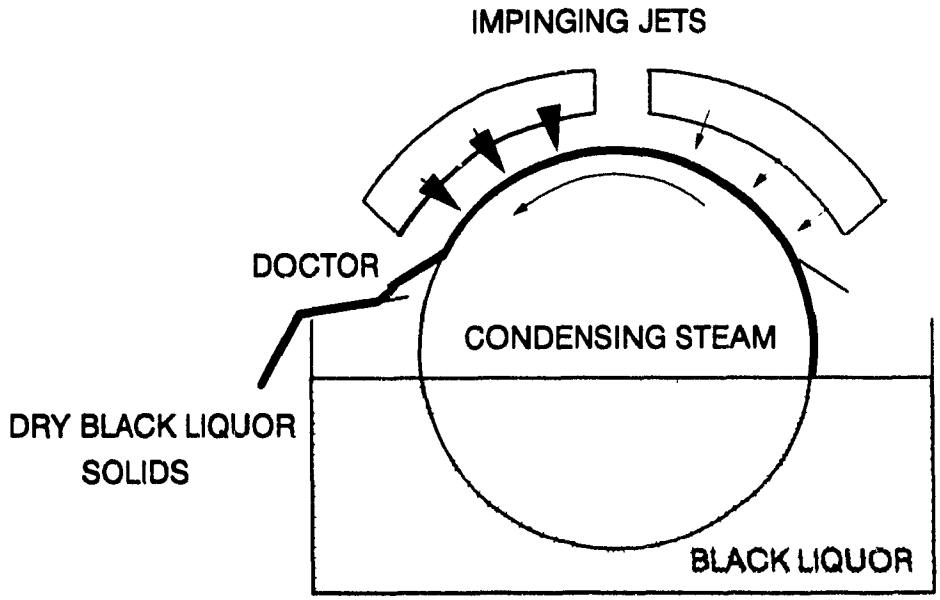

Fig. 1.3 : Proposed black liquor dryer with impinging jets of superheated steam.

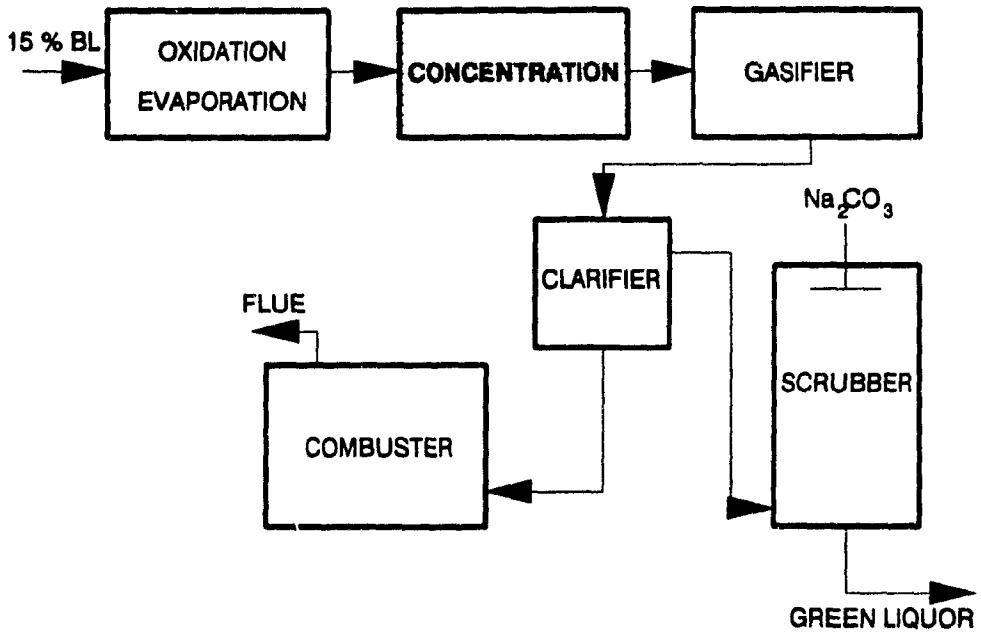

Fig. 1.4 : Proposed alternative recovery process (Avedesian et al.1988).

It was also proposed to study the influence of chemical treatment, namely, oxidation, increasing the sulfate and alkali concentrations, study model compounds (Indulin C and carboxy-methyl cellulose) and numerically simulate the drying behavior. For purposes of this thesis it was decided to neglect the presence of condensing steam in the drum

1.3 LITERATURE REVIEW

The literature review presented here pertains only to the overall objective, namely the drying of black liquor with superheated steam. The literature pertaining to other details such as the drying characteristics of superheated steam, swelling of black liquor, etc are included in the appropriate sections in the following chapters.

There have been 3 projects reported on superheated steam drying of black liquor. They are discussed below according to the date of publication.

1.3.-1. Bergström-Trobeck Process

The Bergström-Trobeck (BT) process (Bergström and Trobeck, 1946 and 1950) utilized circulating low pressure steam superheated to about 400°C to concentrate black liquor to 85 - 90 % solids. The evaporation system consisted of an evaporation apparatus in which superheated steam was brought in direct contact with the liquor, e.g. by being forced directly through the liquor or by being showered with a spray of the same, whereby black liquor was concentrated to such an extent that the product at normal temperature (exit from the dryer) would be in a solid state They proposed that the apparatus in which the evaporation was carried out, be arranged so that the vapor would leave saturated or near saturated.. It was proposed that the superheated steam be injected tangentially or near tangentially or in some other manner whereby the liquid was brought into vigorous motion. They observed that the

superheated steam should be introduced in such a manner that the means of introduction would not present any heating surfaces in the liquid, as this could cause liquor decomposition by overheating.

The main problem with the BT system was the entrainment and subsequent scaling of and hence damage to the superheater (Delin and Wennberg, 1983). There was also a large pressure drop in the nozzle which led to high power consumption. This also caused entrainment problems since the injection of steam into the liquor caused heavy froth.

1.3.-2. Delin-Wennberg Process

The Delin-Wennberg (DW) process (Delin and Wennberg, 1983) is similar to the BT process since superheated steam comes in direct contact with the black liquor. The primary difference is that Delin and Wennberg propose a distillation column to provide intimate contact between the steam and the liquor. The advantages claimed by them are given below.

By running the black liquor countercurrently, the lowest plate/tray will have the most concentrated black liquor. Further since the top tray would have a relatively low solids, and hence low viscosity and low boiling point, the steam leaving the top of the distillation column would have a low degree of superheat and hence be recovered in a condenser.

However in their pilot scale study, Delin and Wennberg found extensive fouling of the steam (due to intimate contact with the liquor), plugging of valves due to solidifying liquor, and poor tray efficiencies (due to high viscosity of black liquor above 75 % solids). They were able to achieve only 85% solids level (with poor drying rates, and fouling of apparatus).

1.3.-3 Clay-Cartwright Process

In the Clay-Cartwright (CC) process (Clay and Cartwright, 1986), the pulping liquor, which has been preconcentrated to 50% solids, is dried in a fluidized bed dryer to produce a solid in particulate form. In the fluidized bed dryer, preformed particulates were fluidized by a gaseous medium substantially of superheated steam Additional heat is supplied to the fluidized bed by passing high pressure saturated steam through heat-exchange tubing within the fluidized bed region. Liquor is introduced into the fluidized bed where the superheated steam vaporizes a substantial portion of its water content The fluidizing steam becomes saturated during its passage through the bed The solid particulates are withdrawn continuously from the bed However, no attempt has been made to use actual wet black liquor in their study and all trial used on dry black liquor in fluidization test

Dalin and Wennberg (1983) concluded that a fluidized bed would be a likely unsuitable for black liquor drying due to its sticky nature. However they propose that the introduction of a small amount of air bled into the fluidized bed substantially decreased the extent of bed collapse.

Based on the literature review it can be concluded that though the concept of using superheated steam as a drying medium for black liquor had been proposed and pursued several times during the last half of this century, no fundamental study describing the drying rates, physical behavior, and influence of liquor properties has been reported The use of superheated steam as a drying medium has been studied intensively for other applications, especially for wood drying. A classical study on superheated steam drying of droplets containing suspended solids was published by Trommelen and Crosby (1970) They found that " even though the drying rate during the first period of drying was both predicted and measured to be lower in superheated steam than in air, complete drying was sometimes found to occur more rapidly in steam than in air This

resulted when the first period of drying was effectively longer because the skin which was formed around the drop had relatively less resistance to mass transfer for drying in steam as opposed to air." They found no substantial differences in physical appearance between the particles dried in air and steam.

1.4 STRATEGY

The experimental plan consisted of five phases :

i) Development of an experimental program and design of the evaporation equipment.

ii) Preliminary experiments to obtain fundamental information on black liquor quality (chemical) and its behavior during evaporation and drying such as thermal degradation, hygroscopic nature, viscosity etc.

iii) Calibration of equipment and comparison of control experiments with previously published data.

iv) Evaporation of black liquor and some model compounds.

v) Analysis of results.

1.5 OUTLINE OF THE THESIS

This thesis concentrates on the measurement of evaporation rates of water from black liquor films using impinging jets of hot air and superheated steam. The thesis is divided into six chapters.

Chapter I deals with the background information pertaining to this thesis.

Chapter II details the experimental apparatus used, preliminary

experiments and calculations to determine the range of variables studied and experimental program.

Chapter III contains the results and discussion of drying of black liquor and model compounds.

Chapter IV contains the numerical predictions of the drying of black liquor.

Chapter V pertains to research results not directly a part of the main objective.

Chapter VI lists the conclusions and summarizes the work

1.6 CITED REFERENCES

Avedesian, M.M , G.J. Kubes, A.R.P. van Heiningen "Development of an Alternative Kraft Black Liquor Recovery Process based on Low Temperature processing in Fluidized Beds". A proposal to the International Energy Agency

Barde, D. K , J.C. Patel : "Optimum Efficiency in the Recovery Area" Chemical Engineering Progress 79(9), pp 27-30 (1983)

Bergström H,O,V., K G. Trobeck · "Process of Utilizing Waste Liquors" US Patent 2,406,581, Aug 27, 1946

Blackwell, B . "The importance of High Temperatures in the Lower Furnace of Kraft Recovery Boilers" Pulp and Paper Canada 87(1), pp 27 (1986)

Clay, D.T : "Drying liquor in Fluid Bed Reactor with Superheated Steam" Paper presented at the US Department of Energy Review Meeting (1987).

Clay, D.T., M.A. Karnofski : "Black Liquor Solid Formation during Oil Flash Evaporation". TAPPI J, 64 (12), pp 45 (1981)

Clay, D.T., T.B. Cartwright : "Method for drying Pulping Liquor to a Burnable Solid". U S. Patent 4,619,732, Oct 28, 1986

Delin, L., O. Wennberg : "Methods of obtaining High Concentration Black Liquor". International Energy Agency Research Project - Annex 1 (1983).

Grace, T.M. : "Black Liquor solids content : How high is up?". PIMA, October (1987). pp 39-40.

Harrison, R.E., P.J. Chung, B.A. Crowell, E.A. Ketcham : "Ultra-High Solids Evaporation of Black Liquor". TAPPI J. 71(2), pp 61-66 (1988).

Hurley, P.J. : "Energy Balances for Alternative Recovery Systems". Chemical Engineering Progress 76(2), pp 43 (1980)

Krogh, G.N.E. . "The Brazilian method for an improved Recovery Process". Proceedings of International Chemical Recovery Process, New Orleans. pp 235 (1985).

Räsänen, O, Alajarvi, T · "Evaporation to ultra high solids Benefits and Possiblities" Recovery symposium, 1991, Helsinki.

Sandquist, K : "Rheological properties and evaporation of black liquor at high dry-solids content. Part 1 : Rheology". Pulp and Paper Canada 84 (2), pp 30-34 (1983).

Trommellen,A M , E.J Crosby : "Drying of solute droplets in superheated steam". AIChE J 16(5), pp 857-867 (1970).

Wennberg, O . "A new concept for evaporating black liquor". Recovery symposium, 1991, Helsinki.

CHAPTER II

EXPERIMENTAL APPARATUS

This chapter consists of a description of the experimental apparatus used and the experimental design studied in this thesis. As mentioned earlier, this is the first fundamental study on the concentration of black liquor to high solids using superheated steam as an environment, hence it was imperative to learn about the limitations and boundaries for the detailed experimental design A discussion of the preliminary experimental design is also included here. Since the apparatus was designed and built in the local machine shop (Paprican), a detailed characterization and optimization of the apparatus was done.

While a substantial amount of articles and patents have been published in the area of superheated steam drying, the literature is scattered and a section of this chapter is devoted to review the literature on superheated steam drying. In any experimental study, before presenting new results and discussion, it is imperative to perform control experiments or established experiments The control experiments studied here were drying of aluminum oxide slurry (this can be compared to sand slurry which has been investigated before)

2.1 EXPERIMENTAL CONCEPT

An experimental facility was designed and constructed to study the drying characteristics of black liquor using impinging jets of air or steam. The experimental apparatus was capable of the measuring the drying characteristics with respect to the drying times from 15 seconds onwards. The primary design constraints were to achieve rapid measurements of the dried sample (for accuracy) and to obtain uniform transfer coefficients on the evaporation surface (to avoid dry spots). Accuracy is defined here as closeness of the measured value to the

actual value of a parameter (mass in this case). This study pertains to the use of impinging jets (nozzle made with circular holes drilled in a plate) and hence one could have areas where there is a high transport coefficient (under a jet) and areas of low transfer coefficient (away from the jet). This could lead to dry spots vertically under the jet compared to the regions away from the jet.

A survey of the literature indicates a number of techniques used to measure the drying characteristics on a laboratory scale. Notable references are those by Trommlen and Crosby (1970), Cui et al (1985), Sparrow et al (1986) and Bond (1991).

Trommlen and Crosby (1970) studied the evaporation of drops in superheated vapors. They studied both pure liquid drops and drops containing dissolved solids. Hence, they used a droplet of liquid as the sample on a thermocouple bead and controlled the drying time by a quick opening baffle. A convergent nozzle was used to produce a flat velocity profile. The drop was suspended at the junction of a chromel-constantan thermocouple which itself was affixed to the end of a balance. Simultaneous measurement of the temperature of the drop together with its weight allowed a good check on the nature of the various initial drops investigated. The deflection of the filament varied according to the weight of the drop and was measured by the distance over which the fixed end had to be moved to maintain the free end at its initial position. A slide valve for rapid diversion of the drying medium was attached directly to the convergent nozzle and acted as the support for the drying chamber

Cui et al (1985) used paper on a saturated cotton slab as the wet sample and controlled the drying time for the constant rate period by a quick opening baffle. Saturated steam was superheated using an electrical heater and entered the dryer chamber through a perforated plate and impinged on wet paper supported on a wet textile fabric that was in good contact with a layer (5 cm) of cotton. The cotton drew the

water up to wet the fabric and the paper, and kept the moisture content of the paper above its critical moisture content. The drying rate was calculated by ensuring saturation of the cotton slab with water and recording the amount of water fed to keep the sample saturated.

Sparrow et al. (1986) studied the evaporation at the liquid surface due to jet impingement. They calculated the drying rate by directly mounting the sample in a pan just above a balance and weighing the sample directly. To achieve well-defined thermal and vapor concentration, and hydrodynamic conditions necessary for the attainment of accurate and reproducible data, the experiments were performed in an environment chamber and in the suction mode. They however do not describe the placement of the thermocouples to measure the temperature of the water in the sample pan.

Bond (1991) studied the drying of paper using impinging jets of hot air and superheated steam. He measured the drying rate by introducing the sample into the drying chamber for a defined period of time and recording the change in weight. The sample was introduced cold into the chamber supported on a glass/metal plate. The temperature of the surface and the bottom of the paper was measured by thermocouples.

The apparatus designed for this work is a combination of the methods used by Cui et al. and Sparrow et al.

2.2 EQUIPMENT DESCRIPTION

The flow sheet for the experimental setup is shown in Figure 2.1 Air and steam installations were provided by the physical plant services at McGill University. The line pressures for both were about 100 psi A pressure regulator (Spriax Sarco BRV Pressure Reducing Valve) was used to supply a 24 psi steam or air to the superheater. A 15 kW electrical heater was used to heat the air and steam to the desired temperature. The flow rate to the apparatus was regulated by a needle valve. The

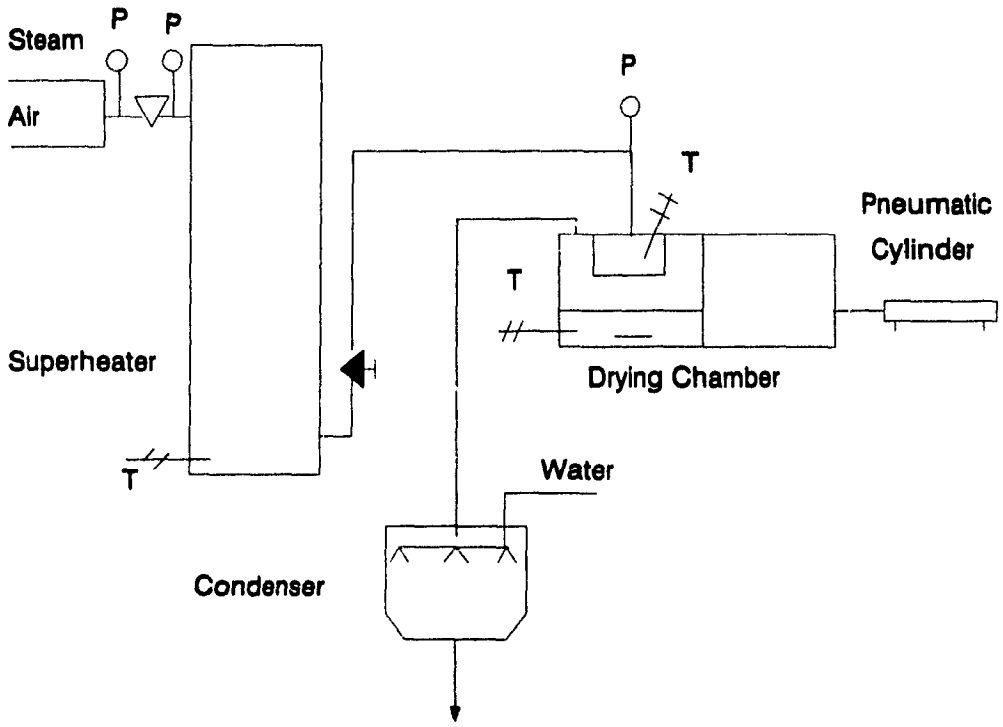

Fig. 2.1 : Flowsheet of the experimental setup

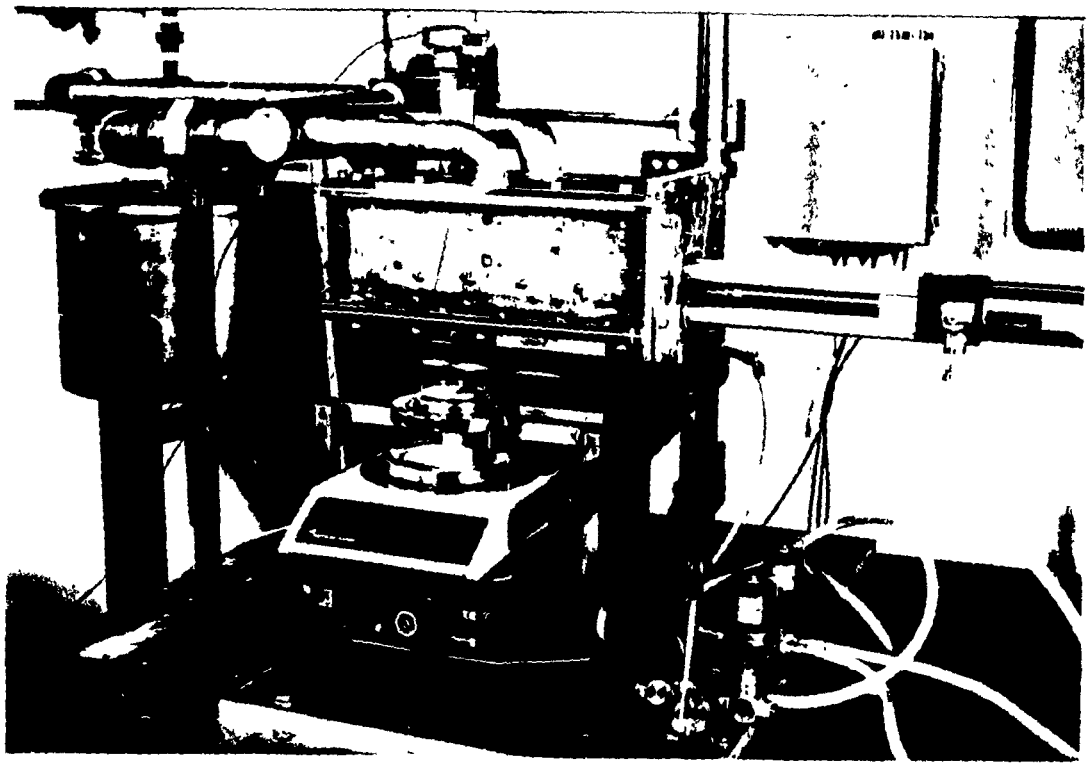

Fig. 2.2 : Photograph of the experimental apparatus.

flow was measured for cold conditions using an diaphragm type dry flow meter. The hot flow conditions were corrected with the same valve opening for density and temperature. The hot fluid was then sent to the drying chamber and finally to a condenser. Figure 2-2 is a photograph of the experimental assembly.

Figures 2-3 and 2-4 show the front and side views of the drying chamber. The chamber is a rectangular, metal-walled enclosure, completely airtight when closed except for a vertical nozzle and 4 exhaust ports at the top. The sample insertion and removal were done manually by opening a window at the bottom of the chamber. The opening and closing of the window were done pneumatically and were manually controlled.

The drying chamber was divided into two parts. The main part where the drying took place was 15 cm (width) x 15 cm (breadth) x 10.5 cm (height). From the top of the drying chamber a nozzle head protruded into the chamber. The outer dimensions of the nozzle head were 8.5 cm (width) x 8.5 cm (breadth) x 7.5 cm (height). The sample pan surface (when filled with material) was 2.5 cm from the nozzle head. The nozzle head consisted of a drilled plate. 0.2778 cm (7/64") holes were drilled at appropriate pitch distance to obtain the desired fraction open area. This configuration gave a nozzle - plate distance to nozzle diameter ratio of 9.0. The fraction open areas investigated were from 0.03 to 1.0. A flow breaker and a wire mesh (75 mesh) were placed ahead of the nozzle to give a more uniform flow at the nozzle exit across the plate. The flow breaker dimension was 30 cm and was experimentally determined to give the most uniform transfer coefficient at the sample surface. Four outlet ports 2.54 cm in diameter were present at the top surface to remove the exhaust fluid. The outlet ports were placed symmetrically to improve uniformity of flow of the impinging medium and hence transfer coefficients on the surface.

Between the nozzle head and the sample or the window there was a

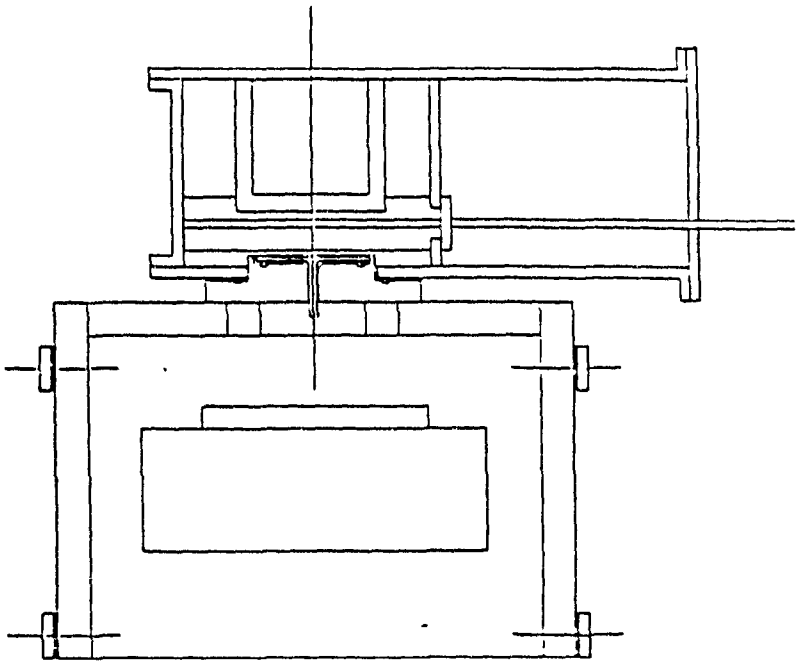

Fig. 2.3 : Front view of the drying equipment.

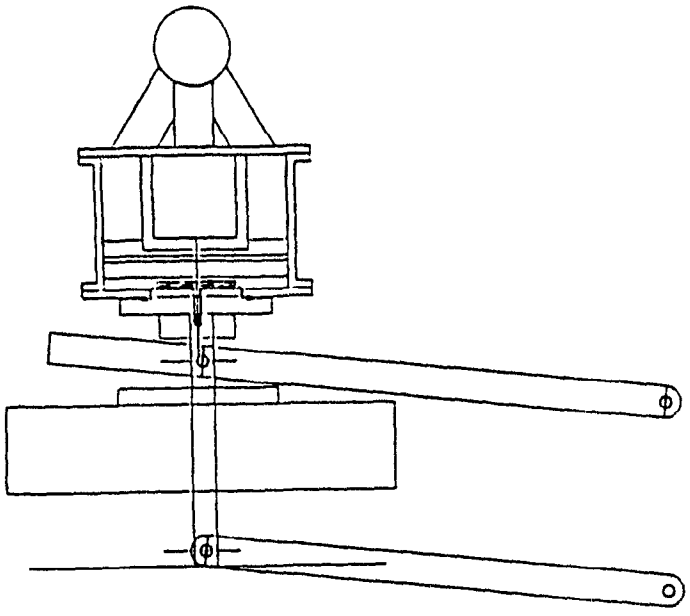

Fig. 2.4 : Side view of the drying equipment.

metal baffle. The baffle was to prevent the drying medium from coming in contact with the sample when it was being loaded or removed. After the sample was loaded, the baffle was withdrawn into a side chamber having the same dimensions as the main drying chamber. The insertion and withdrawal of the baffle which in turn determined the drying cycle or time were pneumatically activated and computer controlled. The side chamber was included to provide good sealing. Two "O rings" were used to seal the window and the sample pan when in operation. All the pipe lines and the drying chamber were insulated for safety and to prevent heat loss.

The sample to be dried was held in a straight sided circular pan supported from below by a cylindrical column. The pan and the column were made of titanium and Macor (a machinable ceramic material). titanium was used as a realistic material (in industrial practice the backing rolls are generally made of a steel alloy of iron, chromium or nickel) and Macor to give a near insulating boundary condition.

2.3 INSTRUMENTATION

Pressure Measurement : The pressures before and after the pressure regulator were measured using Winter's pressure gauges (0 - 200 psig).

Flow Measurement : Air flow rate was measured by diaphragm type dry flow meter at room temperature (18 - 21°C) for different valve opening and upstream pressure and then corrected for temperature and medium.

Temperature measurement : A K - Type thermocouple was used to measure the temperature of the superheater heating element. J - Type thermocouples were used to measure the inlet, exhaust and sample temperatures. A thermocouple holder was designed to measure the temperature at three places on the film as shown in Figure 2-5. The holder was made of teflon with a flat bottom and a tapered top. The diameter of the holder was 2.54 cm and the height of the film was less

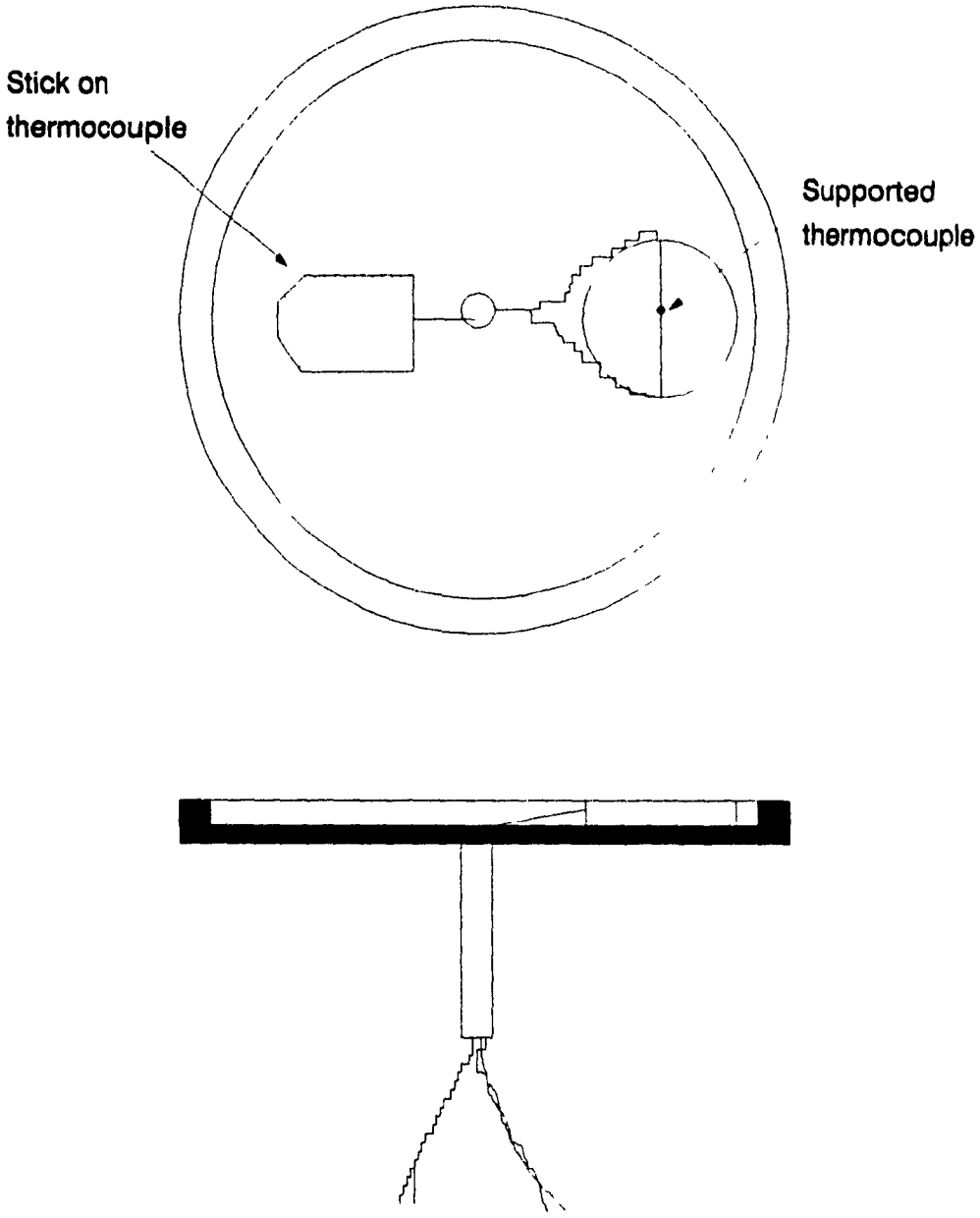

Fig. 2.5 : Thermocouples arrangement for temperature measurement of the black liquor film.

than 0.15 cm. This gave a diameter to height ratio of at least 12 and the process can still assumed to be one dimensional. The thermocouples were horizontally mounted to eliminate any conduction (vertical) effects. The thermocouple wires were made of 0.0127 cm diameter and the thermocouple bead was about twice the diameter of the wire. The beads were coated with thermally conductive Omega thermocoat. The beads were also staggered as shown in the figure by about 4 wire diameters so that the presence of a bead below or above did not affect the representative film significantly. The sample bottom temperature was measured by a self adhesive thermocouple.

Mass measurement : Mass measurements are made with a Mettler 400 J balance. The balance has a maximum mass limit of 400 g, a readability of 0.01 g and and accuracy of 0.02 g. The total amount water evaporated in a typical experiment was in the range of 0.75 - 2 g.

Controls : The superheater temperature was controlled to achieve a constant chamber inlet temperature using an on-off control system. The control system as well as the drying time or exposure time were monitored by a Corbit micro-computer. A Wainbee air cylinder was used to move the baffle. All the temperatures and mass of the sample before and after drying were also recorded by the computer.

Safety : The program to control the superheater temperature assured that the temperature at the superheater coils did not exceed 400°C. The difference in temperature between the superheater and the chamber inlet was also kept less than 200°C at all times. A safety knuckle valve before the superheater ensured that the pressure in the superheater did not exceed 60 psig. In the event of a pressure surge the vent of the knuckle valve was led to the condenser (not shown in Figure 2-1).

2.4 EXPERIMENTAL DESIGN

As mentioned in Chapter I little work has been done on attempting to achieve ultrahigh solids level i.e., greater than 90 - 95% solids. Furthermore this is perhaps the first work on impingement drying of black liquor. As a result the variables had to be investigated and the ranges had to be assessed or estimated at first. The variables considered to be of importance were :

a] Drying medium inlet temperature.
b] Drying medium mass flow rate.
c] Wet film thickness.
d] Film bottom boundary condition.
e] Drying medium.
f] Chemical composition of black liquor.

2.4-1 INLET TEMPERATURE

Since the heat required for evaporation of water from black liquor is supplied by the impinging medium, a higher temperature drying medium will give a higher temperature driving force and hence a higher drying rate. However, the maximum temperature in this study of black liquor drying was limited due to the degradation of black liquor at high temperatures.

In order to estimate the temperature at which black liquor begins to degrade thermogravimetric experiments were performed. The TGA (thermogravemetric analysis) system was a Cahn 113-DC system installed with a Cahn RG-2000 electric balance. A small sample of dry black liquor solids (about 7.5 mg) was placed in the TGA furnace. The temperature of the furnace was increased slowly (about 10°C in 30 min), and the temperature near the sample and mass of the black liquor sample were recorded. A typical output of the weight and temperature history is shown in Figure 2-6. Since the black liquor sample used was dry

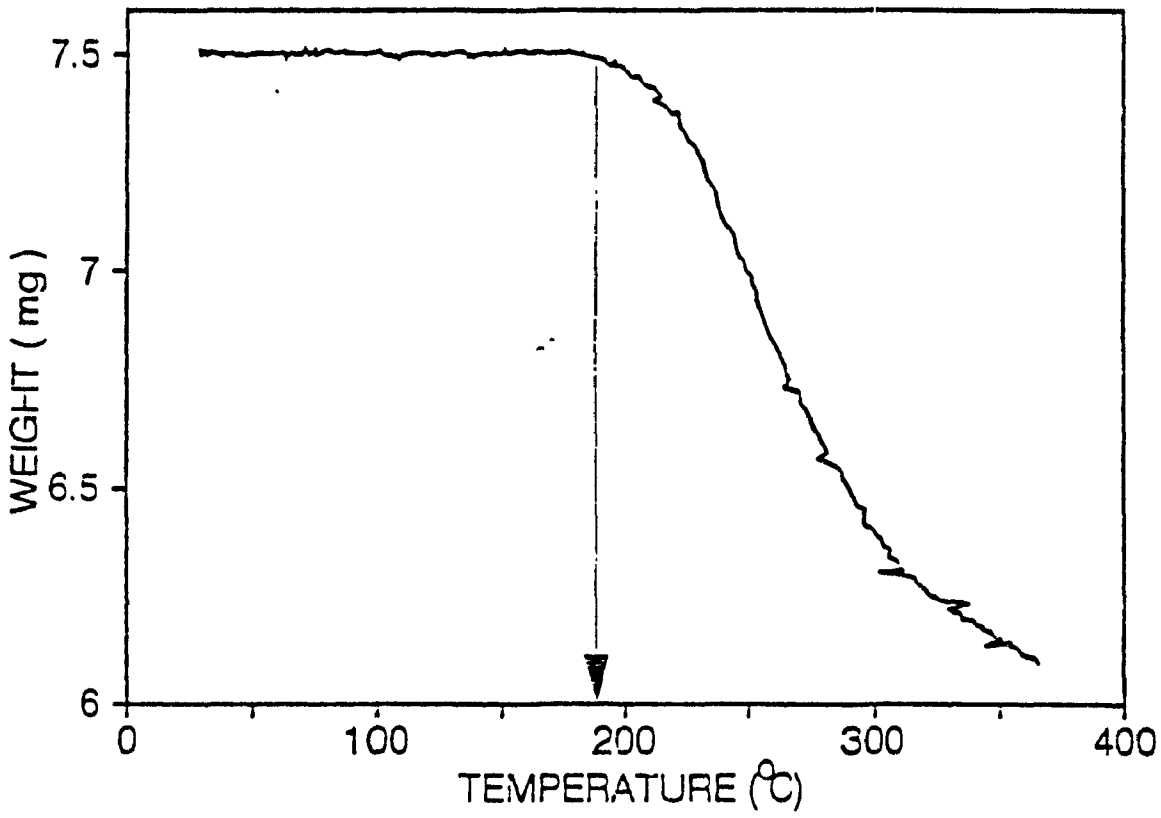

Fig. 2.6 : Thermal degradation of black liquor above ≈ 190 °C.

there was no weight loss at low temperatures. However, at temperatures above 190°C there was a significant decrease in mass of the sample This is attributed to the degradation of the cellulosic materials and lignin in black liquor. As shown in the figure the degradation takes place at roughly 190 °C. This agrees fairly well with the results of others (Harrison et al., 1988).

It has also been described by others that for the evaporation of water into air and superheated steam there exists an inversion point (Yoshida and Hyodo 1970), i.e., a gas temperature below which evaporation in air is more rapid than that in steam (compared at the same mass flow rate) and vice versa at temperatures above the inversion point (Section 2- 7). This implies that steam drying is more advantageous at temperatures above the inversion point where the drying rate in steam is higher. The inversion temperature for laminar flow over a flat plate was determined to be about 240°C and for turbulent flow about 220°C.

Based on these results for purposes of this study, the temperature range of the drying medium investigated was between 150°C and 250°C

2.4-2 MASS FLOW RATE OF IMPINGING MEDIUM

The mass flow rate limitation was determined experimentally. A higher mass flow rate will increase the evaporation rate because of the increase in Sherwood number with Reynolds number It should also be recognized that the sample to be concentrated is initially in a liquid phase (viscosity ≈ 100 cp at 100°C) and therefore the impinging jet of air or steam (specifically, since the temperature of the surface corresponds to the boiling temperature in steam drying) could strip the liquid off the pan. Furthermore when steam is used as the impinging medium there is an initial condensation of the steam because the sample is cold (lower than the boiling temperature). This dilution of the surface causes the viscosity of the surface of black liquor film to drop

even further. This results in a .arger extent of "splashing" of the liquor from the drying surface due to the impinging jet at high mass flow rates.

Based on experiments it was determined that below a mass flow rate of 1.2 kg/m^2s there was no splashing or stripping of the black liquor film. Hence the influence of mass flow rate was studied between 0.80 and 1.2 kg/m^2s.

2.4-3 FILM THICKNESS

The film thickness was chosen based on the assumption that the final industrial equipment would consist of a cylinder rotating in a vat of black liquor. Hence the maximum film thickness that could be achieved due to free roll coating was estimated. The estimation of the film thickness was based on the method developed by Tharmalingam and Wilkinson (1978). The properties for black liquor used in the calculations were taken from "Recovery of Chemical Process" (Hough, 1985) The film thickness was chosen finally to be less than 2 mm. However, at film thicknesses above 1.25 mm it was seen that the black liquor boiled over the pan sides and therefore from a practical point of view the film thickness was chosen to be less than 1.25 mm. In practice this can be easily achieved by doctoring of excess liquor from a free roll.

2.4-4 FILM BOTTOM BOUNDARY CONDITION

The proposed drum dryer will contain condensing steam on the inside to supply heat from the bottom of the film while hot steam/air impinge on the top. However in this study it was proposed that heat would not be supplied from the bottom. Hence the two boundary conditions studied were a low heat loss (approaching insulating) boundary condition and an ill defined boundary where heat loss occurred by radiation and convection to the surroundings. A machinable ceramic (MACOR) was used

to represent an insulating boundary, however it had a thermal conductivity higher than that for black liquor. A titanium pan was used as the other ill defined boundary (since the thermal conductivity and also loss to atmosphere is high).

2.4-5 DRYING MEDIUM

Steam and Air were chosen to be the drying mediums. The choice was based on industrial applicability of the project. Steam has been shown to be economical if efficient recycling of the exhaust is possible (Bond 1991) and if the steam exiting from the concentrator could leave close to saturation so that it could be used as condensing steam elsewhere (specifically in multiple effect evaporators as suggested by Avedesian et al. (1988)). The comparison of superheated steam and air as drying mediums are discussed later in this chapter (Section 2-7)

2.4-6 DRYING SAMPLE

The main objective of this thesis was to study the evaporation of water from black liquor. However, to get an insight to the behavior of black liquor drying, lignin in the form of Indulin C (precipitated lignin by acid hydrolysis) and cellulose derivative (carboxy methyl cellulose) were also investigated. It has been proposed in the literature (Bergstrom and Trobeck 1946, Cartwright and Clay 1986) that the oxidation and increased content of residual alkali load would have a beneficial effect on black liquor drying in the fluidized bed or spray drying. To provide data and to study the influence of chemical modification of black liquor, it was oxidized and content of residual alkali was increased.

In order to calibrate the equipment and to compare the results of this work to that of others, drying of aluminum oxide slurries were also studied. A list of the variables investigated and their ranges are given in Figure 2-7.

VARIABLES INVESTIGATED

IMPINGEMENT MEDIUM		AIR	STEAM	
TEMPERATURE (°C)	180	200	225	245
SAMPLE HOLDER			TITANIUM	MACOR
FILM THICKNESS (mm)		0.8	1.05	1.16
MASS FLOW RATE ($kg/s\text{-}m^2$)			0.8	1.0
INITIAL SOLIDS LEVEL (%)		60	67.7	74

SAMPLE: AL_2O_3 | BLACK LIQUOR | CMC | INDULIN C

BLACK LIQUOR: NaOH | Oxidized BL | Na_2SO_4

Fig. 2.7 : Variables investigated in this study.

2.5 CALIBRATION OF THE EQUIPMENT

The equipment described in the previous section was assembled in the Paprican machine shop. Since it was not a "standard" equipment to study the concentration behavior of black liquor, it was imperative to study the transport of energy and mass behavior in the equipment. This study would also lay the basis for other investigators to compare results with this study. It was also essential to see how this apparatus falls within the literature results published before.

2.5-1 MASS TRANSFER COEFFICIENTS

The main quantity to be determined was the rate of mass transfer from the sample holder to the impinging stream of fluid. The naphthalene sublimation technique was used to measure mass transfer coefficients from the surface of the sample. Details of this method are given by Li (1989) and Scholtz (1965).

A film of naphthalene was applied on an aluminum pan. The film was formed by pouring liquid naphthalene on a sloping pan allowing the naphthalene to overflow while some of the poured naphthalene solidifies and forms a film. This process was found to be most effective by Scholtz (1965). The formation of a smooth and uniform naphthalene surface was essential to avoid added turbulence in the boundary layer of the impinging jets.

The mass transfer coefficient "k_g" (m s^{-1}) is defined by

$$(-r) = k_g S (C_w - C_\infty) \qquad (2\text{-}1)$$

where (-r) is the rate of naphthalene sublimation (mol s^{-1}) measured by exposing the naphthalene surface to the jet stream and measuring the weight loss for a given interval of time, S is the surface area of sublimations (m^2), and C_w and C_∞ are the vapor concentrations (mol m^{-3})

of naphthalene at the surface, and in the bulk of the gas respectively. In the present study, C_∞ is zero and C_w is calculated from the ideal gas law using the top surface temperature T_w (K) and the saturated vapor pressure of naphthalene p_w (Pa) at this temperature :

$$C_w = \frac{p_w}{R\,T_w} \qquad (2\text{-}2)$$

where R is the universal gas constant, 8.314 (kJ mol^{-1} K^{-1}). "k_g" the average mass transfer coefficient was calculated by (Li 1989) :

$$k_g = \frac{R\,T_w}{p_w}\,\frac{m}{A} \qquad (2\text{-}3)$$

The mass transfer coefficient k_g was correlated in terms of Sherwood number (Sh), Reynolds number (Re), and Schmidt number (Sc) defined as

$$Sh = \frac{k_g\,d_j}{\mathbb{D}} \;;\quad Re = \frac{V\,\rho\,d_j}{\eta} \;;\quad Sc = \frac{\mu}{\rho\,\mathbb{D}} \qquad (2\text{-}4)$$

where d_j is the diameter of the nozzle, V is the jet velocity of the impinging medium, ρ is the density of the impinging medium, η is the viscosity of the impinging medium, and $\mathbb{D}$ is the diffusion coefficient of naphthalene in the carrier gas. The density and viscosity of the carrier gas (air) were used because the influence of the vapor pressure of naphthalene on the density is negligible over the temperature range studied here (22 - 25°C).

The saturation vapor pressure of Naphthalene is expressed as (Popiel and Boguslowski, 1986) :

$$\log_{10} p_w = B_1 - \frac{B_2}{T_w} \qquad (2\text{-}5)$$

where B_1 = 13.54 and B_2 = 3729 for p_w in Pa and T_w in Kelvin. The diffusion coefficient of naphthalene in air was estimated as $6.1*10^{-6}$ m^2 s^{-1} at 23°C.

In order to measure the local mass transfer coefficients, the surface profile of the naphthalene was measured before and after exposure using a moving stylus. The sample pan had three holes drilled at 120 degrees to each other and was placed on a holder which had three floating pins to match the holes. The holder had three additional fixed pins to keep the entire assembly horizontal The height of the surface was measured at 2 mm intervals. The stylus pin had a diameter of 1 mm. The stylus had a resolution of 0.0005" (0.00127 cm). After sample preparation the naphthalene surface was exposed to the jet stream for 3 - 5 hours (depending on the flow rate) till about 0.015 in (0.318 mm) of the coating had sublimed at the stagnation points. Typical profiles (one 90 degree sector of the pan) is shown in Figure 2-8.

The local mass transfer coefficient was calculated by using

$$k'_g = \delta \rho R T_w / (\tau p_w) \qquad (2\text{-}6)$$

where

k'_g = Local mass transfer coefficient.

δ = Local decrease in height.

ρ = Density of Naphthalene.

τ = Time of exposure.

Local mass transfer calculations were made to ensure uniform evaporation / transfer from the surface of the film by suitable modification to the nozzle head.

2.6 IMPINGING JETS - LITERATURE REVIEW

A brief review of impinging jets is presented here to indicate the importance of the naphthalene sublimation study and to compare the apparats used here to those published in the literature. Martin (1977) presents an excellent review and correlations on the heat and mass transfer between impinging gas jets and solid surfaces. Other reviews are published by Mujumdar and Douglas (1972), and Russell and Hatton

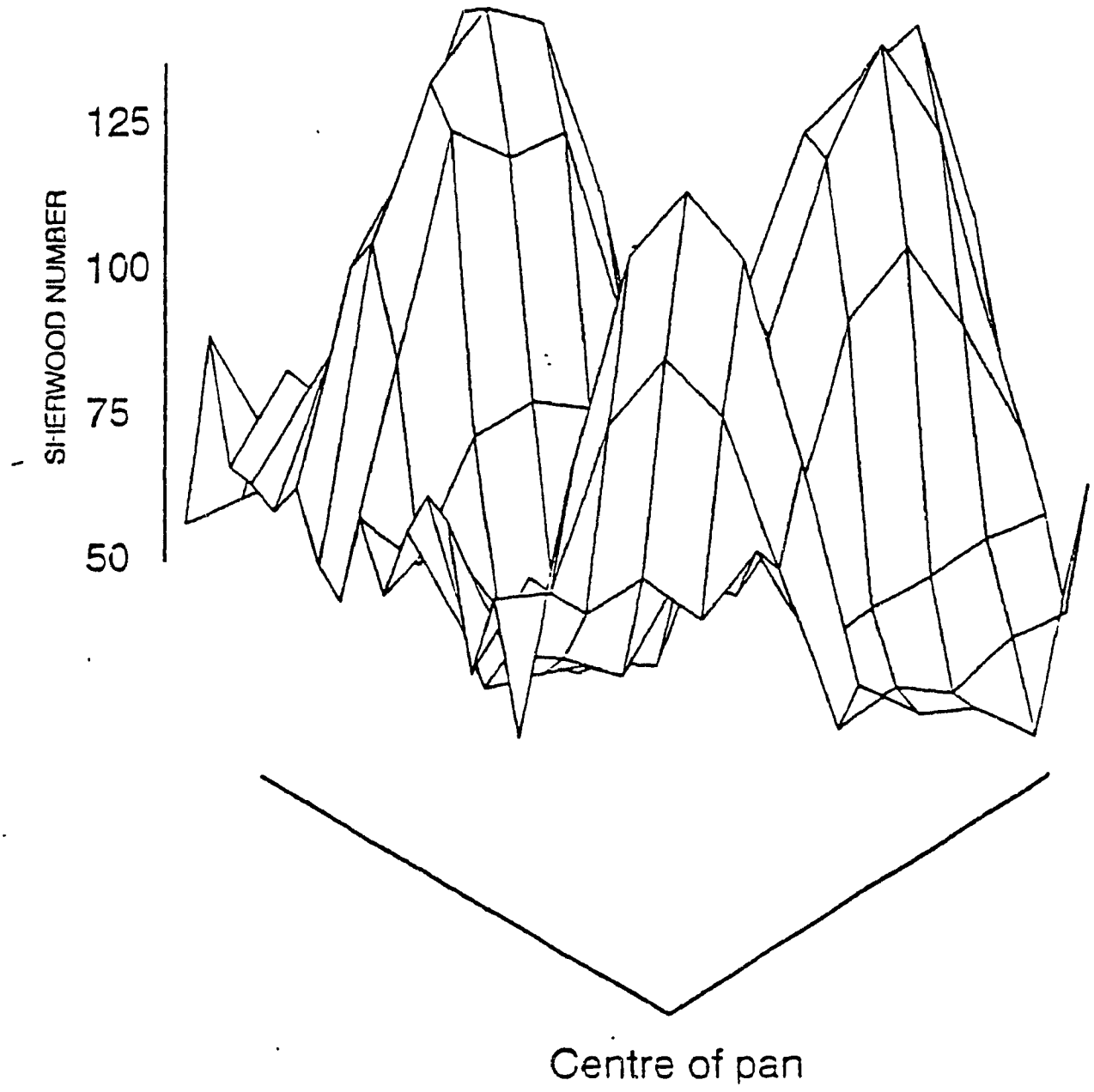

Fig. 2.8 : Surface profile for naphthalene after exposure to air jets - 7% open area, height to nozzle diameter = 9.

(1972).

Gordon and Akfirat (1966,1972) presented good results on heat transfer characteristics of impinging jets. They studied only two dimensional jets, i.e. slot type jets. They compared the spatial variation of heat transfer coefficients produced by a single two-dimensional jet with that of multiple jets. At relatively small nozzle-to-plate spacing, the pressure distribution in the impingement region of one of the multiple jets was substantially the same as that for the single jet, as indeed was also the distribution of heat transfer rates. However, while the pressure outside the impingement region of the single jet remained zero, that for multiple jets increased again in the region where the deflected jets approached one another The positive pressure gradient at first caused a thickening of the boundary layer and hence a progressively more rapid decrease in local heat transfer rates. This was followed by flow separation, which was manifested by marked secondary peaks in heat transfer rate at the secondary stagnation points midway between adjacent nozzles. This behavior was evident in this study also as depicted in Fig. 2-9.

At larger nozzle-to-plate ratios the behavior was different. While a single jet spread through substantially stationary air, the multiple jets must advance against a stream of "spent air" returning from the plate. The longer jet length therefore reduces their arrival velocity more than that of a single jet. This was shown by the pressure distribution curve, and probably the main reason why stagnation-point heat transfer coefficients were lower for multiple jets than for a single jet. Higher uniformity in heat transfer coefficients were achieved with higher nozzle-to-plate ratios. The similar behavior is also reflected when comparing a higher and lower Reynolds number jets as shown in Fig. 2-10. Theoretical analysis on the behavior of impinging jets has been done by Agarwal and Bower (1982).

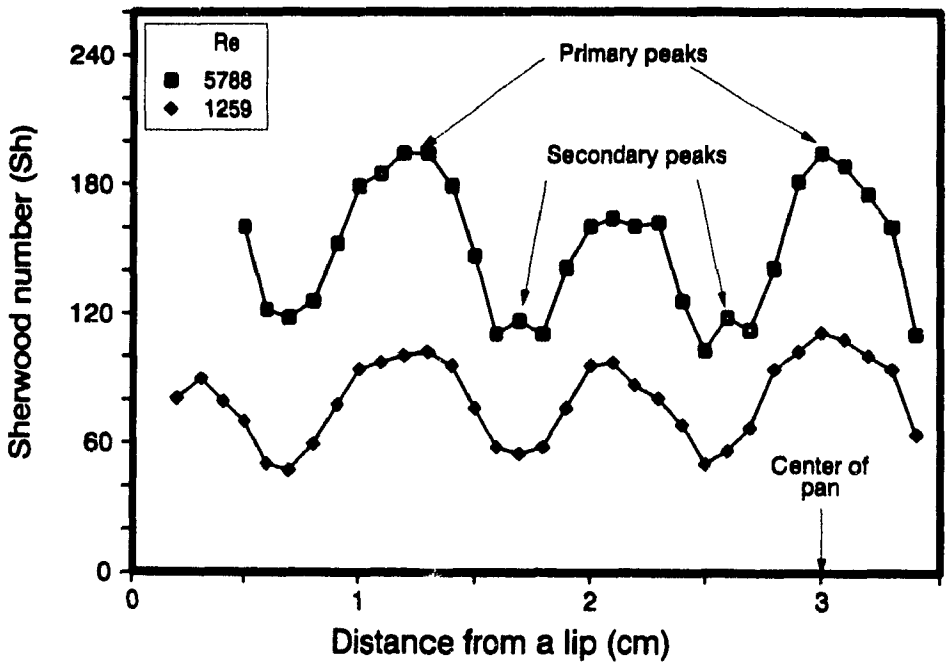

Fig. 2.9 : Local Sherwood number versus distance at 3% open area.

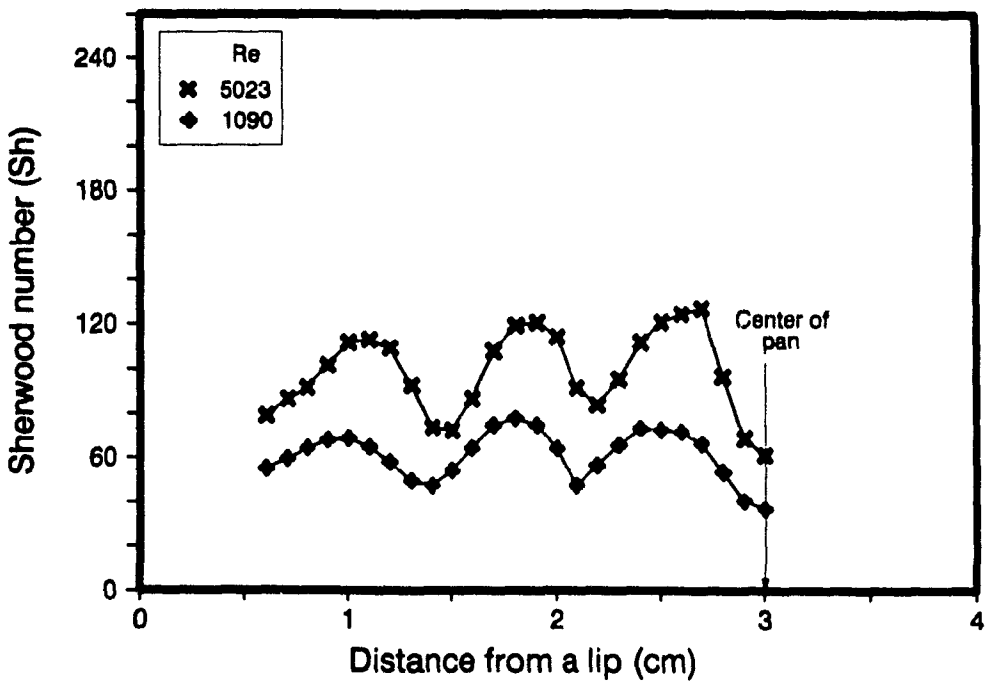

Fig. 2.10 : Local Sherwood number versus distance at 7% open area.

While the above discussion pertains particularly to two dimensional jets arrays of round jets have also been investigated (Huang 1963, Kercher and Tabakoff 1970, Chance 1974, Florschuetz 1980). The study on arrays of jets is not as comprehensive on single or two dimensional jets.

For a large number of nozzles and different arrays, Kercher and Tabakoff (1970) found that that (a) heat transfer by multiple square array could not be correlated by power function expressions of dimensionless parameters; (b) heat transfer is dominated by the hole diameter Reynolds number and hole spacing-to-hole diameter; (c) the exponent on Reynolds number is a strong function of percent opening; increasing crossflow of the jet decreases heat transfer performance; and (d) decreasing hole diameter with increasing number of holes, improves heat transfer performance.

Chance (1974) highlighted the importance of incorporating well-designed exhaust passages to minimize crossflow interference and obtain increased performance at large open areas. He also determined that if the performance of an array of jets is described as :

$$Nu\ Pr^{-1/3} = C\ Re^{n} \qquad (2\text{-}7)$$

where "n" is the slope of the linear line on a log ($Nu\ Pr^{-1/3}$) vs log(Re) plot, the exponent "n" is a function of the plate perforation (% open area) "n" decreases with increase in open area. He also found that there was no substantial difference between using a square array and an equilateral array of round jets.

Florschuetz et al (1980) determined that large amplitudes of upstream periodic variations were significantly reduced downstream by the influence of crossflow from upstream jets. They also recommended that the use of smaller hole diameters would increase the transfer

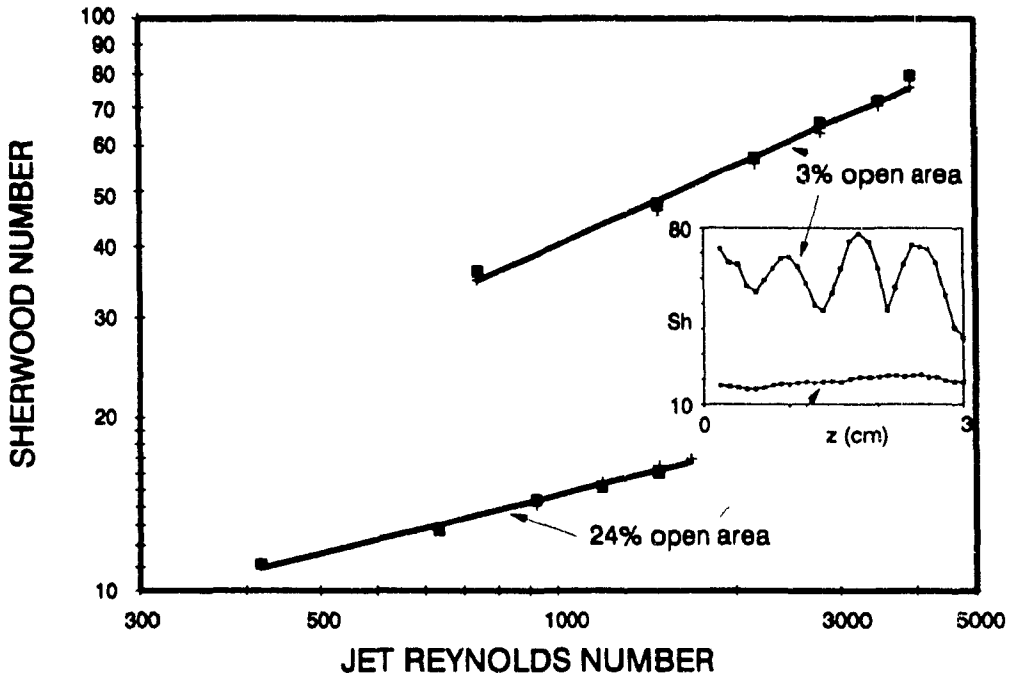

Fig. 2.11 : Sherwood number versus Reynolds number for two different nozzles.

Inset : Sherwood number as a function of distance of the two nozzles.

coefficients. However they cautioned that this would lead to significantly increased pressure drop, plugging of holes with foreign matter, and potential stress problems.

Figure 2-11 shows the effect of Reynolds Number on the Sherwood Number for two different nozzle open areas used in this study. The two curves follow the equation

$$Sh * (Sc)^{-1/3} = C \ Re^{n} \qquad (2\text{-}8)$$

The exponent "n" for 6 % open area is ≈ 0.5 and that for 24 % open area is ≈ 0.3. These values are lower than those published earlier (6 % open area n ≈ 0.66) however agree with previous results that the exponent of Reynolds number decreases with increase in the percent open area (Chance 1974).

Inset in the Fig. 2-11, is the profile of the local Sherwood number. As the figure indicates at low open areas there is a large variation in the local coefficients, however at higher open ares the variations decrease. If however a single large hole would be used then one would have a higher heat transfer coefficient in the middle with decreasing heat transfer coefficients away from the center.

Uniformity of the heat transfer coefficient on the surface of the black liquor is essential. Since the entire heat is obtained from the jet of hot air or superheated steam, local variations in the heat transfer coefficient would result in local drying of the black liquor. This would lead to dry spots and overheating resulting in the decomposition of black liquor. In order to avoid this phenomenon from occurring, the nozzle with 24 % open area was used to study the behavior of black liquor concentration.

In all subsequent chapters where calculations or predictions for the drying rate are to be made, the measured Sherwood number - Reynolds

number relation will be used since it is believed that this represents the transport phenomena in the experimental equipment better than previous correlations (generally generated under ideal conditions [low cross flow, contoured nozzles]).

2.7 SUPERHEATED HEATED STEAM DRYING

The use of superheated vapor as a drying medium has been used in a number of industries, eg. pulp (Swenson, 1976), particle board (Salin 1988), wood (Kauman 1956, Kollmann 1961, Atherton and Welty 1972, Laity et al. 1974, Rosen et al. 1983, Vermaas 1987, Resch et al 1988), paper (Cui et al. 1985), cellulose acetate (Yoshida and Hyodo 1963), and polypropylene (Basel and Gray 1962). As evident from the references listed above most of the interest has been in the area of wood drying.

2.7-1 LITERATURE REVIEW AND THEORY OF SUPERHEATED STEAM DRYING

Svenson (1976) determined that the effective burning of solid moist fuel (bark) for steam production was favored by drying the fuel in steam. He also claimed that the process makes it possible to get 50% more exergy than by a conventional air drying system.

Kollman (1961) concluded that above the fiber saturation point the wood temperature rarely exceeded the temperature of the wet-bulb thermometer. He also mentioned that since, the moisture conductivity increases in a large scale with the temperature, superheated steam drying with respect to rate of drying, had to be superior to conventional drying with steam-air mixture. He also cautioned that the construction of driers had to be carried out with special care, which means that corrosion resistant construction materials would be required if hardwoods were to be dried. Heat insulation had to be provided very carefully.

Laity et al. (1974) concluded that veneer samples dried more

rapidly and charred less readily in steam than in air for drying conditions at 600°F., and that steam would remain more effective than air at higher temperatures. They attributed the greater effectiveness of steam at higher temperatures to the higher Prandtl number of steam compared to air, which, based on convective heat transfer theory would contribute to a higher heat transfer coefficient for veneer in steam as the drying medium. Vermaas (1987) used empirical models developed for air drying to fit his data for steam drying.

Yoshida and Hyodo (1963) found that dry spinning of synthetic fiber with superheated solvent vapor as a drying agent produced a stronger, finer fiber. The also determined that the recovery plant was simpler than that required in air drying, and the spinning chamber was smaller.

While the above discussion refers to the results published on industrial scale studies, fundamental studies of superheated steam drying have also been performed. One of the most interesting investigations on superheated steam drying fundamentals was presented by Malmquist (1959).

Malmquist (1959) investigated the drying of hygroscopical materials such as wood, and found a number of anomalies in their drying behavior. He argued that the evaporation process was not completed in the surface, but was continued in an entropy boundary layer outside the surface. He calculated the change in heat transfer coefficient in a drying process, according to change in specific volume of the surface moisture from the Bolzmann entropy relation. In entropy boundary layers the matter is far from thermodynamical equilibrium and a phase change surface would contain a transition region between phases. This transition region would be of importance , when the entropy boundary layer volume is of the same order as the total volume of the material. This would be the case in porous and colloidal structures.

He expressed the heat of evaporation "r" as the entropy difference

between the vapor and liquid in equilibrium, multiplied by the absolute temperature :

$$r = T (s^v - s^l) \qquad (2\text{-}9)$$

The entropy difference ($s^v - s^l$) involves one of pure geometrical part according to the difference in specific volume in vapor and liquid phases V^v and V^l respectively. From the Bolzmann entropy relation

$$\Delta s = R * \ln (G_2/G_1) \qquad (2\text{-}10)$$

where G is the number of microstates possible, (in phases 2 and 1). The geometrical difference was represented as :

$$\Delta s^v = R * \ln (V^v / V^l - 1) \qquad (2\text{-}11)$$

He thus calculated the heat of evaporation transferred to the liquid surface as

$$r_* = r - R T \ln (V^v / V^l - 1) \qquad (2\text{-}12)$$

where "r" is the total equilibrium heat of evaporation and "r_*" is the heat of evaporation, transferred to the liquor surface through the temperature boundary layer. His results matched closely with those published by Wenzel and White (1953).

Vermaas (1987) has also presented an interesting discussion of the principles involved when drying with dry bulb temperatures above 100°C in superheated steam / air - steam mixtures He claims that " the driving force in superheated steam drying is an absolute or total vapor pressure gradient from the wood to the drying medium, causing evaporation of water into an atmosphere containing only water vapor " He suggested that without this pressure build-up in the wood (caused by structural resistances) with respect to vapor pressure of the steam, no

drying could be possible in a pure superheated steam atmosphere.

Weber (1989) presented an argument of the advantage of using superheated steam as a drying medium by drawing a control volume on the surface of a droplet evaporating in superheated steam, and stated that the driving force for evaporation in superheated steam is density. He also derived the equation for the bulk velocity of the water vapor in superheated steam and hot air. The velocity of water vapor in superheated steam was dependent only on the heat transfer, while that in air was dependent on both diffusion and heat transfer.

A simple approach to establish the behavior of superheated steam drying is taken here. Consider two closed systems as shown in Fig. 2.12 a. One is a two component system (air - water) and the other is a single component system (water). The two systems also exist in two phases in equilibrium (liquid and vapor). When two phases exist in equilibrium, the fugacity of a component in one phase is equal to the fugacity in the other phase. This is expressed as

$$f^v = f^l \tag{2-13}$$

or in terms of chemical potentials

$$\mu^v = \mu^l \tag{2-13a}$$

$$y P \phi^v = x P_s \phi^l \tag{2-13b}$$

If the liquid and the vapor phases are considered to be ideal ($\phi = 1$, $\gamma = 1$), and since only one component is assumed to be in the liquid phase (water in this study), $x = 1$, hence

$$y P = P_s \tag{2-14}$$

For a two component system, the partial pressure exerted by the

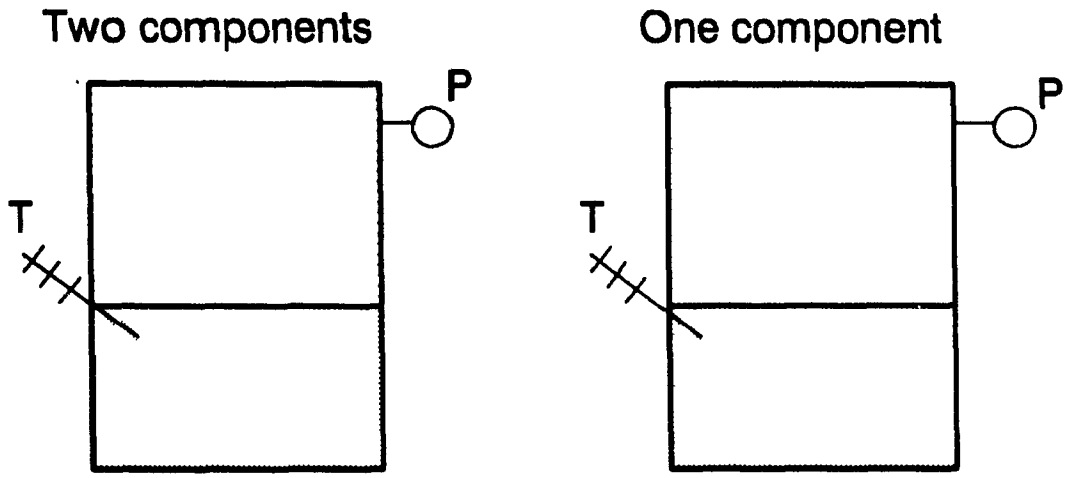

Fig. 2.12 a : Comparison of air-water and pure water systems.

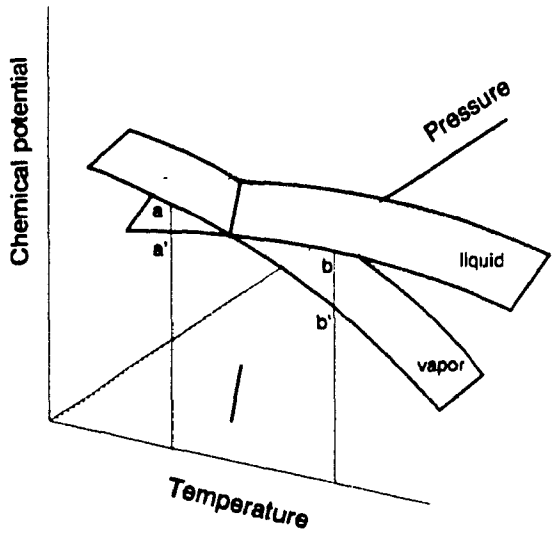

Fig 2.12 b : Chemical potential-pressure-temperature diagram for a pure component system.

component of interest (that exists in both phases, water here) is equal to the saturation vapor pressure at the given temperature. However for a single component system y = 1, hence

$$P = P_s \qquad (2\text{-}14a)$$

or, the total pressure is equal to the saturation pressure of the component of interest at the given temperature.

The above analysis is valid for systems in equilibrium. However if the system is removed from equilibrium, then there exists a non-equilibrium process. For evaporation to occur (i.e. transfer of matter from the liquid phase to the vapor phase) the fugacity / chemical potential of the vapor phase should be lower than the fugacity / chemical potential of the liquid phase. The simplest form describing mass transfer in terms of chemical potential is given by the linear phenomenological equation :

$$j_m = L_{em} \nabla \frac{1}{T} - L_{mm} \nabla \frac{\mu}{T} \qquad (2\text{-}15)$$

where L's are the transport coefficients.

The chemical potential - temperature (at constant pressure) behavior of a single component (pure) system in two phases is given schematically in Fig. 2-12 b. As can be seen from the figure, if the pressure of the system is maintained constant, if the temperature is below the boiling point then the chemical potential of the liquid (a') is lower than the chemical potential of the vapor phase (a) and hence condensation will occur. However if the temperature is maintained above the boiling point (as in the case of superheated steam) then evaporation will occur. The corresponding behavior for a two component system is that if the partial pressure is less than the vapor pressure (at the given temperature) then evaporation occurs.

Once a material has been transformed from the liquid to the vapor phase, in a two component the driving force is concentration gradient. This can be derived from Eqn 2-15, as described by Fitts (1962) and Prigogine (1967). However for a single component system the driving force is density (Weber 1989). Hence for a *two component* system, the transfer of material in the gaseous phase occurs by *diffusion*, and for a *single component* system, by *bulk flow* (Hastopolous and Keenan 1965). It is surmised that the transfer behaves like free expansion since the water vapor generated (due to evaporation) expands into the bulk of the vapor. For an ideal gas

$$\frac{1}{T} = \frac{3}{2} R \frac{N}{U} \qquad (2\text{-}16)$$

and

$$\frac{P}{T} = \frac{N R}{V} \qquad (2\text{-}17)$$

From Gibbs-Duhem equation :

$$d\left[\frac{\mu}{T}\right] = u\, d\left[\frac{1}{T}\right] + v\, d\left[\frac{P}{T}\right]$$

$$= u\left[-\frac{3R}{2u^2}\right] du + v\left[-\frac{R}{v^2}\right] dv \qquad (2\text{-}18)$$

This implies that during free expansion (constant internal energy) the chemical potential gradient is given by :

$$\left[\frac{\mu}{T}\right]_A - \left[\frac{\mu}{T}\right]_B = R \ln \frac{\rho_A}{\rho_B} \qquad (2\text{-}19)$$

Since the equilibrium approached in a single component system is a mechanical equilibrium unlike diffusion equilibrium in a multi-component system or in energy transfer, the mass transfer rate is faster than the heat transfer rate. Hence the limiting factor in superheated steam drying (of pure liquids) is the external heat transfer resistance.

Wenzel and White (1951) were one of the first investigators to

study experimentally the drying rates of water into superheated steam. They claimed that the use of steam rather than air as a medium for drying granular solids did not alter the general characteristics of drying. They concluded that higher drying rates and greater thermal efficiencies were possible when drying with superheated steam rather than with air.

Chu et al (1953, 1959) stated that under the same conditions of mass flow and temperature, superheated steam gave faster drying rate during the constant rate period than air. However at high Reynolds numbers they found no substantial difference between steam and air drying. They also mention that mixture of air and steam performed better than air alone and worse than steam alone.

Yoshida and Hyõdõ presented a excellent paper which laid the corner stone for superheated steam drying as understood today. They proposed the concept of "**Inversion point**". They stated that " *the statement that the rate of water evaporation decreases as the humidity of air increases should be revised. The rate of evaporation of water has a limit point (inversion point) with respect to air temperature. The above statement holds below this point, but at higher temperature the rate of water evaporation increases as the humidity of air increases*".

Chow and Chung (1983) proposed a theory for the existence of the inversion temperature and calculated it theoretically. They proposed that the existence of the inversion temperature could be explained by the combined effects of higher heat transfer coefficients for steam flows and the interfacial temperature depression by the presence of air (wet bulb effect).

The heat transfer from the free steam to the water surface is given as

$$Q = h\ (T_{\infty} - T_s) \qquad (2\text{-}20)$$

where "h" is the heat transfer coefficient, T_∞ is the bulk temperature of the free stream, and T_s is the surface temperature. The surface temperature in air drying corresponds to the wet bulb temperature and for steam drying corresponds to the boiling point (which is 100°C at 1 atm).

At low T_∞ the temperature depression of T_s due to air-water vapor diffusion causes a significant percentage increase in temperature gradient ($T_\infty - T_s$), compared to the temperature gradient for pure steam This explains the fact that water evaporates faster into air than humid / moist air. However if T_∞ is large, the percentage change in temperature gradient is not very large when T_s is depressed.

The other parameter that governs the heat transfer in Eqn. 2-20, is the heat transfer coefficient "h". This depends on the Reynolds number, the Prandtl number, and the thermal conductivity of the drying medium approximately by

$$h = C\, Re^m\, Pr^n\, k/L \qquad (2\text{-}21)$$

where C a constant, m and n are positive fractions (less than 1, 0 5 and 0.33 approximately). The Prandtl number of steam is approximately unity, whereas that for air is about 0.7. The Prandtl number effect gives a 12% heating advantage to steam over air. Steam has a smaller dynamic viscosity compared to air, and hence at a given mass flow rate, steam can have a Reynolds number over 60% higher than that for air. This effect gives a 30 % heating advantage to steam over air. However, the thermal conductivity of air is higher than that for steam and this attributes to a 25% disadvantage to steam over air. Another factor that contributes effectively to steam is the fact that at high temperatures the latent heat of vaporization is lower.

At high free stream temperatures, the effect of interfacial temperature depression due to the presence of air is not as significant

as the factors which affect the heat transfer coefficient. Thus at high T_∞, the evaporation rate of water actually increases as the free stream steam mass concentration increases.

2.8 COMPARISON WITH PREVIOUS RESULTS

Having calibrated the equipment for mass transport by naphthalene sublimation, it was first attempted to repeat some of the previous experimental results. As stated in the introduction little drying data is available for the evaporation/drying of solutions, and none which use impinging jets. However some work has been done on the evaporation of water from an open trough placed in a wind tunnel through which steam and hot air are passed (Wenzel & White 1951, Chu et al. 1953, Haji & Chow 1988). Numerical calculations have also been done for evaporation from a flat plate (boundary layer type flow) by Chow & Chung (1983), Taleb et al (1985), Hasan et al. (1986). For the constant rate period drying of wood pulp, Cui et al. have published some data (1985). Most of the experimental data and numerical results published are only for the constant rate period.

While it was demonstrated in the section that the repeatability of the experiment was good for naphthalene sublimation it was essential to verify the repeatability of the equipment / experiment for water loss.

In order to achieve the above two objectives, the evaporation of water from a bed of "aluminum oxide" was studied in the drying apparatus. Aluminum oxide was chosen because it is a non-hygroscopic, non crust forming, non swelling material and has a well defined constant rate period.

Figure 2-13 shows the amount of water lost as a function of time at different temperatures when air at 1.2 $kg/s\text{-}m^2$ is used as the impinging medium. As is evident from the graph the repeatability of the equipment is good. It can also be seen from the figure that in the time interval

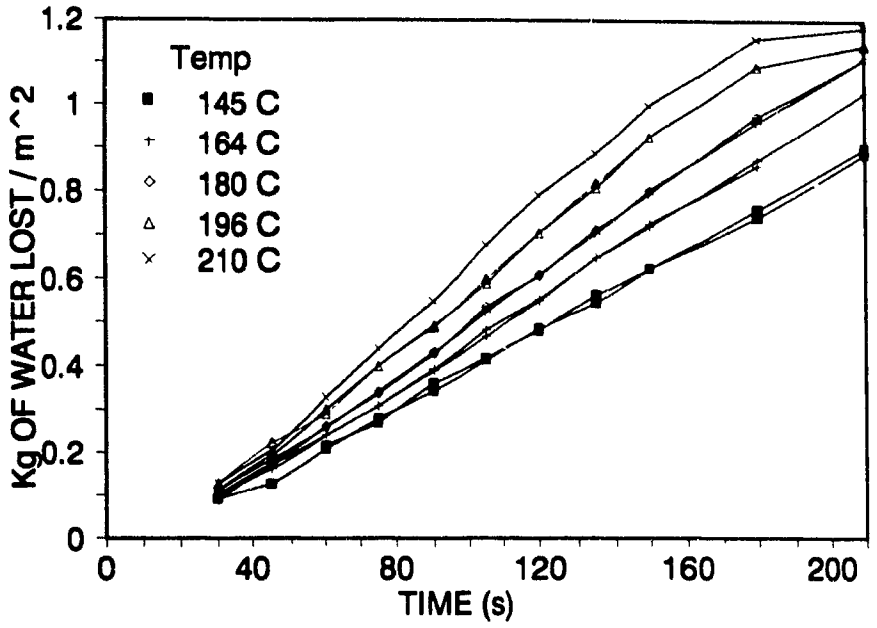

Fig. 2.13 : Water loss from a slurry of aluminum oxide as a function of time at different air temperatures. Pan material : titanium.

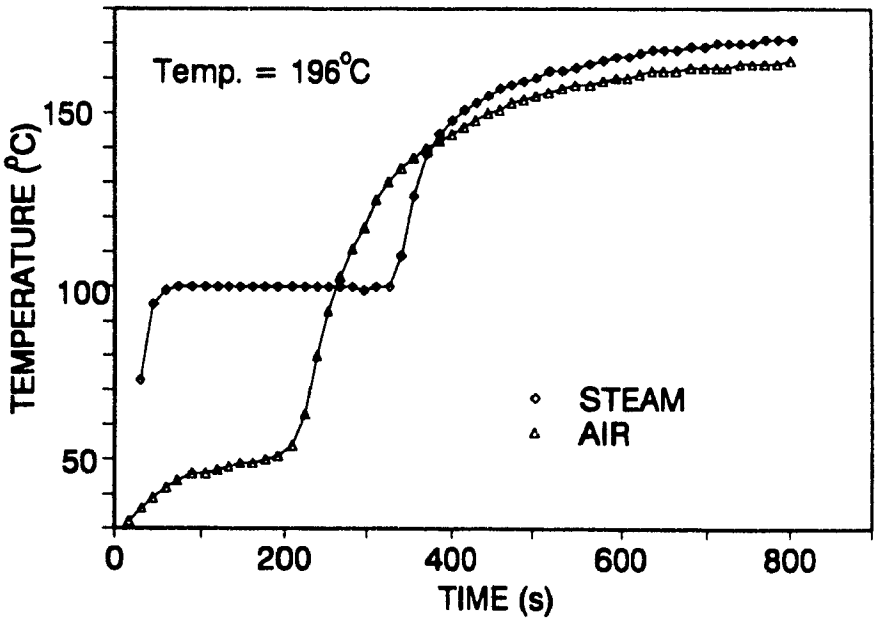

Fig. 2.14 : Surface temperature of aluminum oxide film. Same conditions as above.

from 60 to 180 seconds, the curves are linear. This implies that in that time interval the gradient of moisture content with time is a constant, which in turn indicates the existence of a constant rate period. From the slope of the line the drying rate can be calculated. Figure 2-14 is a plot of the surface temperature (the thermocouple is initially at the surface of the bed of Aluminum Oxide) as a function of time.

This set of experiments was repeated for different temperatures, impinging media, and pan material. From the water loss curves, the drying rates were calculated. A plot of the drying rate versus impinging jet temperature is plotted in Figure 2-15 for air and steam, and at two different flow rates (0.8 and 1.2 $kg/s\text{-}m^2$).

Figure 2-15 shows that at low temperatures (below the inversion point) the rate of evaporation in air is higher than in steam and the trend is reversed at higher temperatures. It can also be seen that an increase in mass flow rate decreases the inversion temperature. This was also determined earlier theoretically by Hasan et al. (1985), Taleb et al. (1985), Chow and Chung (1983). The range of inversion temperatures found agree very well with those predicted theoretically. However, it should be mentioned that the absolute value of the drying rate is higher in this study than those presented for boundary layer flow over a flat plate. This is due to the fact that the transfer coefficients here with impinging jets are substantially higher than those for flow over a flat plate. These drying rate results are lower than those published by Bond (1990) and Cui et al (1985) who used much higher flow rates.

A simple calculation can be performed to predict the constant rate period drying rate. During the constant rate period, the temperature of the drying surface is the wet bulb temperature for adiabatic conditions. However in the case of conduction and radiation this temperature tends to increase above the wet bulb temperature. The value

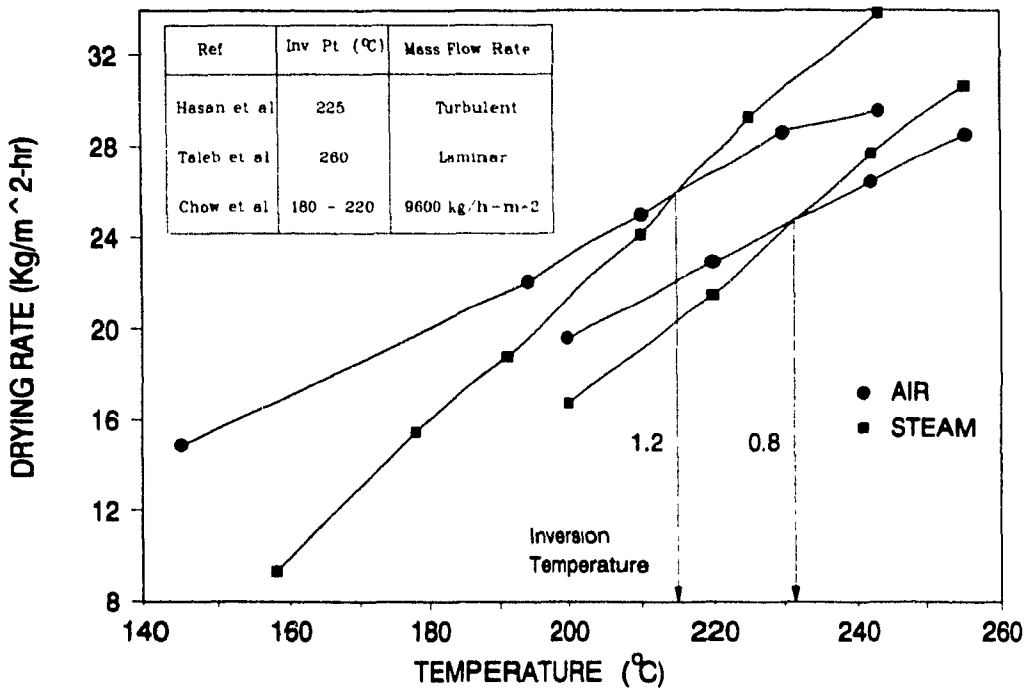

Fig. 2.15 : Comparison of air and steam as drying mediums at 0.8 and 1.0 kg/s m^2 mass flow.

of the steady state heat flux can be calculated using the following expression :

$$j_q = h (T_g - T_s) \qquad (2\text{-}22)$$

where h is the heat transfer coefficient, T_g is the temperature of the impinging jet stream, and T_s is the surface temperature.

The value of j_q can also be calculated using the constant drying rate :

$$j_q = N_{Wc} \Delta H \qquad (2\text{-}23)$$

where N_{Wc} is the constant drying rate, and ΔH is the latent heat of vaporization. Thus,

$$N_{Wc} = h \frac{(T_g - T_s)}{\Delta H} \qquad (2\text{-}24)$$

The value of the heat transfer coefficient can be calculated from the mass transfer data using the transport analogy and by correcting for Prandtl - Schmidt, and Nusselt - Sherwood Numbers. The value of T_s is taken from the plot of temperature versus time is shown in Figure 2-13.

A plot of the drying rate versus temperature calculated from eqn. 2-24 and measured from Figure 2-15 is plotted in Figure 2-16. There is a very good correlation between the two curves.

2.9 CONCLUSION

The designed equipment is well calibrated, the drying experiments are reproducible, and the results for the constant rate period drying of aluminum oxide compare well with those predicted from naphthalene sublimation data. The inversion points measured here also compare well with previous publications.

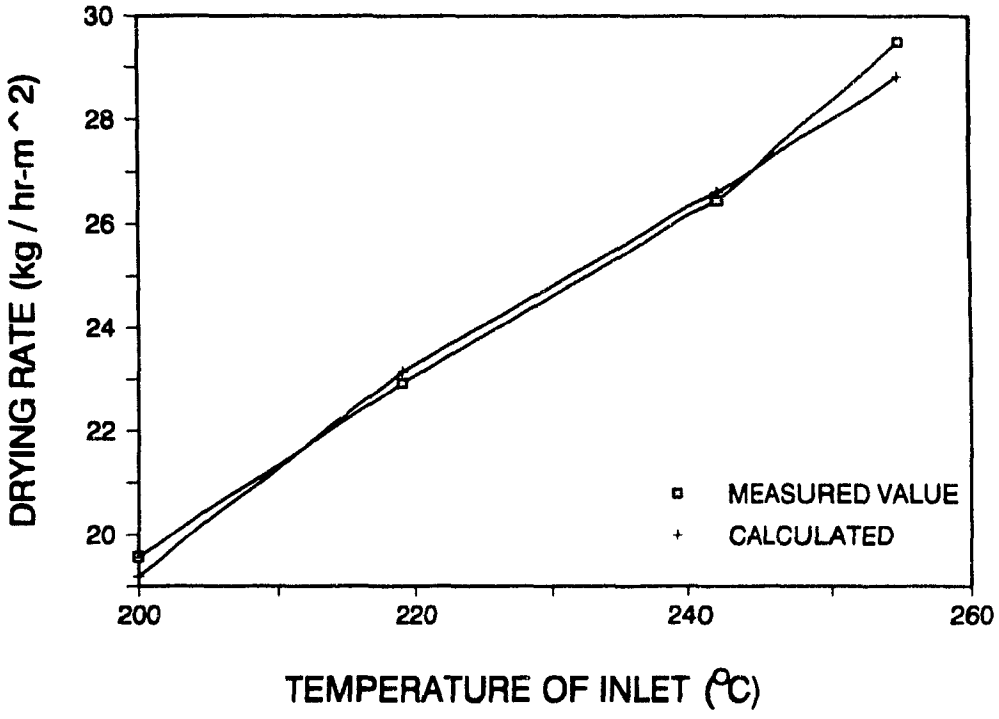

Fig. 2.16 : Comparison of calculated and measured values for drying rates.

2.10 NOMENCLATURE

A	:	Area on surface for sublimation or evaporation (m^2)
C_w	:	Wall (surface) concentration (mol m^{-3})
C_∞	:	Bulk concentration (mol m^{-3})
d_j	:	Jet diameter (m)
f	:	Fugacity (Pa)
h	:	Heat transfer coefficient (W $m^{-2}K^{-1}$)
j_q	:	Heat flux (W m^{-2})
j_m	:	Mass flux (kg m^{-2})
k_g	:	Overall mass transfer coefficient (m s^{-1})
k'_g	:	Local mass transfer coefficient (m s^{-1})
L_{em} & L_{mm}	:	Onsager coefficients in equation
m	:	Mass of naphthalene lost (kg m^{-2})
N	:	Avagadro Number ($6.023 * 10^{23}$ mol^{-1})
N_{wc}	:	Constant drying rate (kg $m^{-2}s^{-1}$)
p_w	:	Saturated vapor pressure (Pa)
r	:	Heat of evaporation.
R	:	Universal Gas Constant (8.314 kJ mol^{-1} K^{-1})
Re	:	Reynolds Number
Sc	:	Schmidt Number
Sh	:	Sherwood Number
T_w	:	Wall temperature (K)
T_g	:	Temperature of impinging jet stream (K)
T_s	:	Temperature of drying surface (K)
V_j	:	Jet velocity (m s^{-1})
V	:	Volume (m^3)
v	:	molar volume (m^3 mol^{-1})

Greek letters :

λ	:	Latent heat of vaporization (J kg^{-1})
ρ	:	Density (kg m^{-3})
η	:	Viscosity (mPa s)
$\mathbb{D}$	:	Diffusivity (m^2 s^{-1})
δ	:	Decrease in height (m)

τ : Time of exposure for sublimation (s)

μ : Chemical Potential.

ϕ : fugacity coefficient

Subscripts and superscripts :

l : liquid

v : vapor

2.11 CITED REFERENCES

Agarwal, R.K., W.W. Bower : "Navier-Stokes Computations of Turbulent Compressible Two-Dimensional Impinging Jet Flowfields". AIAA J 20(5), pp 577-584 (1982).

Atherton, G.H., J.R. Welty : "Drying Rates of Douglas-Fir Veneer In Superheated Steam at Temperatures to 800°F" Wood Science 4(4), pp 209-218 (1972).

Avedesian, M.M., G.J Kubes, A.R.P. van Heiningen : "Development of an Alternative Kraft Black Liquor Recovery Process based on Low Temperature processing in Fluidized Beds" A proposal to the US Department of Energy.

Basel, L., E. Gray : "Superheated solvent drying in a fluidized bed" CEP, 58(6). pp 67-70 (1962).

Beeby, C., O.E. Potter : "Steam Drying". Drying '86. Ed. A.S. Mujumdar, pp 41-59 (1986).

Bond, J.-F.: "Superheated Steam Drying of Paper". PhD Thesis McGill University (1991).

Chu, J.C., A.M. Lane, D. Conklin : "Evaporation of Liquids into Their Superheated Vapors". I&E. C.45(7), pp 1586-1591 (1953).

Chu, J.C., W. Hoerrner, M-S. Lin : "Drying with Superheated Steam-Air Mixtures". I&E C. 51(3). pp 275-280 (1959).

Chance, J.L.: "Experimental invesitigation of air impingement heat transfer undera an array of round jets". Tappi 57(6), pp 108-112 (1974).

Chow, L.C., J.N. Chung : "Evaporation of Water into a Laminar Stream of Air and Superheated Steam". Int. J. Heat and Mass Tr. 26(3), pp 373-380 (1983)

Cui, W.K., W.J.M. Douglas, A.S. Mujumdar : "Impingement Steam Drying of

Paper". Drying Tech. 3(2), pp 307-320 (1985).

Fitts, D.D : "Nonequilibrium Thermodynamics : A Phenomenological Theory of Irreversible Processes in Fluid Systems". McGraw Hill Book Co. pp 46,47. (1962).

Florschuetz, L.W., R.A. Berry, D.E. Metzger : "Periodic Streamwise Variations of Heat Transfer Coefficients for Inline and Staggered Arrays of Circular Jets with Crossflow of Spent Air". J. Heat Tr. 102(1), pp 132-137 (1980).

Gardon, R., J.C. Akfirat : "Heat Transfer Characteristics of Impinging Two Dimensional Air Jets". J. Heat Tr. 108, pp 101-108 (1966).

Gardon, R., J.C. Akfirat : "The Role of Turbulence in determining the Heat-Transfer characteristics of Impinging Jets". 8, pp 1261-1272 (1965).

Harrison, R.E., P J. Chung, B.A. Crowell, E.A. Ketcham : "Ultra-High Solids Evaporation of Black Liquor". TAPPI J. 71(2), pp 61-66 (1988).

Haji, M., Chow, L.C. : "Experimental measurement of water evaporation rates into air and superheated steam". J. Heat Tr. 110, pp 237-242 (1988).

Hasan, M., A.S. Mujumdar, M Al-Taleb : "Laminar evaporation from Flat surfaces into unsaturated and Superheated solvent vapor". Drying 86, Ed A.S. Mujundar Hemisphere Pub. N.Y. (1986).

Hastopolous, G.N., J.H Keenan : "Principles of General Thermodynamics". Wiley, NY, pp 108 (1965).

Hough, G . "Chemical Recovery in the Alkaline Pulping Processes". TAPPI, Atlanta, pp 15 - 85 (1985).

Huang, G.C. : "Investigation of Heat-Transfer Coefficients for Air Flow Through Round Jets Impinging Normal to a Heat-Transfer Surface". J. Heat Tr. 82, pp 237-243 (1963).

Kauman, W G. · "Equilibrium Moisture Content Relations and Drying Control in Superheated Steam Drying". Forest Prod. J. pp 328-332 (1956).

Kercher, D.M., W. Tabakoff : "Heat Transfer by a Square Array of Round Air Jets Impinging Perpendicular to a Flat Surface Including the Effect of Spent Air" J. of Eng. for Power. pp 73-82 (1970).

Kollman, F.F.P. : "High Temperature Drying : research, application and experience in Germany". Forest Prod. J. pp 508-515 (1961).

Laity, W.W., G.H Atherton, J.R. Welty : "Comparisons of Air and Steam

As Veneer Drying Media". Forest Prod. J 24(6), pp 21-29 (1974).

Li, J : "Rate Processes during Gasification and Reduction of Black Liquor Char". PhD Thesis, McGill University (1989).

Malmquist, L : "Drying Physics - an Introduction to Biology?". Papper och Trä, 6, pp 301-308 (1959).

Martin, H. : "Heat and mass Transfer between Impinging Gas Jets and Solid Surfaces". Advances in Heat Transfer, pp 1-60 (1977)

Mujumdar, A.S., W.J.M. Doug'as : "Impingement Heat Transfer : A Literature Survey". Proceeding of TAPPI Eng. Cong. pp 107-136 (1972).

Prigogine, I. : "Introduction to Thermodynamics of Irreversible Processes", pp 19-23, Interscience Publishers, Third Edition, 1967

Popiel, C.O., L. Boguslawski : "Mass and Heat transfer in Impinging Single, Round Jet emitted by a Bell-Shaped nozzle and Sharp-Ended orifice". Heat Transfer pp 1187-1192 (1986)

Resch, H., M.L. Hoag, H.N. Rosen : "Desorption of yellow-poplar in superheated steam" Forest Prod. J 38(3), pp 13-18 (1988)

Rosen, H.N.,R.E. Bodkin, K.D. Gaddis "Pressure steam drying of Lumber" Forest Prod. J. 33(1), pp 17-24 (1983).

Russell, P.J., A.P. Hatton . "Turbulent flow characteristics of an Impinging Jet". Proc. Inst. Mech Engrs 186(52), pp 635-644 (1972).

Salin, J.-G. "Steam drying of wood for imporved particle board and lower energy consumption". Paperi ja Puu 9, pp 806-809 (1988).

Scholtz M.T. : PhD dissertation, Univ Toronto, (1965).

Sogin, H.H. : "Sublimation From Disks to Air Streams Flowing Normal to Their Surfaces". Trans. ASME pp 61-69 (1956).

Sparrow, E.M., S.W. Celere, L.F.A. Azevedo : "Evaporation at a Liquid Surface Due to Jet Impingement". J of Heat Tr 108, pp 411-417 (1986).

Svensson, C . "Back pressure drying, a new system for hogged fuels" Svensk Papperstidning 10, pp 281-287 (1979)

Taleb, M.A., M. Hasan, A.S Mujumdar : "Evaporation of Liquids from a wet stretching surface into air, unsaturated air and superheated solvents". Drying 87, Ed. A.S. Mujumdar, pp 261-269 (1987)

Tharmalingam, S., W.L. Wilkinson : "The Coating of Newtonian Liquids

onto a Rotating Roll". Chem. Eng. Sci. 33, pp 1481-1487 (1978).

Trommelen, A.M., E.J. Crosby : "Evaporation and Drying of Drops in Superheated Vapors". AIChE J. 16(5), pp 857-867 (1970).

Vermaas, H.F : "Fundamentals of Superheated Steam and Superheated Vapor Drying". Suid-Afrikaanse Bosboutydskrif, 142, pp 17-23. (1987).

Vermaas, H.F : "Drying Curve Characterization for Pinus radiata and Pinus patula for Temperatures above 100°C". Holzforschung 41(6), pp 389-394 (1987)

Weber, M.E : "Class notes : 302-611B", McGill University (1989).

Wenzel, L., R R. White : "Drying Granular Solids in Superheated Steam". I&E C, 43(8), pp 1829-1837 (1951).

Yoshida, T., T. Hyõdõ : "Superheated vapor as a Drying agent in Spinning Fiber" I&E C Proc. Des. and Dev. 2(1), pp 52-56 (1963).

Yoshida, T., T. Hyõdõ . "Evaporation of water in air, humid air, and superheated steam". I&E C Proc. Des. and Dev 9(2), pp 207-214 (1970)

CHAPTER III

RESULTS AND DISCUSSION : BLACK LIQUOR DRYING

3.1 INTRODUCTION

This chapter contains all the experimental results and discussion pertaining to concentration of black liquor studied in this thesis A detailed search at the start of the experimental program, showed that the only information in the open literature on concentration of black liquor to dry solids is in the form of patents and a project report

Bergström and Trobeck (1946) mentioned that the "black stuff" was in the form of a powder when fully dry, but stuck to the walls of the flash dryer. They did not give any drying rates or times While Dalin and Wennberg (1983) discuss the difficulties in concentrating black liquor, they do not report any of the concentration characteristics Clay and Cartwright (1986) mention that fluidizing black liquor in superheated steam was extremely difficult Since the literature review indicated the absence of data on concentration rates or the drying characteristics of high solids black liquor, the present study focuses primarily on these two issues

In this chapter the data reduction procedure to obtain the drying rates will be given first This is followed by a presentation of the influence of the different operating variables such as impinging medium, film thickness, jet temperature, jet mass flow rate, and oxidation of liquor. Based on these results the drying characteristics of black liquor in superheated steam and air will be formulated It is also attempted to interpret these characteristics in terms of the drying behavior of the main constituents of black liquor

3.2 DATA REDUCTION PROCEDURE

As described in the previous chapter, the weight of the sample along with the sample holder and film temperatures were recorded during the experiments. The weight and temperature measurements were obtained in separate experiments. The weight loss experiments were performed by drying fresh black liquor at a given set of operating conditions for different intervals of time. The amount of water evaporated is obtained from the difference in mass of the sample before and after drying. Since the loss of mass could also be due to decomposition of the black liquor, experiments were performed in the drying apparatus with online CO and CO_2 analysis of the spent air However, no CO or CO_2 was detected when drying black liquor to 95% solids with air at 245°C, the highest temperature used in this study The experiment was repeated in a thermogravimetric analysis setup because of its smaller volumetric flow rate to sample weight ratio. However even in this case no CO or CO_2 was detected over the range of temperatures of the present investigation

The raw data of two duplicate experiments are depicted in Fig.3.1. The experimental conditions were Impinging medium : superheated steam of 225°C, Initial weight : 4 11 g of 67.7 % black liquor, or a film thickness of 1 04 mm. The titanium pan was used.

The results in Fig. 3.1 show that the repeatability of the weight loss data is very good especially if it is realized that each data point is a separate experiment The standard deviation in superheated steam drying was determined to be 0 02 g, and that in air was found to be 0.01 g It should be mentioned that the results shown in Fig. 3.1 are typical of many duplicate runs since this particular experiment was repeated every two weeks to verify proper operation of the equipment.

To obtain drying rate data, the first order derivative with respect to time of the water loss-time curves is needed. In order to reduce the

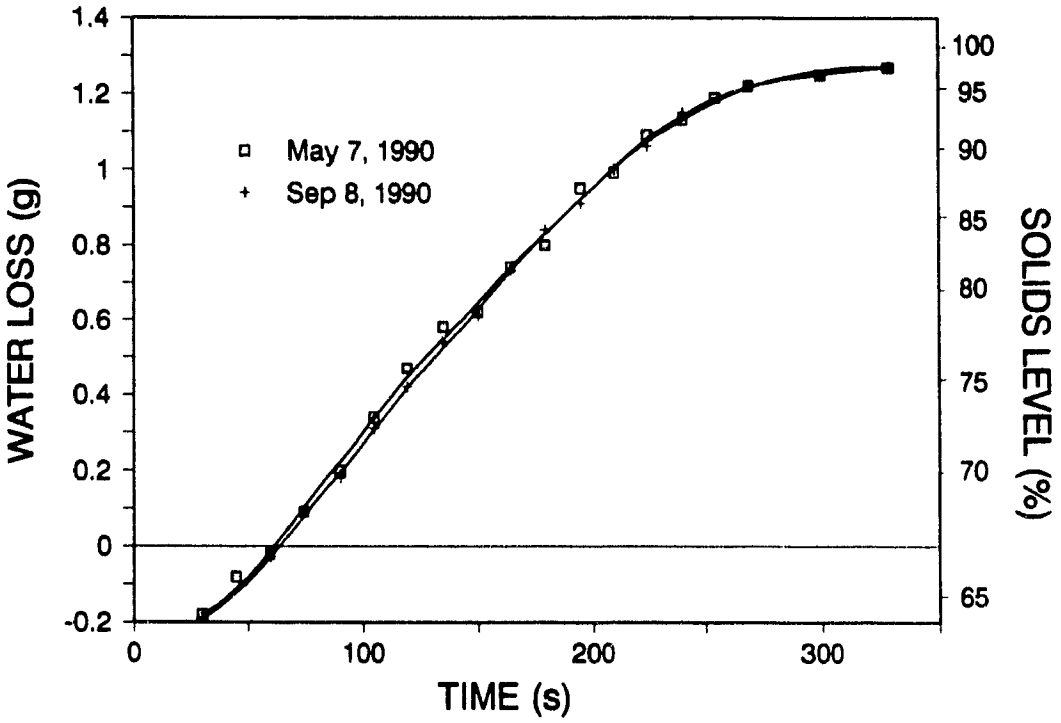

Fig. 3.1 : Repeatability of black liquor drying experiment

Drying medium	:	superheated steam
Jet temperature	:	225°C
Solids level	:	67.7%
Film thickness	:	1.04 mm
Jet mass flow rate	:	0.8 kg/m^{2}s

noise inherent to differentiation of discrete data, the water loss - time curves were fitted using a variable knot (node location) extended spline fit procedure. The method, discussed in detail by Klass and Van Ness (1967) and by de Boor (1978), is summarized below.

The traditional spline fit method consists of connecting all data points with cubic spline functions in such a way that the values and the slopes of the cubic spline functions are the same at all meeting points However the traditional spline fit method leads to very noisy and unrealistic drying rates, since this method is suitable only for data which have little noise. To overcome this difficulty the extended spline fit method was used The extended spline fit method consists of dividing the entire range in a certain number of intervals (less than the number of data points), and use the traditional spline fit method, with the cubics regressing over the points in the chosen interval. Unlike the regular spline fit method, the ordinates of the nodes where the cubics meet in the extended procedure must be calculated based on the regression results This method generally provides smooth differentiated curves. With increasing number of intervals the method approaches that of the traditional spline fit method, which gives rise to unrealistic drying rates With very few intervals, different regions of the drying curve are ignored and tend to give a poor residual diagram. Therefore some experimentation is required to determine the optimum number of intervals and their locations.

Fig. 3 2 and 3.3 show the influence of element location on the drying rate versus moisture plot for the data in Fig. 3.1 As can be seen from Fig. 3.2, the choice of interval location has little influence on the calculated drying rate Fig. 3.3 compares the influence of spacing for the first two intervals listed in Fig. 3.2 This clearly indicates that the influence of element location is small Fig. 3.2 also indicates the smoothing of the differentiated data. Fig. 3.4 and 3.5 show the influence of the number of elements on the drying rate calculation. As mentioned above, a very high number (> 6) of elements

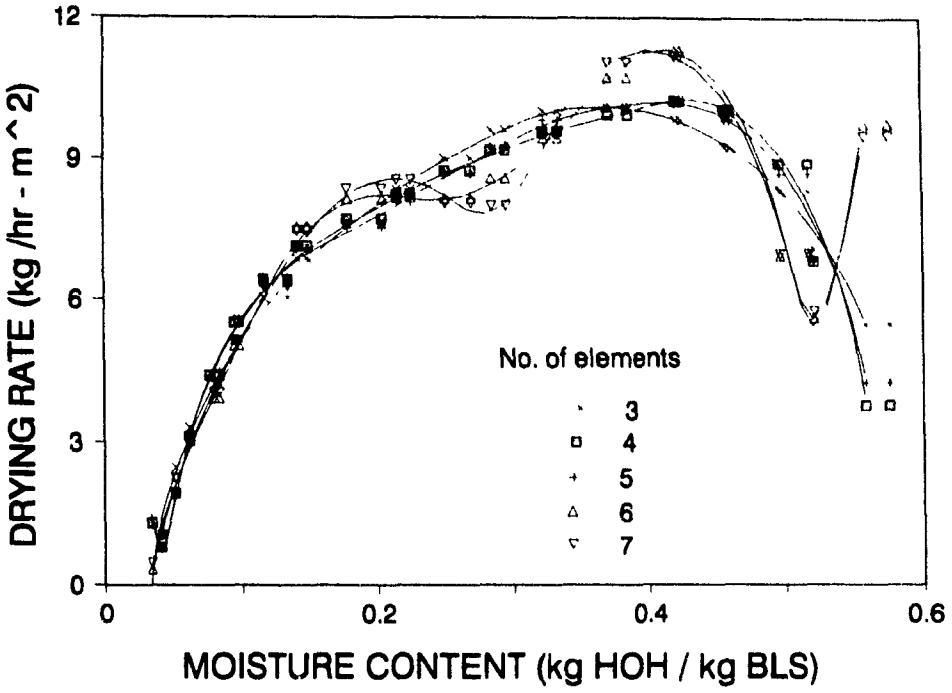

Fig 3.2 : Influence of node location on gradient estimation (4 elements).

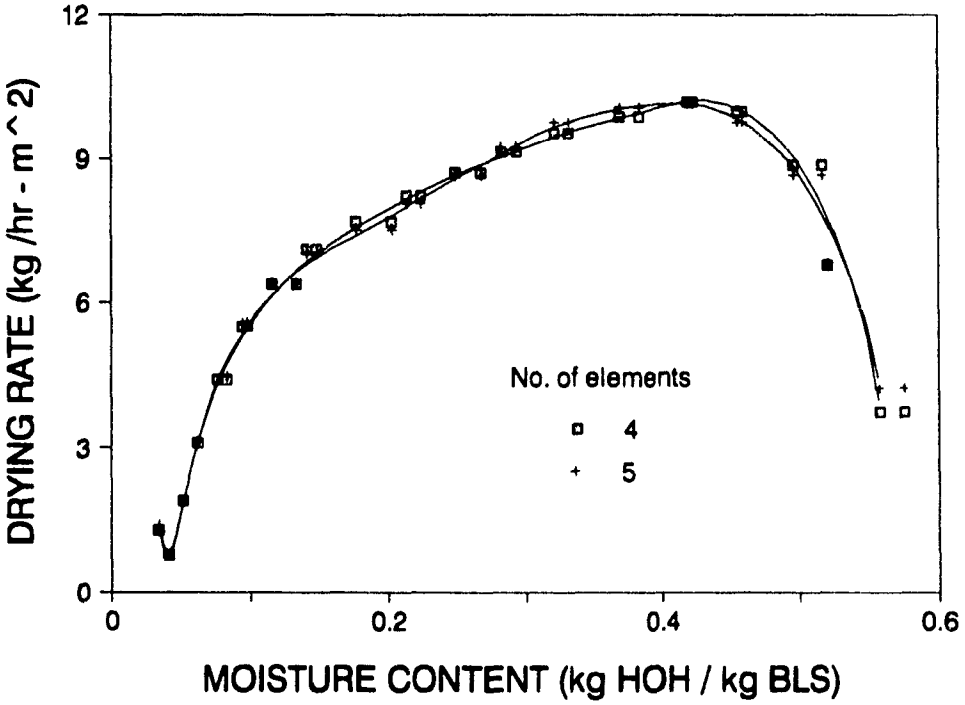

Fig. 3.3 : Influence of node location on gradient estimation

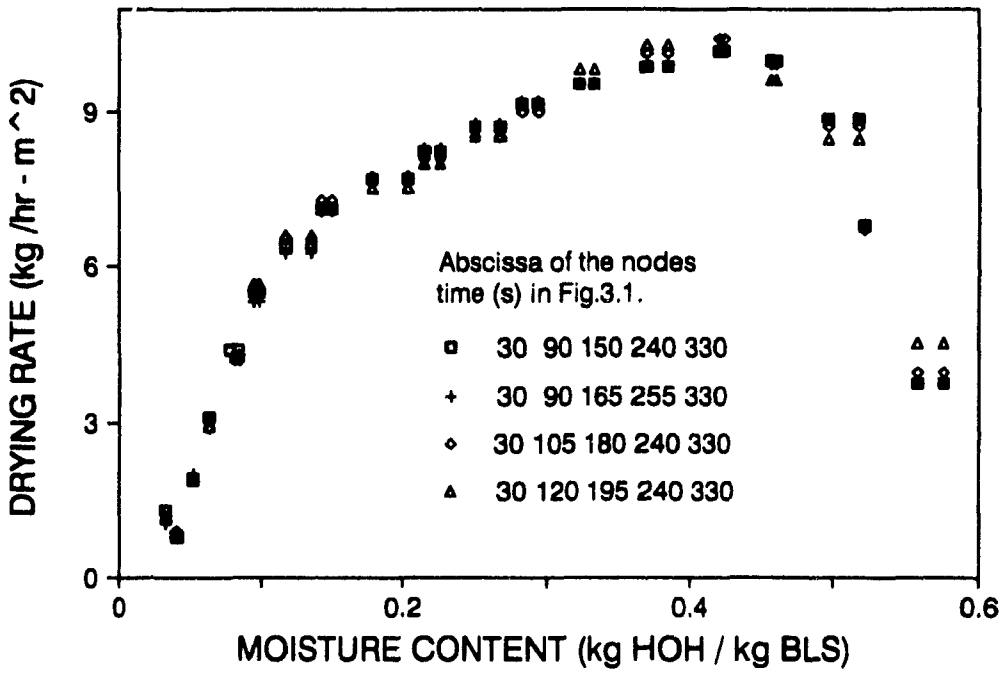

Fig. 3.4 : Influence of number of elements on gradient estimation.

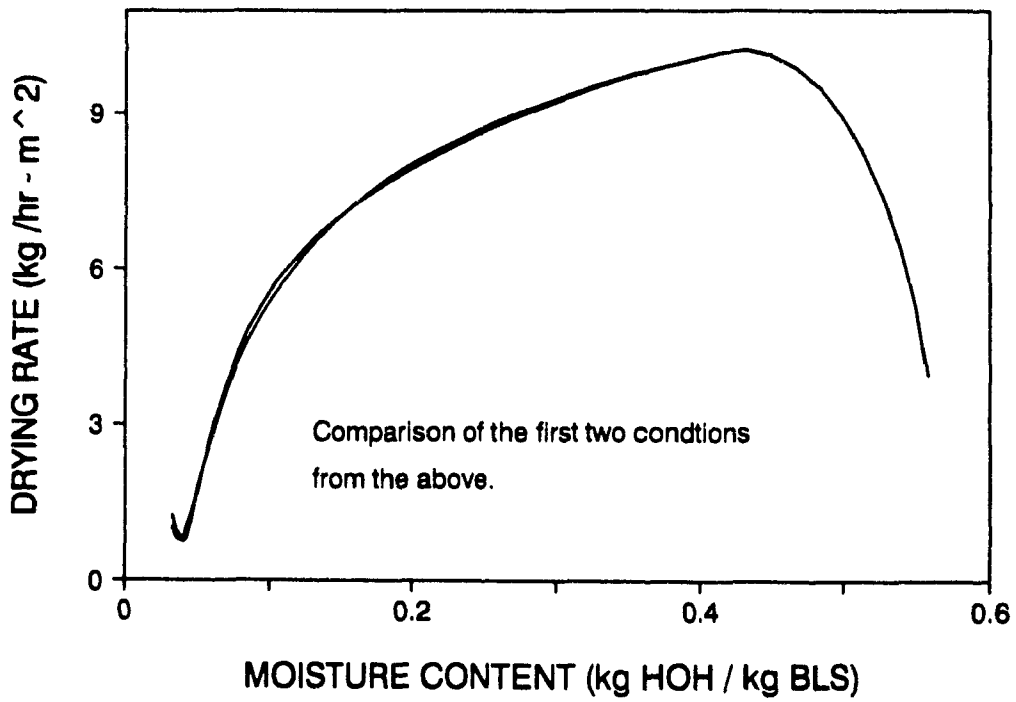

Fig. 3.5 : Influence of number of elements on gradient estimation.

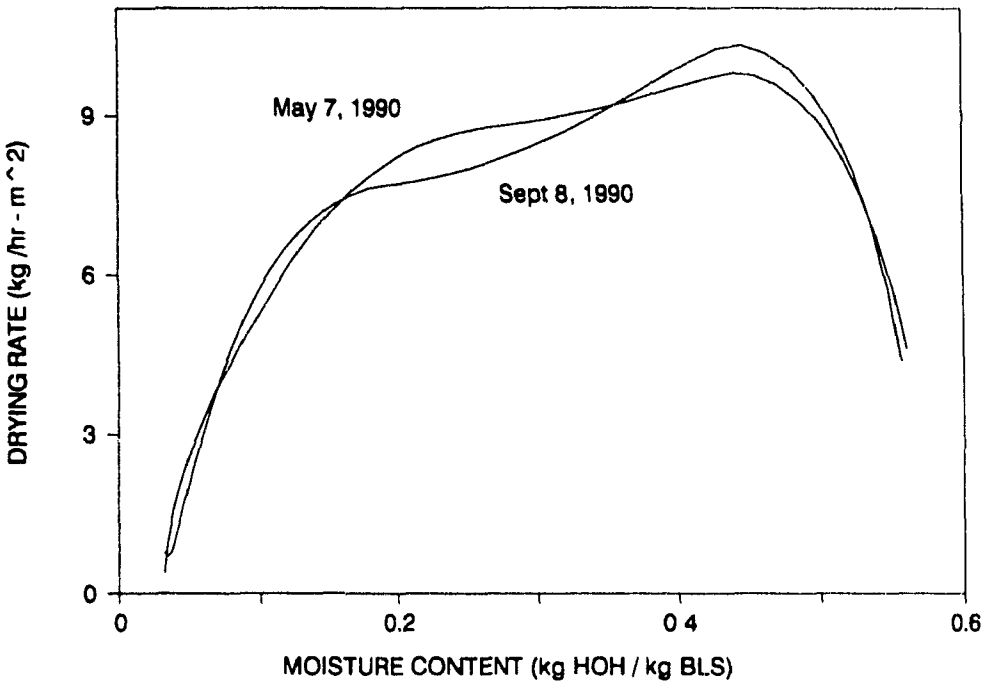

Fig. 3.6 : Repeatability of black liquor drying experiment drying rates.

Drying medium	:	superheated steam
Jet temperature	:	225°C
Solids level	:	67.7%
Film thickness	:	1.04 mm
Jet mass flow rate	:	0.8 kg/m^{2}s

tend to give unrealistic drying rate predictions, and too few elements (< 3) do not properly describe all portions of the curve. Fig. 3.5 shows that the drying rate results when using 4 and 5 elements for the fit are almost identical. Therefore for all further tests the extended spline fit method with 4 or 5 intervals was used. Application of this method to the data in Fig. 3.1 confirms that the present method leads to reproducible drying rate versus moisture content curves as shown in Fig.3.6.

3.3 PHYSICAL BEHAVIOR OF BLACK LIQUOR DURING THE DRYING PROCESS

Before discussing the influence of individual variables on the drying rate and comparing the results quantitatively, it is first attempted to describe the physics of the problem. Substantial work has been done on the physics of the problem of water removal from solutions. Perhaps the most cited study is the classical paper by Charlesworth and Marshall (1960) Figure 4 of their paper has appeared in many books and publications, and it is also partly reproduced in Fig 3.7.

Initially, irrespective of the drying conditions, all droplets lose water and a **crust** is formed on the surface Depending on whether the air temperature is above or below the boiling point of the solution, and whether the crust is rigid and porous, rigid and less porous, or pliable, many different drying behaviors are observed. Kubes (1983) explained the extensive swelling of kraft black liquor during pyrolysis at high temperature (> 400°C), by the formation of a plastic pliable skin at relatively low temperatures. Hence, for the discussion of black liquor it will be assumed that the formed crust is plastic and pliable.

In Fig 3 7 it is shown that when the air temperature is below the boiling point of the solution, the removal of water leads to a decrease in particle volume and thus to a shriveled dry product (sequence III) However, with an air temperature above the boiling point, vapor was formed below the crust when the liquid temperature reached the boiling point. Depending on the characteristics of the crust, the positive

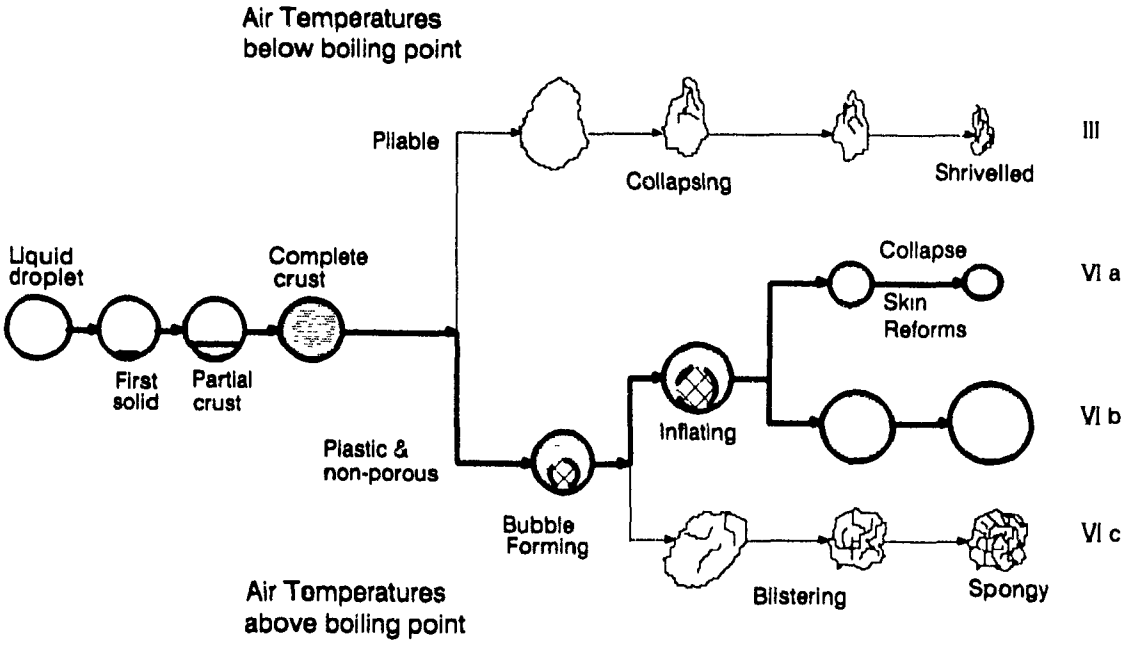

Fig. 3.7 : Appearance changes in drying droplets (Charlesworth and Marshall, 1960).

pressure of the vapor leads to different drying behavior of the particles. In the case where the crust was pliable, the particle generally inflated (sequence VI a,b). Charlesworth and Marshall (1960) also stated that in most cases the final product consisted of hollow particles with a thin shell and a rather smooth outer surface.

The effect of exposing crust forming solutions to superheated steam is described by Dolinsky and Ivansitsky (1987). They postulated that when superheated steam is used as the drying medium, the crust formation process is qualitatively different from that in air. When a drop is introduced in superheated steam, its temperature is raised almost instantaneously to the boiling point. Moyers (1978) showed that water subsequently evaporates without any internal resistance until a condition is reached at which solute solidification begins. The point on the solute concentration - temperature diagram where solidification begins is the intersection of the solidification / saturation and boiling point curves This point is called the invariant point. A schematic description of Moyers proposal is presented in Fig 3.8. He suggested that the crust formation and growth occurred under the condition that the pressure on both sides of the crust remained equal. Thus, with superheated steam, as a result of limited mass transfer through the crust, an increase in the vapor pressure under the crust results in crust deformation that restores the mass transfer to its original value before crust formation.

Figure 3 9 (a - 1) shows the behavior of black liquor in air and steam at the lowest and highest temperature studied, respectively 180 and 245°C. As is evident from Fig. 3.9, the amount of swelling in steam was negligible when compared to that in air Also for air drying the swelling decreased with increasing temperature. Hence it appears that black liquor drying in air follows scheme "VI a" or "VI b" depending on whether a high or low temperature is used respectively. However when steam is used as the drying medium, it is postulated that route "VI a" of Fig. 3.7 is followed, since the boiling activity in the film leads to rapid successions of crust formation and collapse.

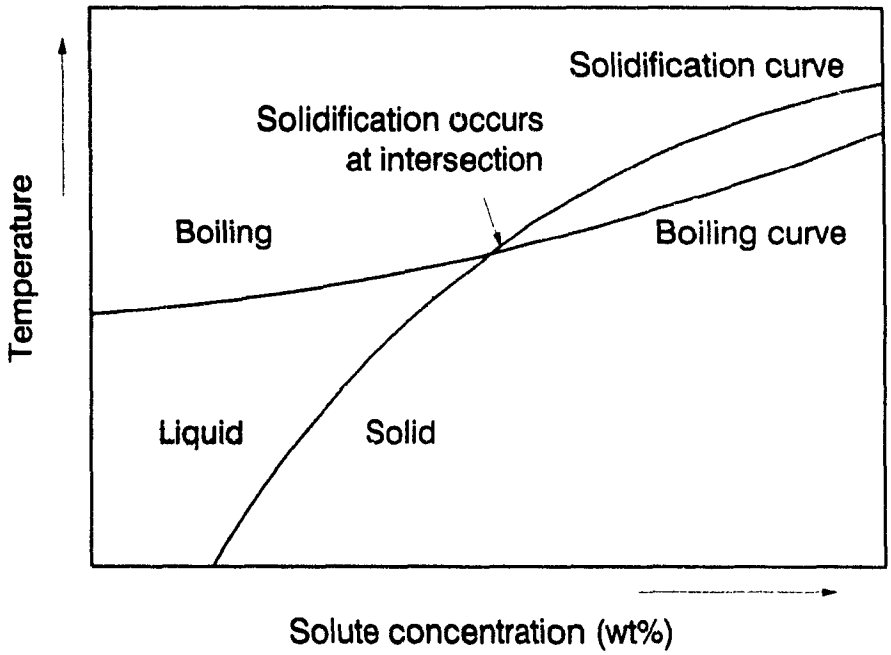

Fig. 3.8 : Solution freezing and boiling curves (Moyers, 1978)

Based on comparison of the drying characteristics in Fig. 3.9 with the phenomenological description given by Charlesworth and Marshall (1960), the following drying behavior seems likely for black liquor in air and superheated steam.

When air is used as drying medium, the temperature of the surface is lower than the boiling point. In fact, the surface temperature corresponds to the wet bulb temperature if there is free moisture available (Geankoplis 1986) Once a crust is formed, and all free moisture near the surface is evaporated, the resistance to evaporation is primarily located in the crust of the black liquor film. The crust becomes thicker as drying continues. Simultaneously the temperature of the black liquor film increases to the boiling point since the drying process is now not limited by external heat and mass transfer. At this point the internal steam pressure leads to swelling of the black liquor film since the crust retains its integrity due to the plasticity offered by the dissolved polymeric lignin and small amount of carbohydrates.

When steam is used as drying medium, the temperature of the surface reaches the boiling temperature almost instantaneously The viscosity and surface tension of black liquor are low as a result of the relatively high boiling temperature Therefore the solidification as proposed by Moyers in Fig 3 8 leads to a weak crust or skin which can be easily disrupted by boiling This boiling behavior can be clearly seen when black liquor is exposed to superheated steam. The above description will serve as a guideline for interpretation of the present drying results of black liquor, and will be verified where possible.

3.4 DRYING RATE CURVES FOR BLACK LIQUOR

When drying a material one can usually identify three regimes: the rising rate, constant rate and falling rate period. The rising rate is obtained when the material heats up, which leads to an increasing water vapor pressure at the exposed surface, and thus a rising evaporation rate. The constant rate period is obtained when the surface reaches a

Table 3.1 : Legend for physical characteristics of black liquor drying shown in Fig 3.9

Legend	Impinging Medium	Inlet Temperature (°C)	≈ Solids level (%)
a	Air	180	68
b	Air	180	84
c	Air	180	93
d	Steam	180	68
e	Steam	180	84
f	Steam	180	93
g	Air	240	68
h	Air	240	84
i	Air	240	93
j	Steam	240	68
k	Steam	240	84
l	Steam	240	93

Pan material : Titanium
Liquor initial solids : 67.7
Jet mass flow rate : 0.8 kg/s m^2
Initial film thickness : 1 04 mm

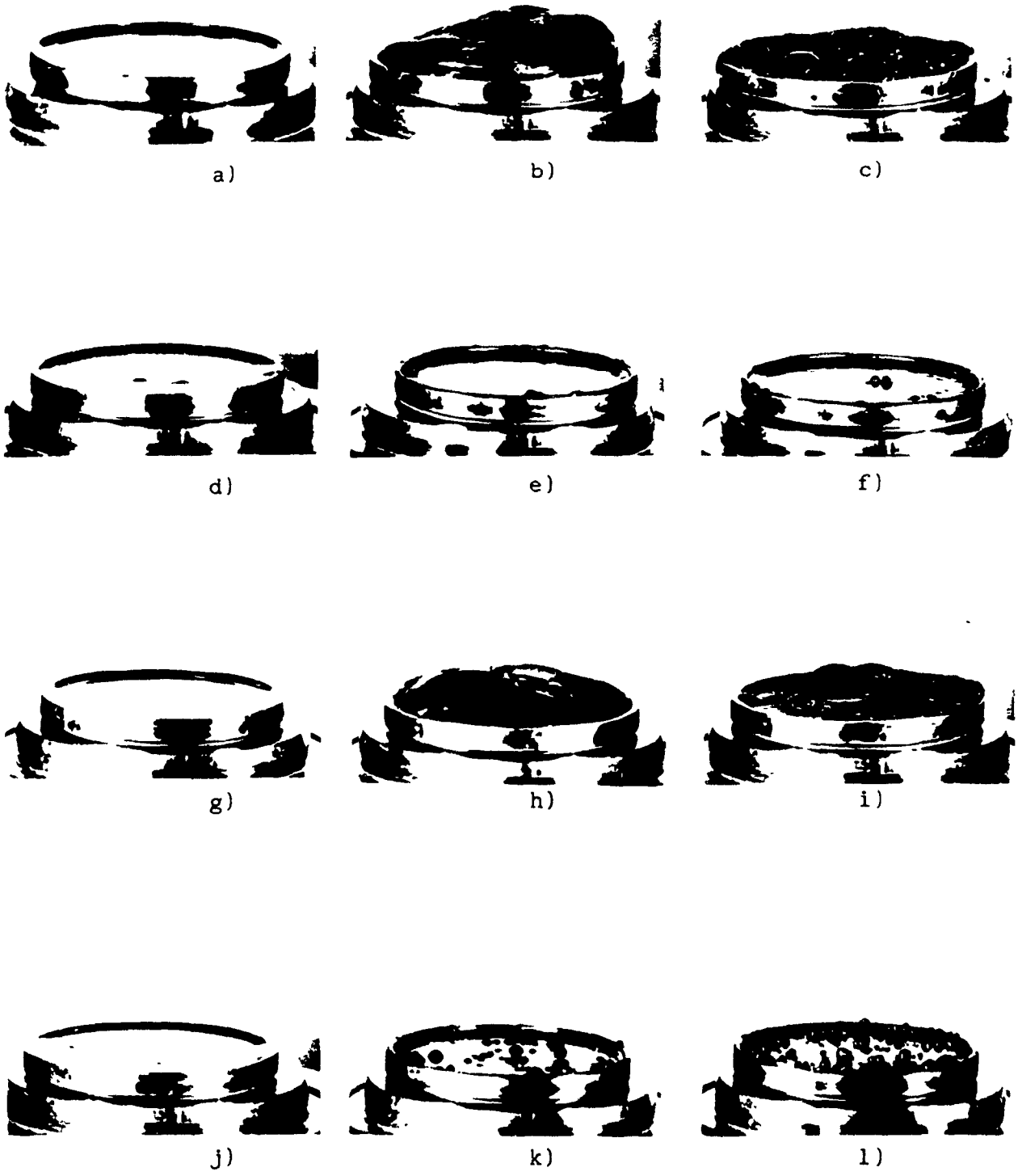

Fig. 3.9 : Physical behavior of black liquor drying. Legend : Table 3.1

constant temperature such as the wet bulb temperature in air drying or the boiling point in superheated steam drying. During this drying period free water is available at the surface. Following the constant rate period there is generally a falling rate period where the drying rate is limited by the transport of water inside the material. The falling rate period is usually divided into two parts: one where the drying rate is proportional to the water content, the other where the removal of bound water requires the additional supply of the adsorption energy.

The presence of these three often cited regions depends on a number of parameters such as the material to be dried, its initial temperature and moisture content, the characteristics of the drying medium etc.

A feature which is not included in the above generalized description is the formation of a crust on the drying surface. As will be seen in the subsequent sections, it is the crust formation which leads to a different drying rate behavior of high solids black liquor.

3.4.1 EFFECT OF DRYING MEDIUM

Fig. 3-10 and 3-11 show the mass loss and temperature curves for black liquor exposed to air and steam jets at 225 and 245°C respectively. These temperatures are selected since it would be desirable in practice to use the high jet temperatures which would achieve the maximum drying rates.

When air is used as the drying medium, water evaporation starts as soon as the black liquor sample is introduced in the drying chamber. As can be seen from Fig. 3-10 and 3-11, the temperatures of the black liquor film and the water loss rate increase gradually from the start in accordance with the rising rate behavior. While the sample is heating up, surface water is removed and a crust (Figure 3 - 9 b) builds up. The crust forms a barrier to mass transfer and eventually limits

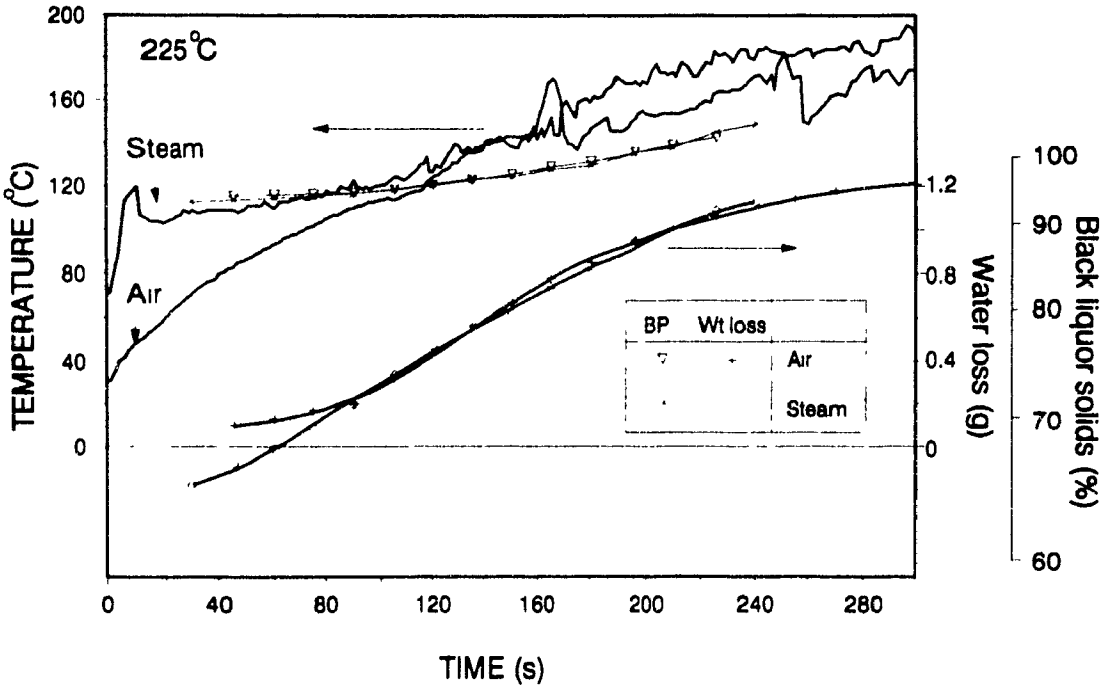

Fig 3 10 : Water loss and temperature curves for air and steam drying. Jet temperature = 225°C

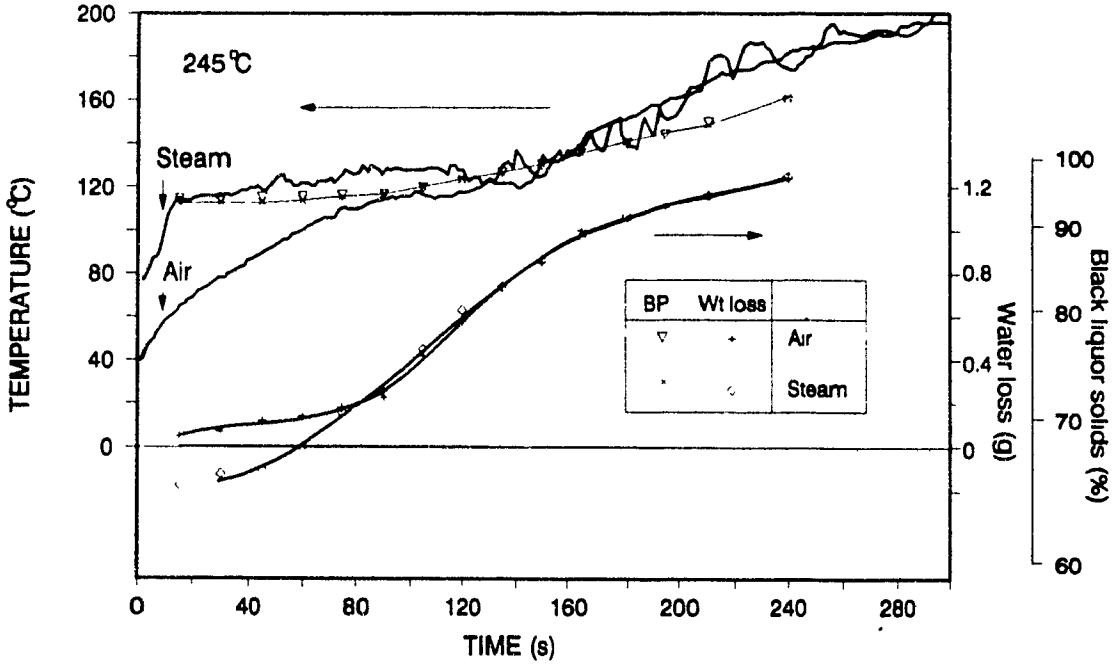

Fig 3.11 : Water loss and temperature curves for air and steam drying Jet temperature = 245°C

further increase in the water loss rate. With further growth and decrease in permeability of the crust a decreasing water loss rate is subsequently observed.

During the constant rate period the material to be dried should reach the wet bulb temperature However the black liquor film temperature in Fig 3 10 and 3.11 increases continuously and eventually reaches the boiling point The boiling point temperature of the black liquor calculated from the average moisture content during drying is represented by the triangular symbols in Fig 3-10 and 3-11 The boiling temperatures were calculated from Robinson and Clay (1986) During this heat-up period the drying rate increases and boiling starts under the crust which causes the black liquor to swell As shown in Figure 3-9, it appears that if the impingement air temperature is less than 200 °C the growth of the crust is slow enough that it does not crack The layer of steam below the crust represents a significant resistance to heat the liquor below so that slowing of the water loss rate is observed

On the other hand if the air temperature is higher than about 200°C, the crust collapses and forms again periodically because the crust is less well developed at the higher water loss rates, and the steam formation rate below it is increased As a result the swelling of black liquor is reduced at these conditions (See Fig 3 9)

From the above it is clear that during air drying of black liquor there is neither free water at the liquor surface nor a constant temperature Hence there is no constant rate drying period as can be seen in Fig 3 12. This is typical for drying of solutions of high solids level (Charlesworth and Marshall, 1960).

When steam is used as the impinging medium a certain amount of steam condenses. This is due to the fact that, the sample is initially at a lower temperature than the boiling point of the black liquor. The two criteria of steam to condense are a] the vapor pressure exerted by

the black liquor is lower than the environment pressure (Weber 1989) and, b] there is thermal inertia in the sample and sample holder to carry away the heat (Othmer 1930) This causes the solids level of the sample to decrease Since, condensation releases a substantial amount of heat, the temperature of the sample rises very rapidly compared to drying in air where there is no condensation.

The black liquor surface temperature reaches the boiling point almost immediately as can be seen from the close agreement with the boiling point temperatures calculated from the average moisture content (the "x" symbols in Fig 3-10 and 3-11). As a result the boiling activity in the black liquor film starts immediately and an uniform crust does not form on the surface of the black liquor With increasing solids content of the black liquor the boiling activity continues Finally the boiling activity becomes very small and the last bound moisture content is slowly removed from the solidified material It should be noted that in Fig. 3 9 at low steam temperatures there is no significant boiling and no swelling is observed This indicates that under these conditions the rigidity of the crust, if formed at all is very low

Hence, the steam drying is characterized by a short initial drying rate period, a long and gradually decreasing falling rate period and finally a rapid falling rate period. One of the reasons for the gradual decrease in drying rate during the falling rate period is that the surface temperature increases continuously as a result of the increase in solids level The increase in boiling point amounts to about 30°C when the solids level increases from 65 to 95 % . Thus the decreasing temperature driving force is partly responsible for the decrease in the drying rate.

There are two rate limiting factors which determine the drying rate in steam. The first is the diffusion of moisture through the film which would determine the drying rate when there is no boiling in the film. However with boiling and complete mixing in the film, the limiting

factor would be the external heat transfer rate (as in the case of aluminum oxide slurry shown in Chapter II) In the latter case the film temperature would correspond to the boiling point of the black liquor. However, it can be observed in Fig 3 11 that in the case of 245°C steam, despite the significant boiling activity (as seen in Fig. 3.9 k, l), the temperature of the film rises above the boiling point temperature. This can occur only if the surface solids concentration is higher than that inside the film, i.e a certain concentration gradient exists through the thickness of the film Since the latter is indicative of internal mass transfer resistance, the diffusional resistance might still be operative when boiling occurs Since Fig 3 9 shows that the film boils in certain locations only (covering a fraction of the surface) it might be that the internal mass transfer resistance limits in the stagnant film areas.

A comparison of the drying rate versus moisture content for air and steam drying at a jet temperature of 225°C is shown in Fig 3-12 It should be noted that there is not a substantial difference in the values of the drying rates However, with reference to the previous discussion of the drying behavior of black liquor the following four differences between air and steam drying can be identified.

1] There is initial condensation of water on the black liquor film when steam is used as the drying medium.

2] The rising rate period in air drying occurs over a larger range of solids level (i.e., the rising rate period is longer) than in steam.

3] The falling rate period decreases more gradually in steam (i.e. over a larger range of solids level) than in air. Thus the drying rate in steam is higher that in air at lower moisture content.

4] The film temperature in steam drying reaches the boiling point of black liquor very rapidly. When air is used as the drying medium the film temperature also reaches the boiling point, only slowly (see Fig.

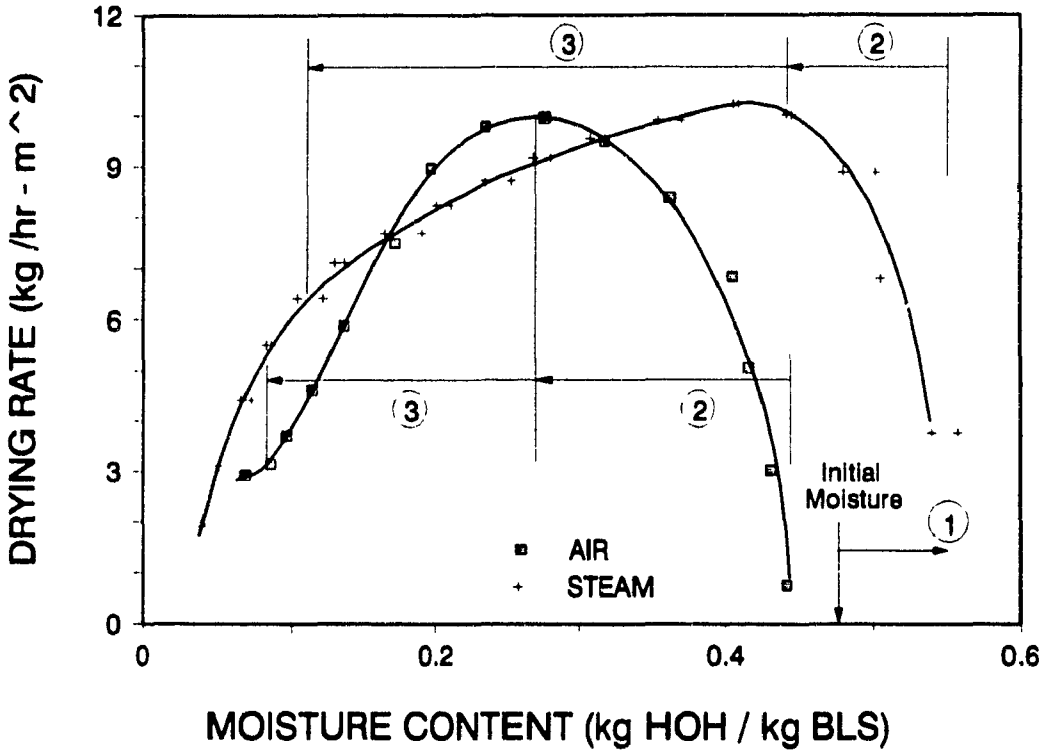

Fig 3.12 : Comparison of air and steam as drying medium. The numbers on the graph correspond to the difference listed on the previous page.

Jet temperature : 225°C
Film thickness : 0.8 mm
Jet flow rate : 0.8 kg/m^2 s

3-10 and 3-11).

3.4-2 EFFECT OF FILM THICKNESS

Before discussing the present results, previous knowledge of the influence of film thickness on the drying behavior of liquids which may or may not form a crust will be briefly reviewed

Without the presence of a crust and for constant drying behavior, the water loss increases linearly with time and is independent of film thickness. This is shown schematically in Fig 3-13 a The onset of the falling period starts earlier for thinner films because less water needs to be removed from these films Once the film is in the falling rate period, the thinner films have a higher drying rate at a given moisture content as is shown in Fig 3 13 a This can be explained by the fact that the diffusional process of water transport is inversely proportional to the square of the transportation distance

The effect of film thickness on the drying behavior of crust forming solutions can be inferred from the drying study for paints and coatings (Croll, 1986) which form a protective crust which cures with time. In this case the crust formation time is independent of the film thickness. Once the crust is formed it controls the drying rate and hence the water loss curves for different film thicknesses separate from a single point as shown in Fig. 3.13 b. Thus, during the rising rate period when the crust being formed, the amount of water lost as a function of time is independent of film thickness Hence the initial drying rates are the same.

However, since the amount of water lost is the same, the moisture content versus time behavior of the different film thickness will be different. Hence during the rising rate period at a given drying rate, the thicker films will have a higher moisture content, or for a given moisture content thicker films will have a higher drying rate. However, during the falling rate period since the crust is assumed to be

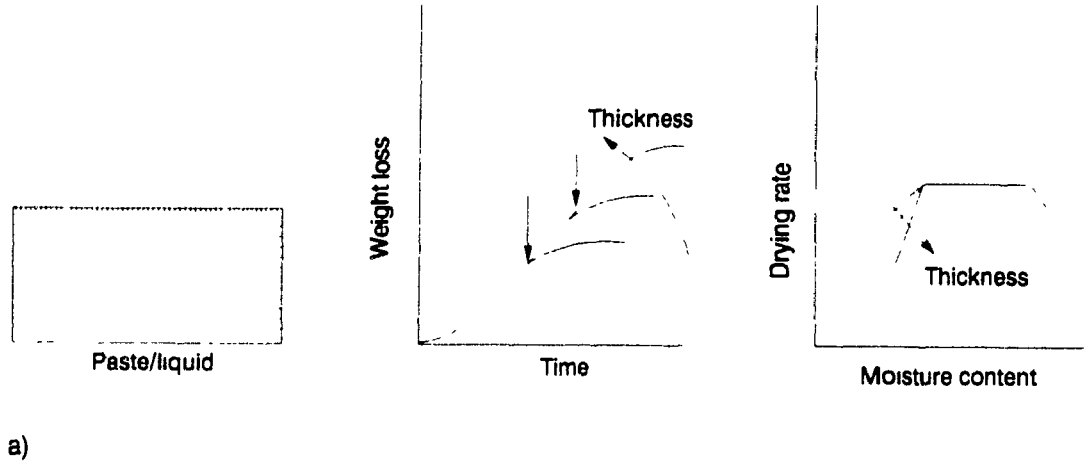

Fig 3.13 : Schematic behavior of paints and coatings (a) without and (b) with crust formation.

the controlling factor, for a given average moisture content, the gradient of moisture across the crust (assumed to be dry) is independent of the film thickness Hence, the drying rates would be similar for all the film thicknesses.

Three film thicknesses were studied in the present work ; 0 8, 1.04 and 1.16 mm. The film thickness was calculated by dividing the weight of the black liquor sample by its density and the cross sectional area of the pan. Figures 3-14 (a), (b) and 3-15 (a), (b) show the weight loss curves for these film thicknesses when drying with air of 180, 200, 225, and 245°C respectively The figures show that the amount of water lost during the initial period is the same for all three film thicknesses. As discussed in the previous section there is no constant rate period when drying black liquor. Indicated by vertical arrows in Fig 3-14 and 3-15 are the points where the weight loss curves of the three film thicknesses diverge from each other It can be seen that both at 180 and 200°C the three curves diverge from each other starting from the same point (located at 270 and 210 seconds respectively), while at 225 and 245°C the water loss curves separate from each other at different locations

Comparison of the water loss curves at the lowest two temperatures of 180 and 200°C in Fig. 3-14 along with the schematic Fig 3-13 b suggests that the crust on the exposed surface is the main transport resistance for water removal. Similarly, since there is no single point of divergence at 225 and 245°C (Fig. 3-15), it appears that at the two highest temperatures the mass transfer resistance is not solely due to water transport through the crust. The points of separation of the water loss curves for the 0.8 mm and 1.04 mm thick films from that of the 1.16 mm thick film occur at about 150 and 180 seconds, and at about 120 and 150 seconds when drying with air of 225 and 245°C respectively. The decrease in time with increasing air temperature is expected as a result of the increased heat transfer characteristics of the hotter jets. Fig. 3-16 a,b show the drying rate - moisture content curves for air drying at 200 and 245°C.

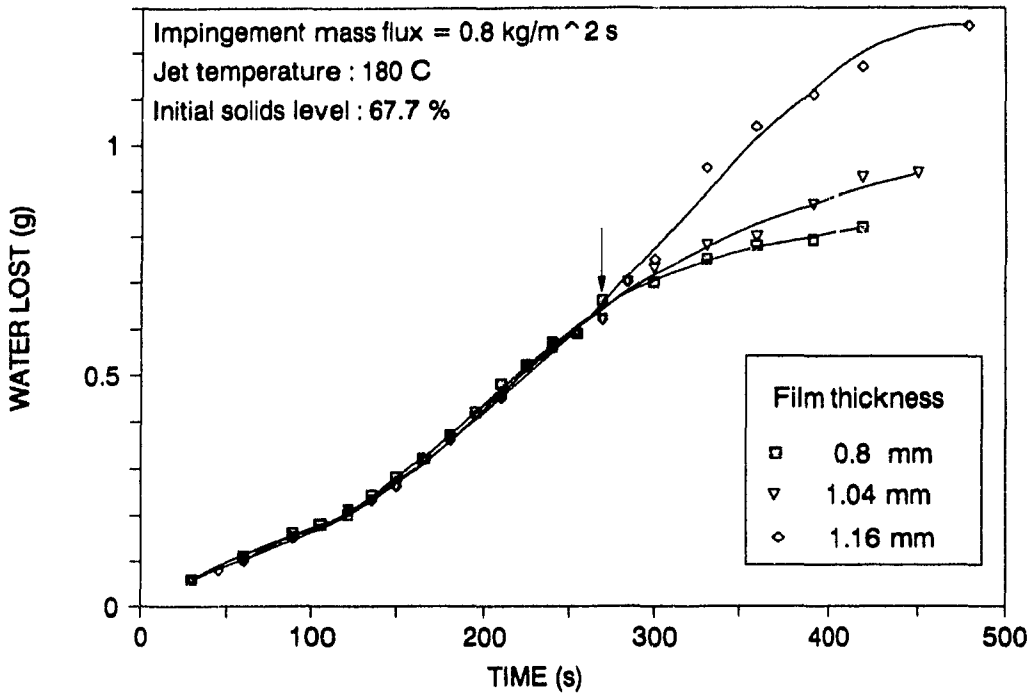

Fig.3.14 a : Influence of film thickness on water loss at 180 °C (air).

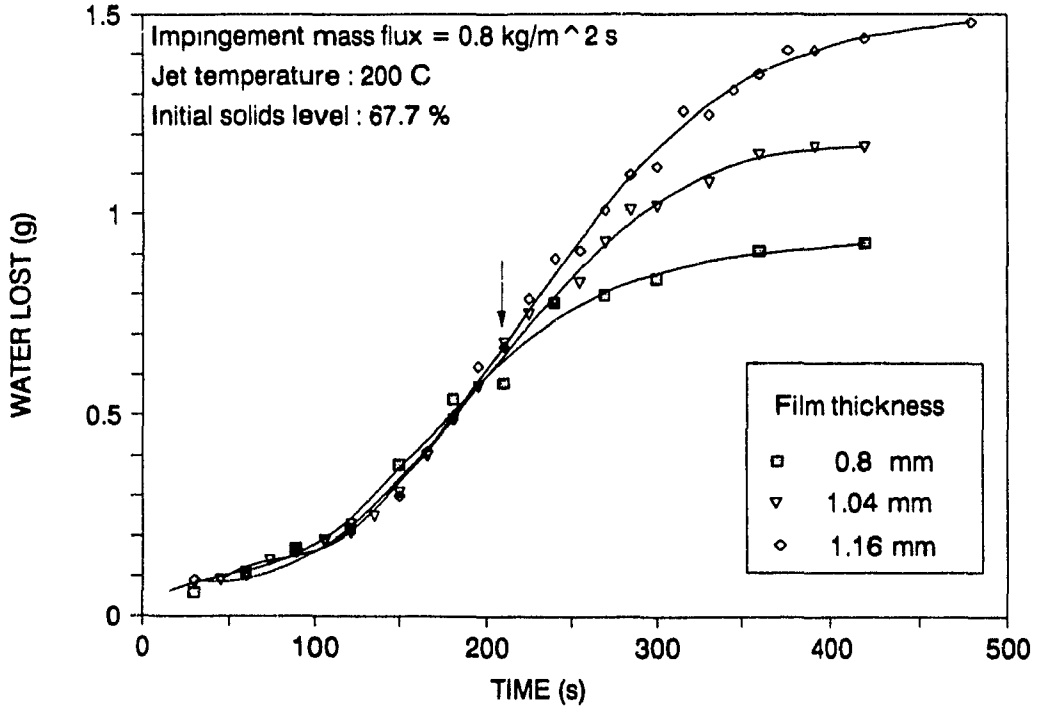

Fig. 3.14 b : Influence of film thickness on water loss at 200 °C (air).

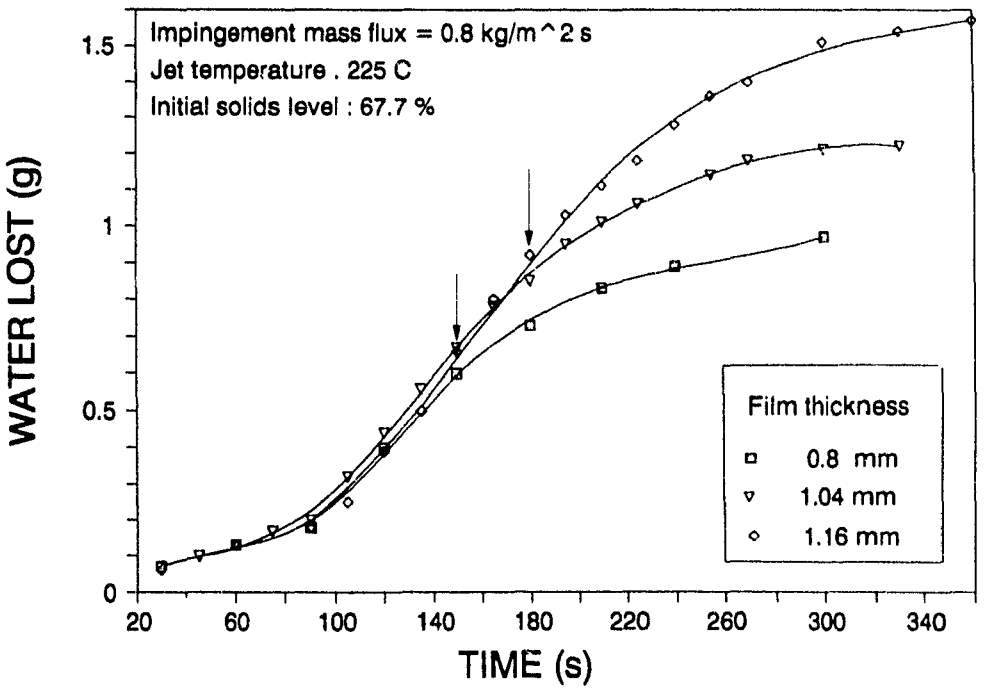

Fig. 3.15 a : Influence of film thickness on water loss at 225 °C (air).

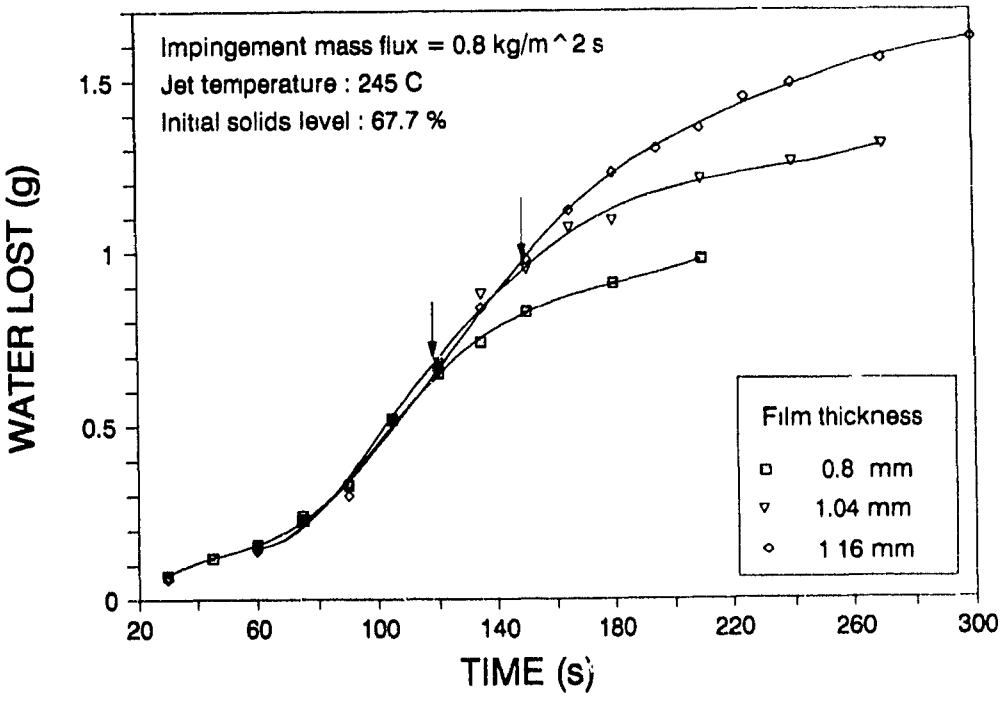

Fig. 3.15 b : Influence of film thickness on water loss at 245°C (air)

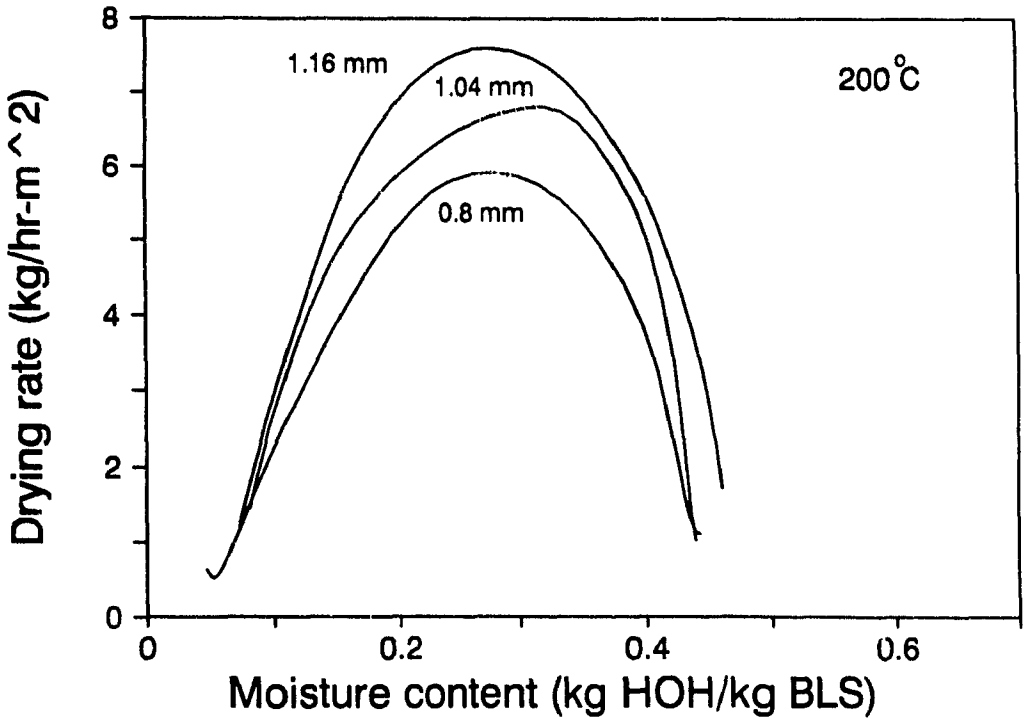

Fig. 3.16 a : Influence of film thickness on drying rate at 200°C.

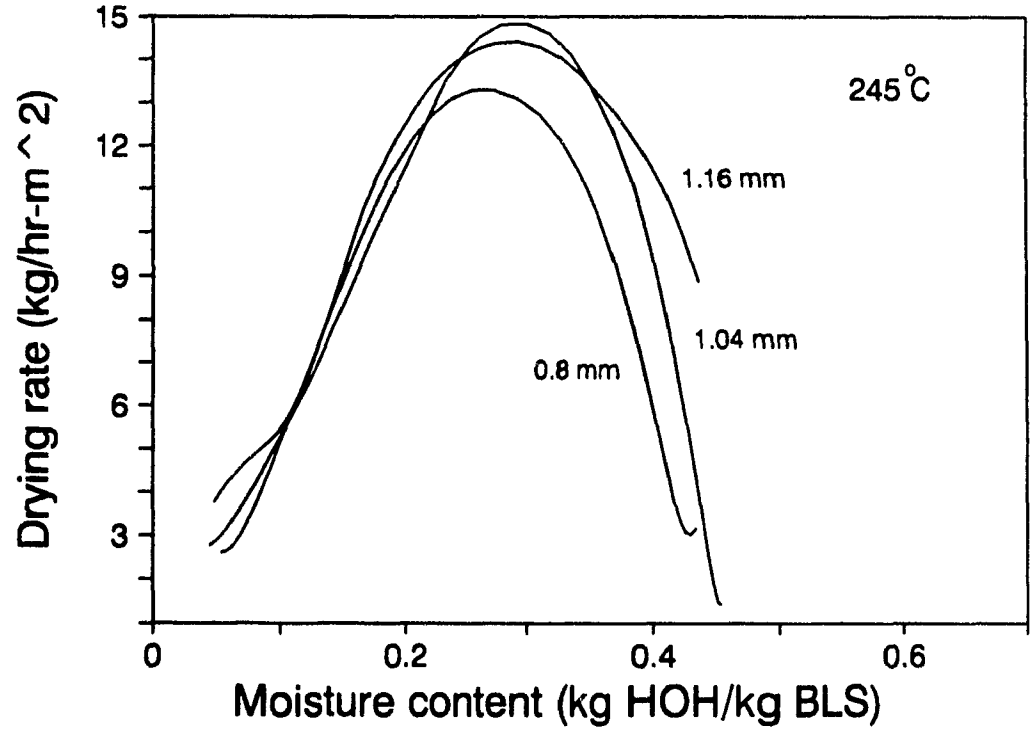

Fig. 3.16 b : Influence of film thickness on drying rate at 245°C.

The effect of film thickness on the drying rates versus moisture content curves using superheated steam as the drying medium is shown in Fig. 3.17 a,b Only two film thicknesses, 0.8 and 1.04 mm, are presented because a film thickness above 1.05 mm lead to extensive splashing of black liquor from the sample holder. As can be seen from Fig. 3.17 a at a low temperature of 180 °C, an increase in the film thickness causes a decrease in the drying rate. Since at 180°C there is almost no boiling in the film (see Fig. 3-9 d,e, and f) diffusion through the film must be the limiting factor. An increase in film thickness causes a decrease in the drying rate since the diffusional transport resistance increases proportional to the square of the diffusion distance.

However, at the high steam temperature of 245°C in Fig.3.18 b an increase in film thickness has little influence on the drying rates. This is attributed to the fact that the boiling behavior of the black liquor film is also a contributing factor (see Fig. 3.9 j,k, and l). Since the bubble diameter is much larger than the film thickness it is unlikely that the drying rate will depend on the film thickness. However, the drying rate will not correspond to that when external heat transfer is the controlling factor because the boiling does not cause the entire area of the pan to be of the same moisture content. The fact that the drying rate versus moisture content curves are almost identical for the two thicknesses in Fig. 3-17 b suggests that in this case the drying behavior is determined by the physical properties of the black liquor

3.4-3 INFLUENCE OF DRYING MEDIUM INLET TEMPERATURE

The influence of temperature on the drying rates of black liquor with air as the drying medium is shown in Fig 3-18 a,b for the 0.8 and 1.04 mm thick film respectively. It can be seen that the drying rate increases with increasing temperature and that the maximum drying rate shifts to slightly lower moisture content.

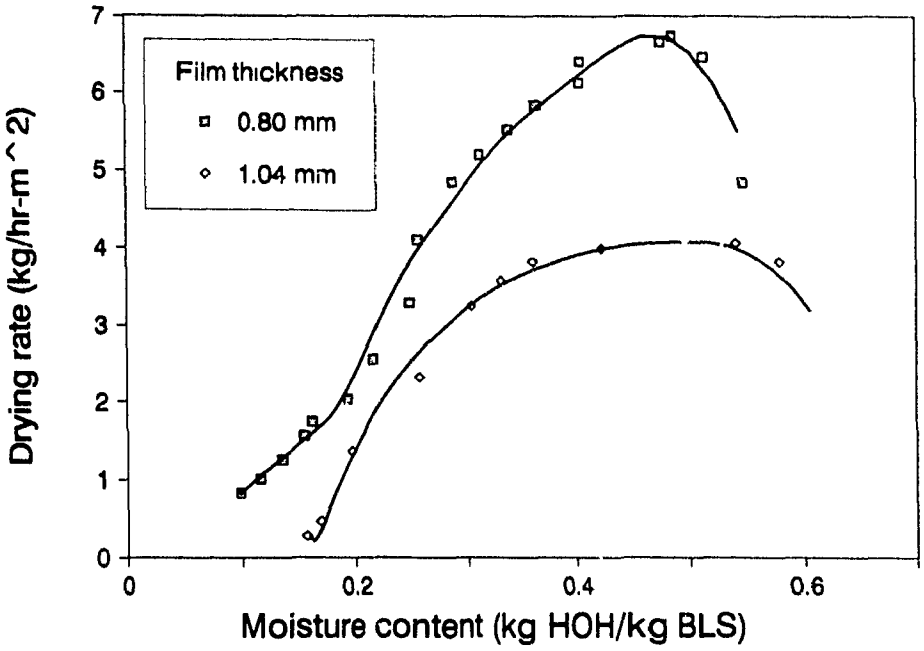

Fig. 3.17 a . Influence of film thickness on drying rates at 180 °C Steam drying.

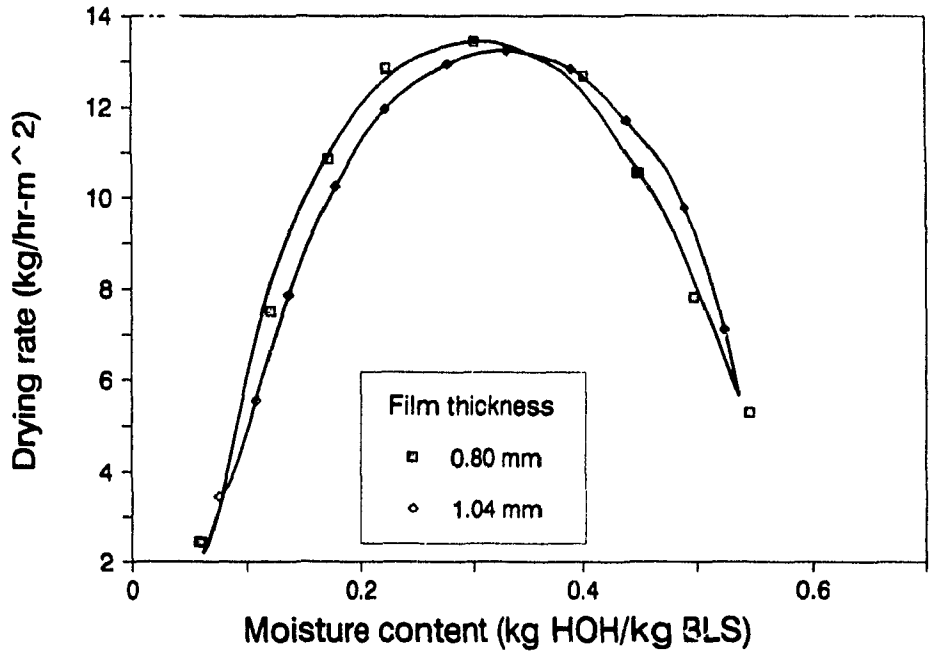

Fig. 3.17 b : Influence of film thickness on drying rates at 245°C

The increase in drying rate with the jet temperature is expected since the driving force for heat transfer increases, which in turn increases the rate of water removal. The shift in the maximum drying rate is caused due to the fact that at higher temperatures the crust is ruptured more frequently and hence the high drying rates can be maintained to a lower moisture level. In the falling rate period the drying rate appears to be a linear function of the moisture content for temperatures of 225°C or higher.

Fig 3 18 also includes two curves indicating the drying rates that would be achieved if the external heat transfer were the limiting factor. It is clear that in both cases the drying rates predicted by the external heat transfer is higher than that measured. This (as mentioned earlier) can be attributed to a) internal mass transfer limiting drying rate, and b) heat loss to the supporting pan and structure A heat and mass balance on the film is presented in Appendix 6.

With steam as the drying medium, the drying rates are shown in Figures 3-19 (a) and (b) At temperatures below 225 °C one can identify an increasing rate period (with condensation), a gradual falling rate period and a rapid falling rate period However, at 245 °C it can be seen that there is only one falling rate period after the maximum drying rate has been reached Apparently the higher boiling activity in the film at a jet temperature of 245°C allows the increasing rate period to continue to lower moisture contents, thus eliminating the gradual falling rate period As mentioned earlier in section 3 4, a comparison of Fig 3-18 and 3-19 shows that the drying curves for steam drying are wider than those obtained in air.

Figures 3-20 (a) and (b) show the solids level vs time curves for air and steam drying at the four different jet temperatures. As can be seen, the amount of steam condensed decreases with increasing temperature.

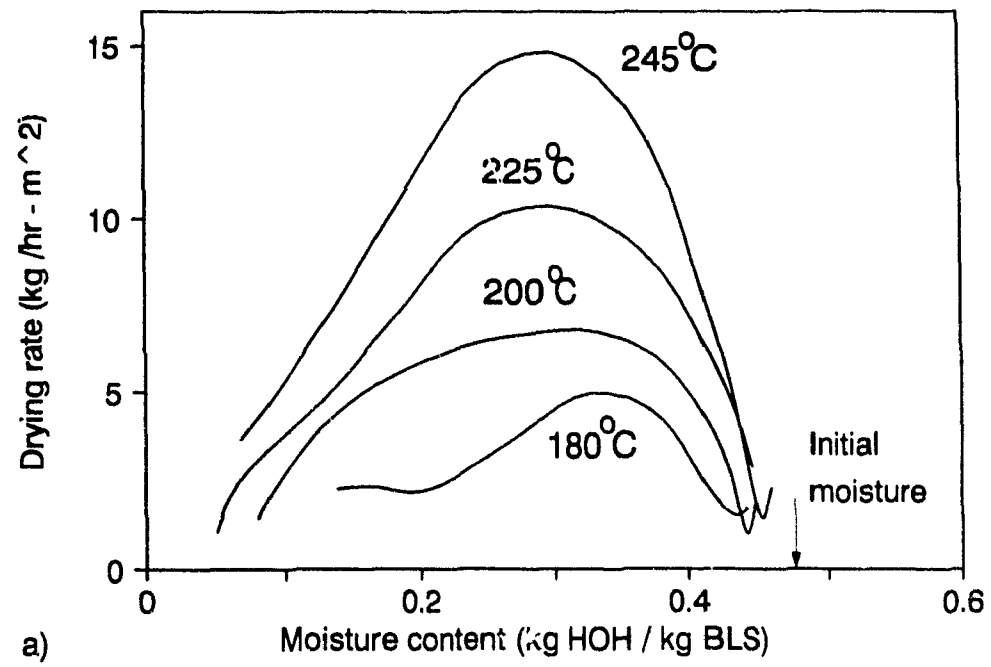

a)

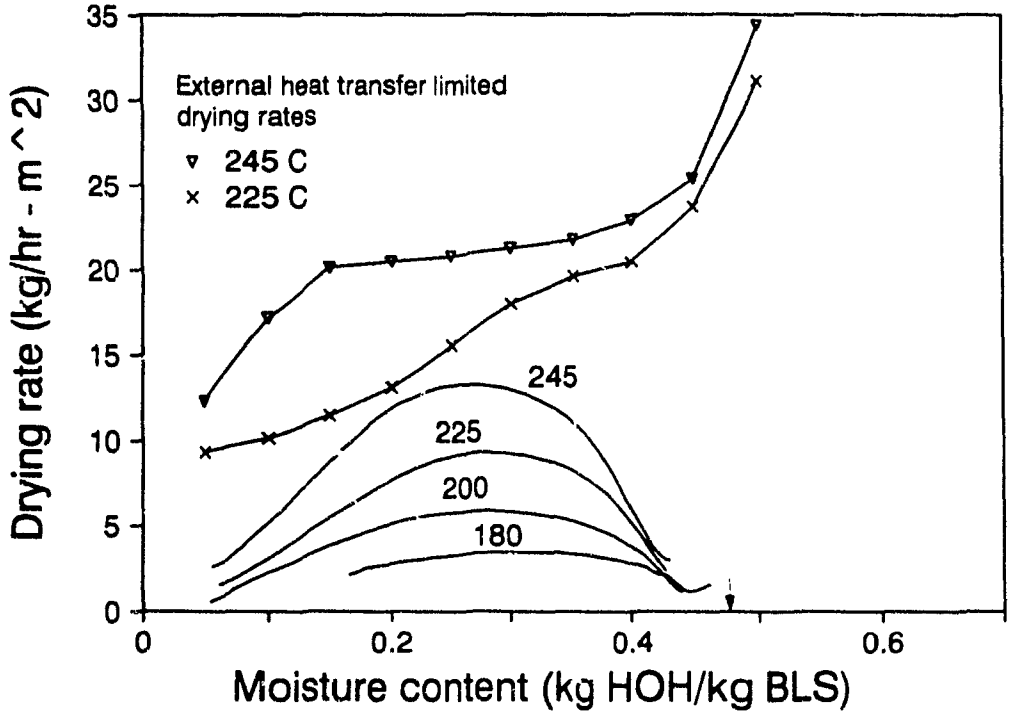

Fig. 3.18 : Influence of temperature on air drying rates of black liquor
Pan material : Titanium, Sample : 67.7% BLS,
Air mass flow : 0.8 kg/s-m^2

a) 0.8 mm BL film, b) 1.04 mm BL film.

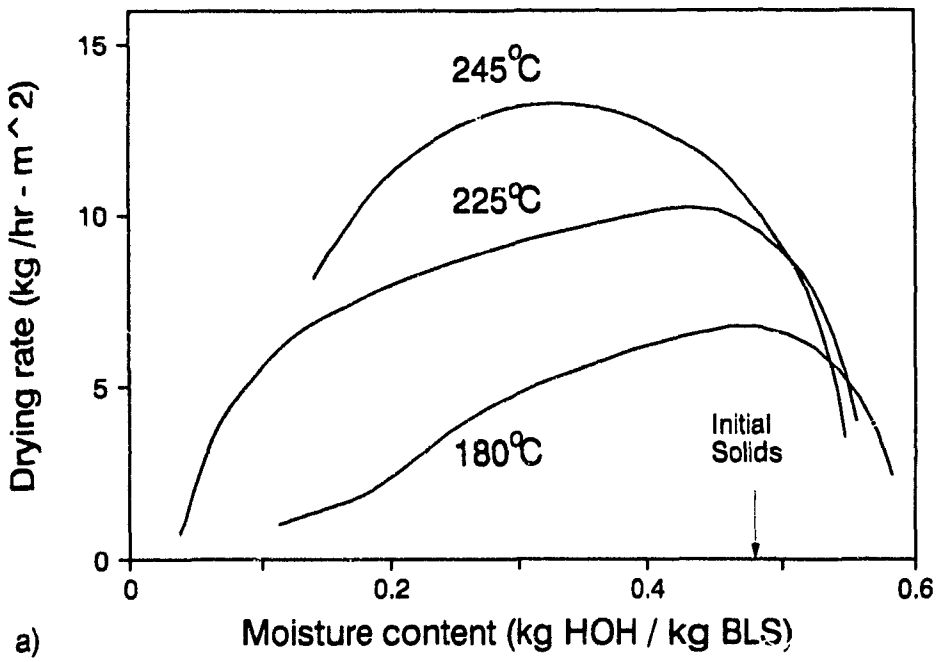

a)

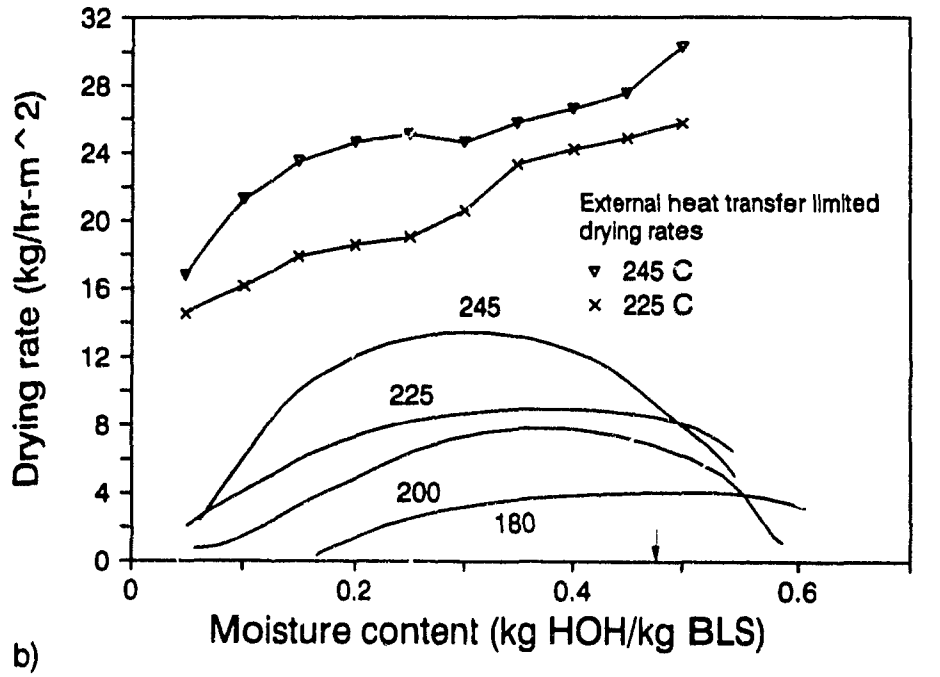

b)

Fig. 3.19 : Influence of temperature on steam drying rates of black liquor. Pan material . Titanium, Sample : 67.7% BLS, Steam mass flow : 0.8 kg/s-m^2

a) 0.8 mm BL film, b) 1.04 mm BL film.

3.4.4 EFFECT OF DRYING MEDIUM MASS FLOW RATE

Figures 3-21 (a) and (b) show the influence of the jet mass flow rate on the drying rates in air and steam respectively It can be seen from Fig.3-21 (a) that an increase in the mass flow rate increases the maximum drying rate However the differences are small during the rising rate and final falling rate periods The small effect of impingement mass flow rate during the rising rate period when the skin is being formed and in the final falling rate period when the rate of breaking of the crust is decreased due to the high solids level is expected because in these cases the external heat transfer resistance is not rate limiting Again the maximum drying rate seems to be shifted slightly to a lower moisture content most likely due to the increased boiling activity with the higher heat flux due to a higher air mass flow rate.

With steam as the impinging medium the drying rates in Fig. 3 21 b increase with increasing jet mass flow rate over the entire range of moisture levels A clear explanation for this is not available. It is assumed that this effect is similar the effect of increasing temperature, in that the increased heat flux causes increased boiling.

3.4.5 EFFECT OF INITIAL SOLIDS LEVEL

The solids level of the black liquor sprayed into the recovery boiler varies over a wide range in the industry. It was also anticipated that at low solids level a constant rate period could be seen. The solids levels investigated were 60, 67.7 and 74 % with air as the drying medium However when steam was used as the drying medium it was seen that black liquor splashed out of the pan when the initial solids level was 60 % and hence only 67.7 and 74 % solids were studied for steam drying.

Figures 3-22 (a) and (b) show the influence of initial solids level on the drying rates of black liquor. As can be seen from Figure 3-22

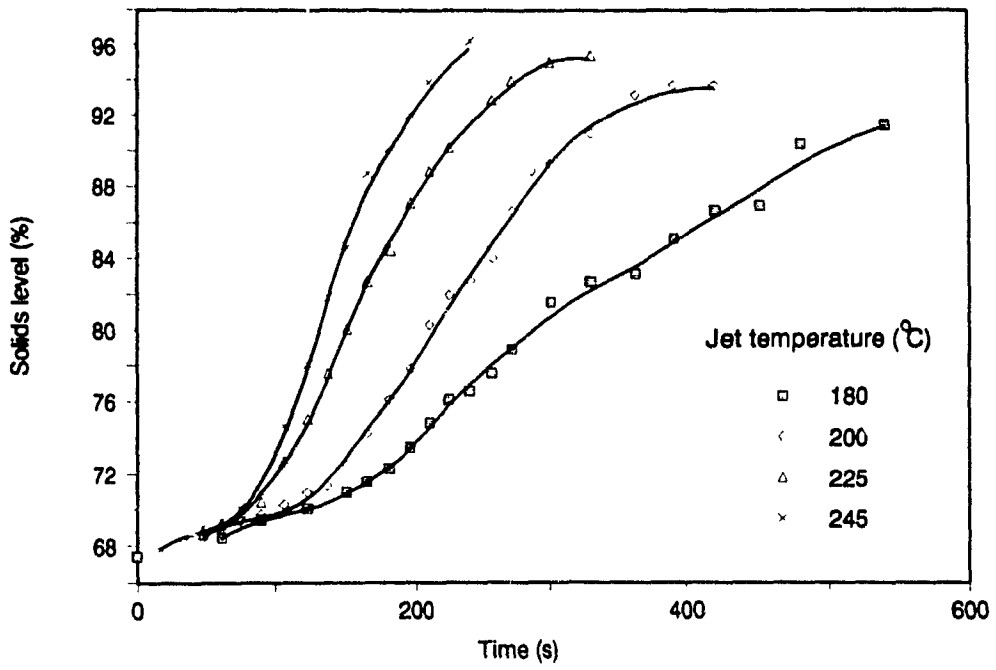

a)

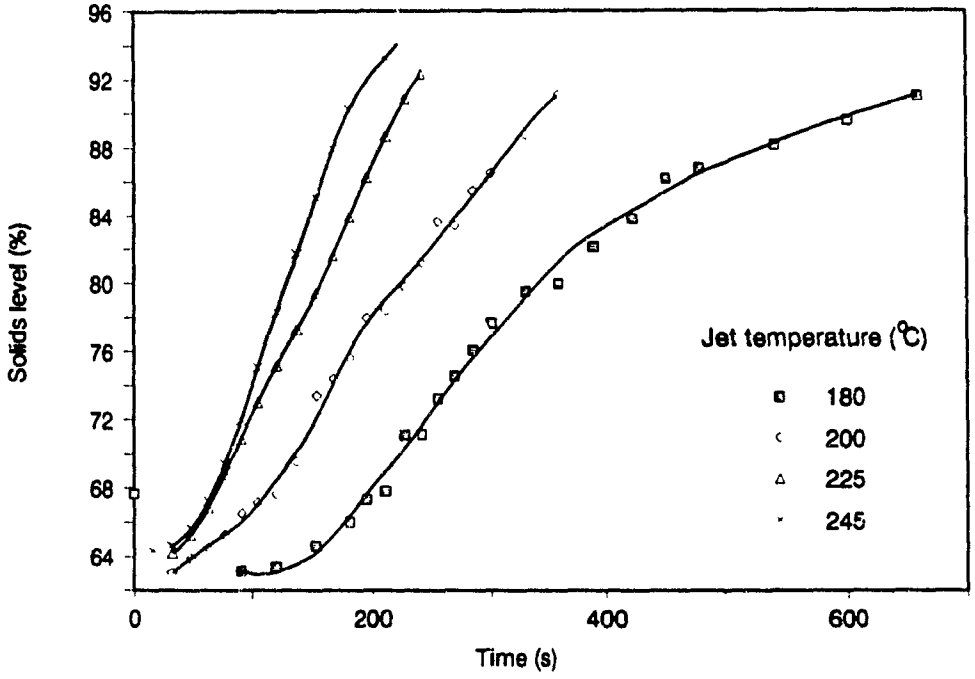

b)

Fig. 3.20 : Solids level versus time for a) air and b) steam drying.
Pan material : Titanium, Sample : 67.7% BLS
Mass flow : 0.8 kg/s m^2

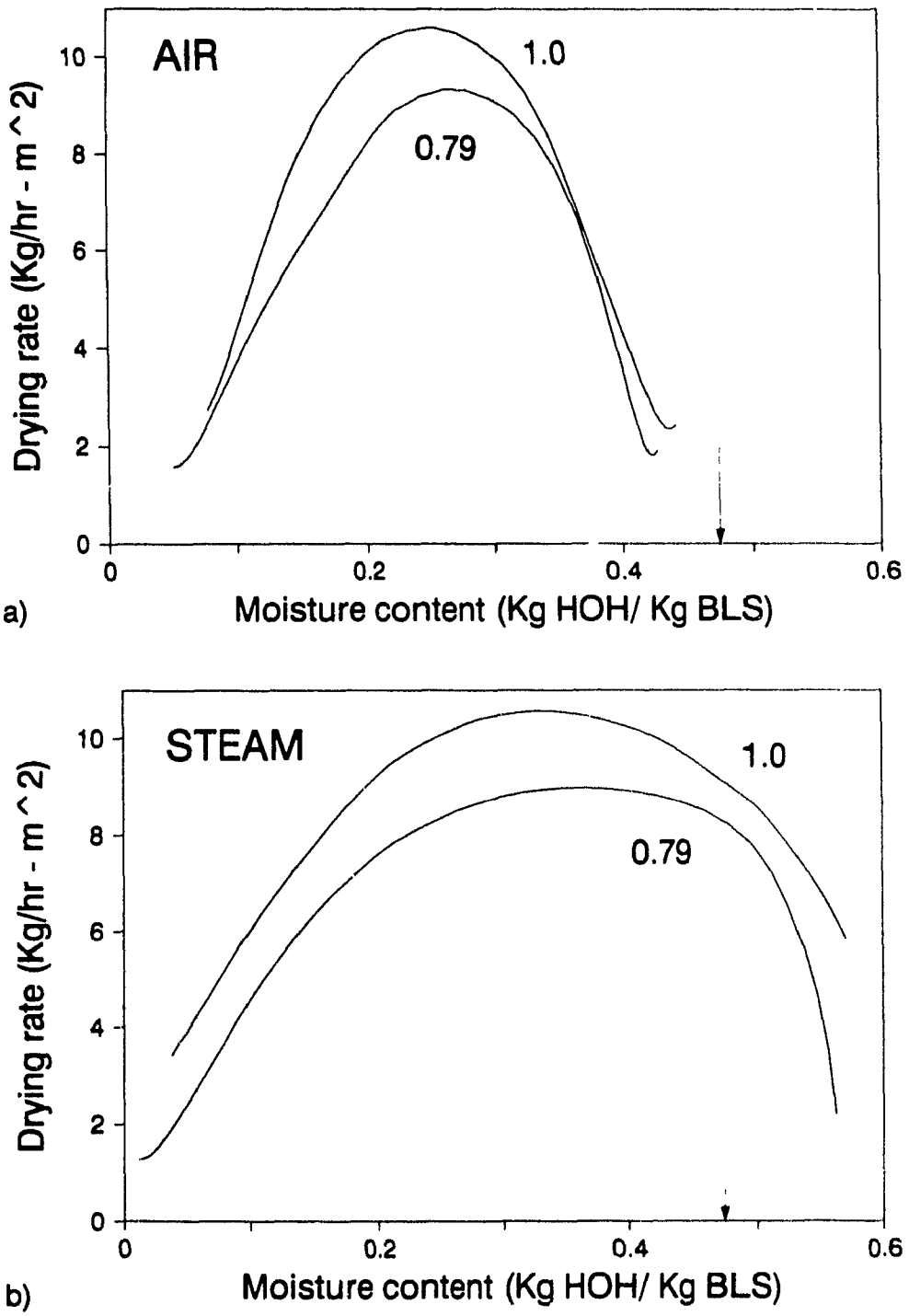

Fig. 3.21 : Influence of mass flow rate on a) air, b) steam drying
Pan material : Titanium, Sample · 67.7% BLS
Film thickness : 1.04 mm, Temperature : 225 °C

(a) the increase in solids level during air drying has two effects : [1] The shift of the drying rate moisture curves to the left persists at low moisture content, [2] the peak drying rate decreases with increase in solids level

It should be recognized that the comparisons are made at constant film thickness (1 04 mm). Hence the total amount of water which must be evaporated is larger at lower solids level. These differences can be explained by the fact that the moisture distribution in the film at the same average moisture level (after some period of drying) are different for experiments with different initial solids content Thus, if drying starts at a lower solids level, then when the total solids level reaches a higher level there is a higher concentration near the surface than the bottom This causes a more rigid crust to be formed when the experiment is started at low solids level. Thus for a given solids level in the falling rate period one would expect that the higher initial solids content would provide a higher drying rate

The same drying rate - moisture content pattern is also seen in the case of steam drying however the highest drying rate does not seem to be influenced by the initial solids level. This could be of practical significance since, it would still be desirable to have black liquor starting at the highest possible solids level. The second implication is that at higher solids content a high velocity impinging jet can be used because the viscosity of black liquor increases with solids content and less splashing (stripping in a continuous process such as a drum dryer) would occur.

3.4.6 INFLUENCE OF PAN MATERIAL

Two materials titanium and Macor (a machinable ceramic) were used as the sample holder for black liquor drying. Macor was chosen to decrease the heat loss through the pan bottom. However, even Macor has as thermal conductivity higher than black liquor. Hence significant improvement was not observed. The Fig. 3-23 (a) and (b) show the water

loss versus time curves for the two pan materials in air and steam respectively. As can be seen from Figure 3-23 (a) the sample holder material does not seem to have any influence on the water loss curves when air is used as the drying medium It can be also seen from Figure 3-23 (a) that the temperatures of the black liquor film are very similar with time.

When steam is used as the drying medium, as shown in Figure 3-23(b) there are two distinct features between titanium and Macor First, the amount of water absorbed when Macor is used as the pan material is higher than for titanium This can be attributed to the pan being introduced cold into the hot drying chamber. Since the thermal diffusivity of titanium is lower the titanium pan heats up faster (in turn heating the black liquor) than Macor. As a result the amount of water which condenses is higher in Macor than titanium The second feature to be observed is that the water loss curve of Macor "catches up" with that for titanium This can be evinced from both the weight loss curves (Figure 3-23 (b)) and temperature curves (Figure 3-24(b))

It can be summed that the experiments with the two materials did not indicate a significant improvement in the analysis of data The best solution to overcome the heat loss condensation factors would be to design an equipment which could introduce the black liquor close to the boiling point.

3.4.7 DRYING OF CARBOXY-METHYL CELLULOSE AND INDULIN C

The drying characteristics of CMC (carboxy-methyl cellulose) and Indulin C were investigated to obtain a better understanding of the behavior of black liquor, particularly swelling Black liquor contains about 60 % organic material (primarily cellulose and lignin) CMC (from Aqualon, CMC 7M) was dissolved in distilled water to obtain a 10 % solution. It should be recognized that the initial solids level for CMC solution was lower than that for black liquor because dissolving higher levels of CMC was difficult and the viscosity of CMC rises very high due

to the high molecular weight of CMC. There was no swelling behavior observed during CMC drying

Indulin C was obtained from Westvaco Corp. Indulin C is lignin precipitated from black liquor by acidification. Indulin C suspension was prepared by dissolving it (obtained as a powder) in hot alkali. Indulin C on drying exhibited extensive swelling, and the swollen structure did not collapse (as it did for black liquor) It is hence *suggested* that the lignin in the black liquor provides the strength for the crust to swell, and that it plays an important role in the formation of the film A physical picture of lignin drying behavior is presented in Fig 3-25

3.4.8 INFLUENCE OF NaOH, OXIDATION, AND Na_2SO_4 ON DRYING OF BLACK LIQUOR

This study was undertaken primarily to provide data which would be useful for work at the Institute of Paper Science and Technology, Atlanta Professor Clay who has advocated the use of a fluidized bed dryer (Clay 1984) suggested that for such an operation it is imperative that the inorganic load in black liquor (either as Alkali or Sulfate) should be high It has been established that oxidation of black liquor results in an increase in the viscosity of black liquor (Grace 1984). It was attempted to study the influence of oxidation on the drying behavior, since some industries would be interested to meet the environmental requirements (oxidation leads to low sulfur emissions). The addition of the NaOH and Na_2SO_4 did not influence the drying rates to any significant degree in either air or steam

The influence of black liquor oxidation on drying rates is depicted in Fig 3-26 a,b. It has been proposed that the oxidation of black liquor is primarily the oxidation of Na_2S to Na_2SO_4 The oxidation of black liquor is seen to increase the viscosity of the black liquor due to the decrease in active alkali and hence the precipitation of lignin. The oxidation of black liquor is also believed to decrease the boiling

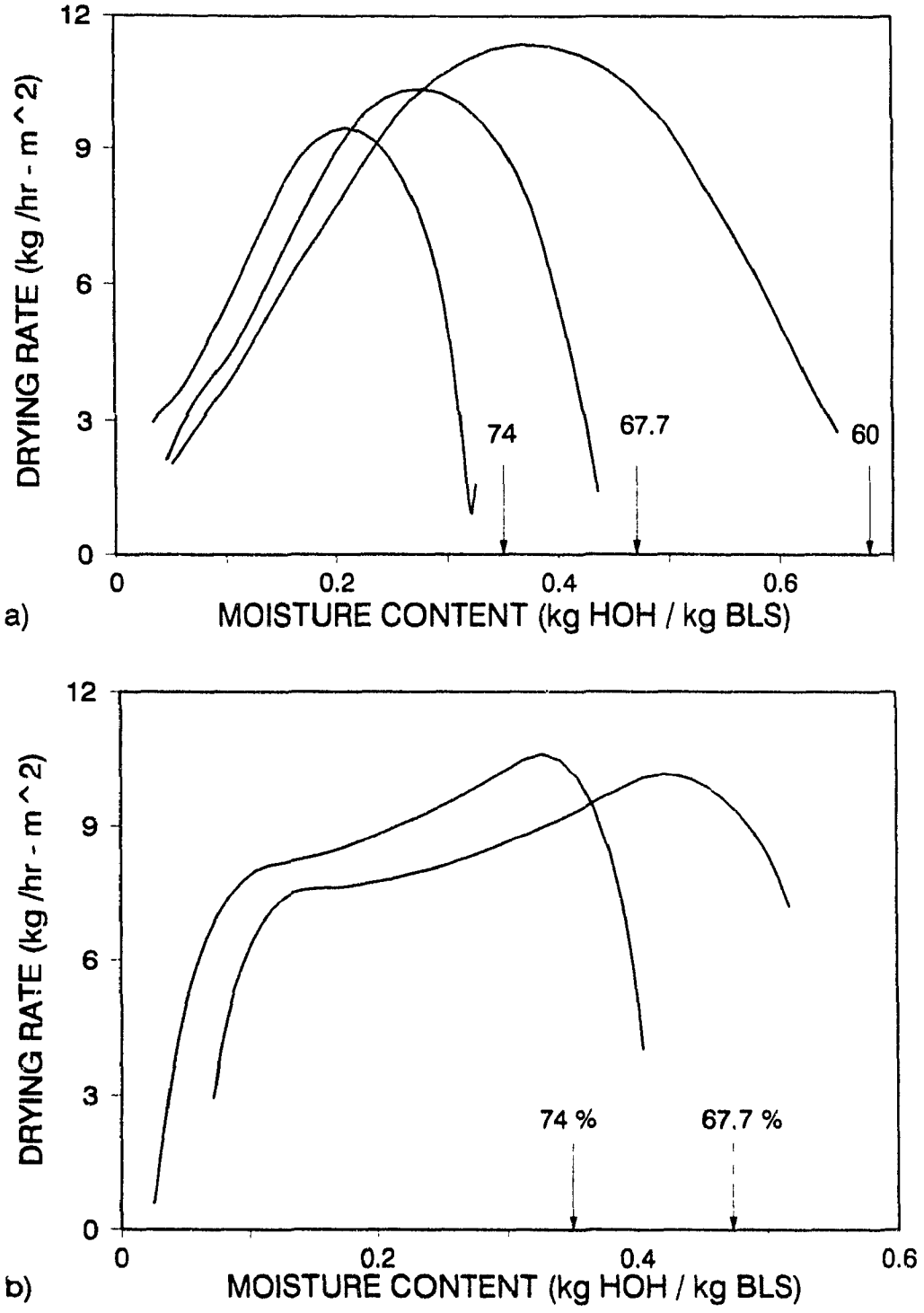

Fig. 3.22 : Effect of initial solids level on a) air, b) steam drying rates. Pan material : Titanium, Mass flow rate : 0.8 kg/s m^2 Film thickness : 1.04 mm, Temperature : 225 C.

point rise (Clay 1986). This would cause the evaporation of oxidized liquor to be faster than unoxidized in superheated steam since less heat is required to raise and maintain the film at a high temperature. Based on the previous discussion on the behavior of black liquor however, the increased viscosity of black liquor, which is caused due to the precipitation of lignin will cause the crust formed during air drying to be predominant. Hence oxidation of black liquor will result in a decrease in air drying rate.

Hence oxidation of black liquor is believed to contribute differently in air and steam drying. In steam drying the oxidation of black liquor will have a positive effect (higher drying rates) where as in air drying will have a detrimental effect (lower drying rates).

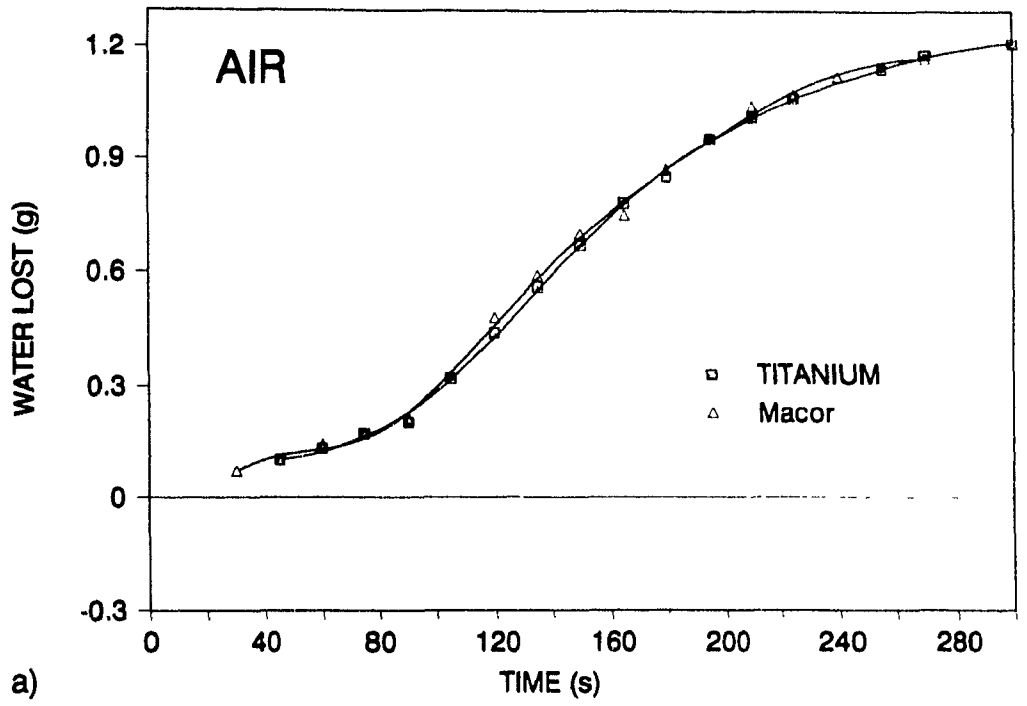

a)

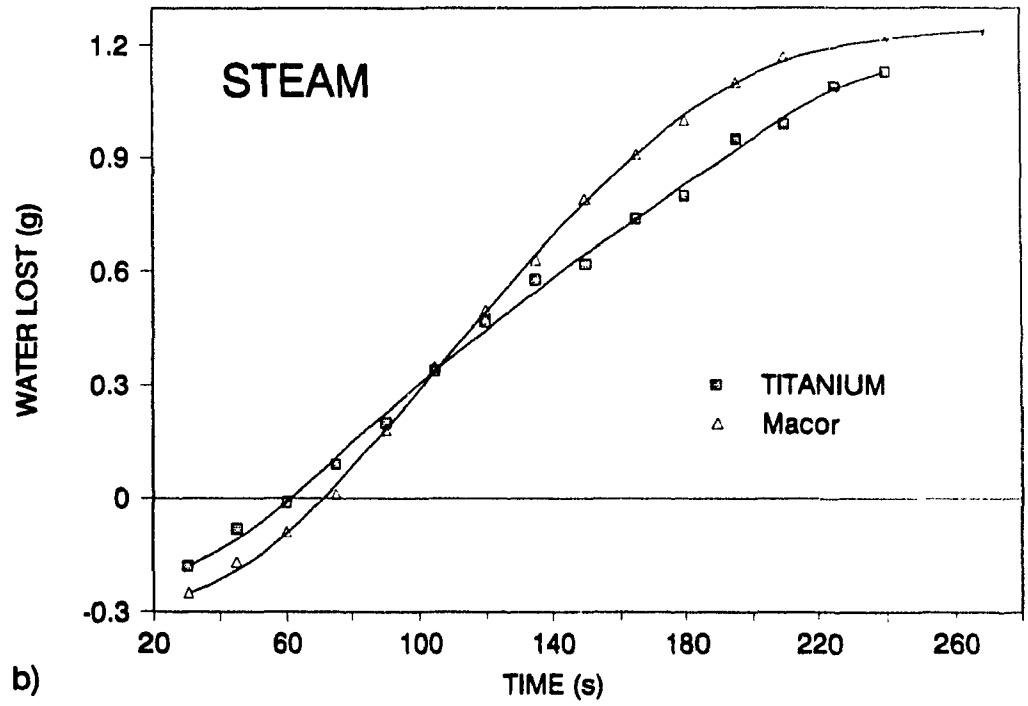

b)

Fig 3.23 : Influence of pan material on water loss. a) air, b) steam drying.

Sample : 67.7% BLS, Mass flow : 0.8 kg/s m^2

Film thickness : 1.04 mm, Temperature : 225°C

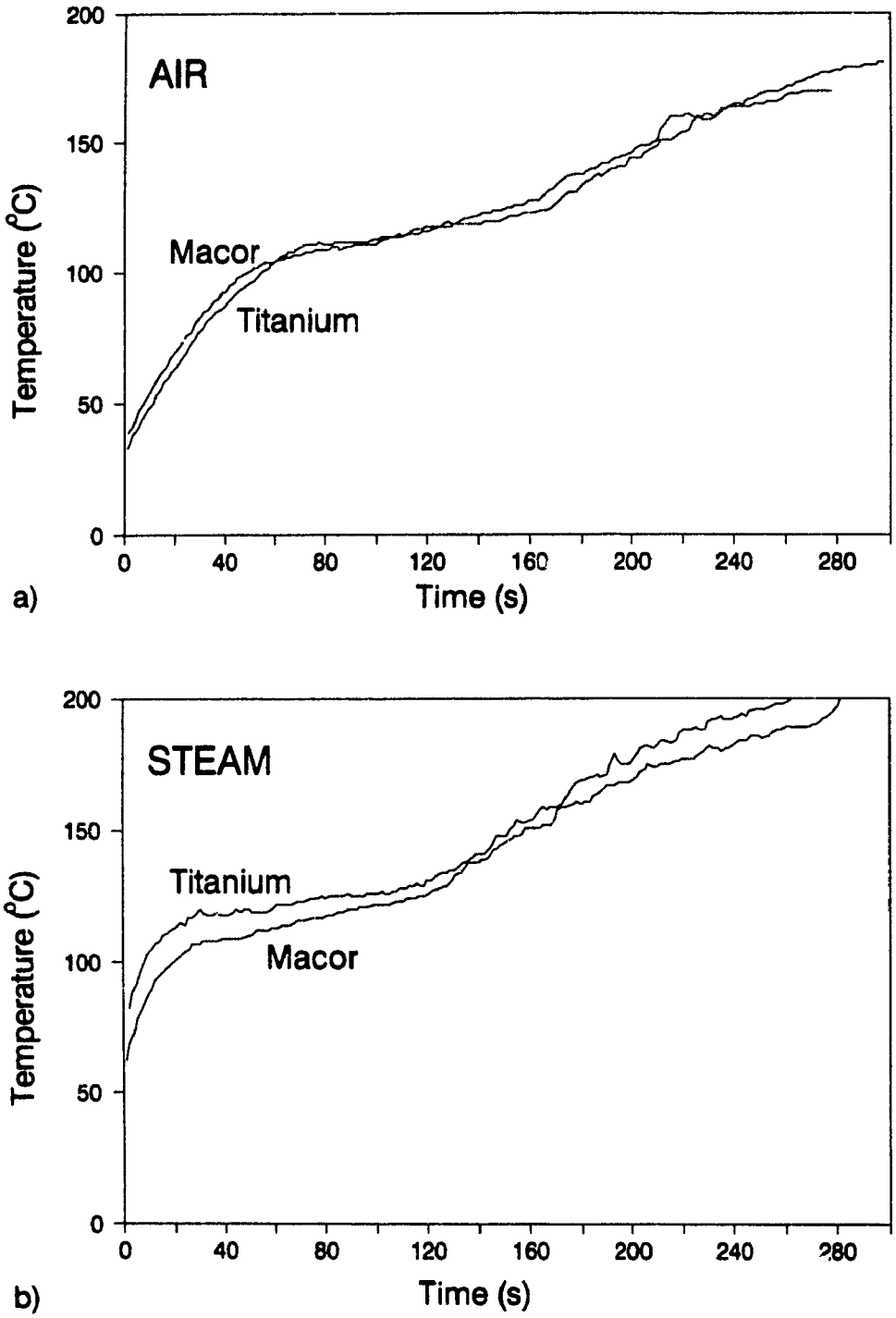

Fig 3.24 : Influence of pan material on film temperature. a)air, b)steam drying.
Sample : 67.7% BLS, Mass flow : 0.8 kg/s m^2
Film thickness : 1.04 mm, Temperature : 225°C.

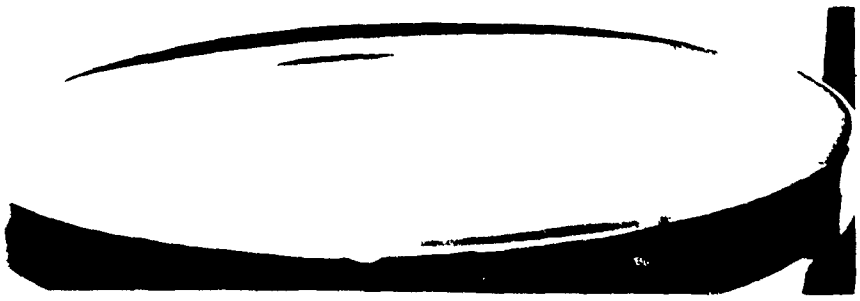

Before drying

Immediately after drying

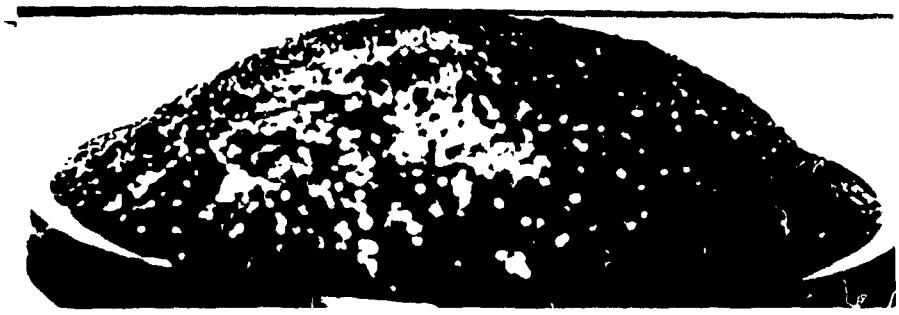

1 hr after drying

Section of crust cut away

Fig. 3.25 : Physical appearance of lignin during drying.

3.5 CITED REFERENCE

Bergström, H.O.V, K G Trobeck : "Process of Utilizing Waste Liquors". U.S. Patent 2,406,581, Aug 27, 1946.

Charlesworth, D.H., W.R. Marshall Jr : "Evaporation from drops containing dissolved solids". AIChE J. 6(1) pp 9 -23 (1960).

Clay, D.T., T.B. Cartwright . "Method of drying Pulping Liquor to a Burnable Solid". U.S. Patent 4,619,732, Oct. 28, 1986.

Croll, S.G : "Drying of Latex Paint". J. Coat. Tech. 58(734) pp 41-49 (1986).

de Boor, C : "A Practical Guide to Splines". Springer-Verlag. pp 235-275, (1978).

Delir, L., O. Wennberg : "Methods of obtaining High Concentration Black Liquor". International Energy Agency Research Project - Annex 1 (1983).

Dolinsky, A.A , G.K. Ivanitsky : "Heat and mass transfer on the interface at evaporation of fluid drops in air and superheated vapor" Proceedings of Int. Drying Symposium, Versailles PC 51-58 (1988).

Geankoplis. C.J . "Transport Processes and Unit Operations". Second Edition Allyn and Bacon Inc pp 539 (1983).

Klaus, R L , H C Van Ness : "An Extension of the Spline Fit Technique and Applications to Thermodynamic Data" AIChE J. 13(6), pp 1132-1136, (1967).

Kubes, G J : "Effect of wood species on Kraft Recovery Furnace Operation". CPPA Ann Mtg, 19-25 (1983).

Moyers Jr., C.G : "Drying of solution droplets in superheated vapor". Proceeding of the First International Symposium on Drying. Ed. A.S Mujumdar, pp 224-229 (1978).

Othmer, D.F : "The Condensation of Steam". I&E C, 21(6), pp 576-583 (1929).

Weber, M.E : "Class notes : 302-621B", McGill University (1989).

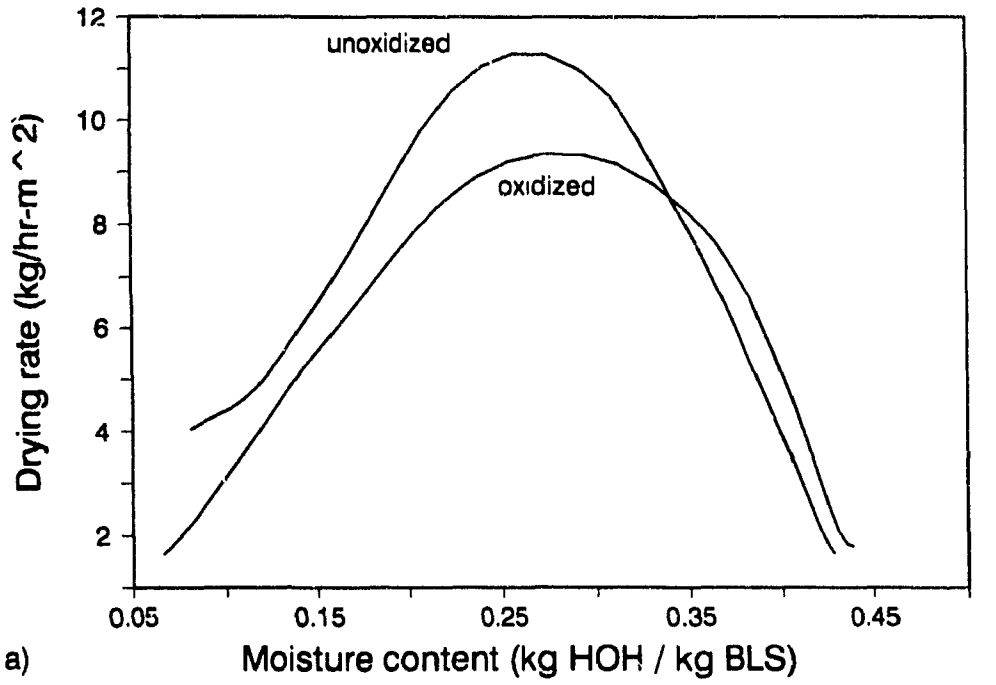

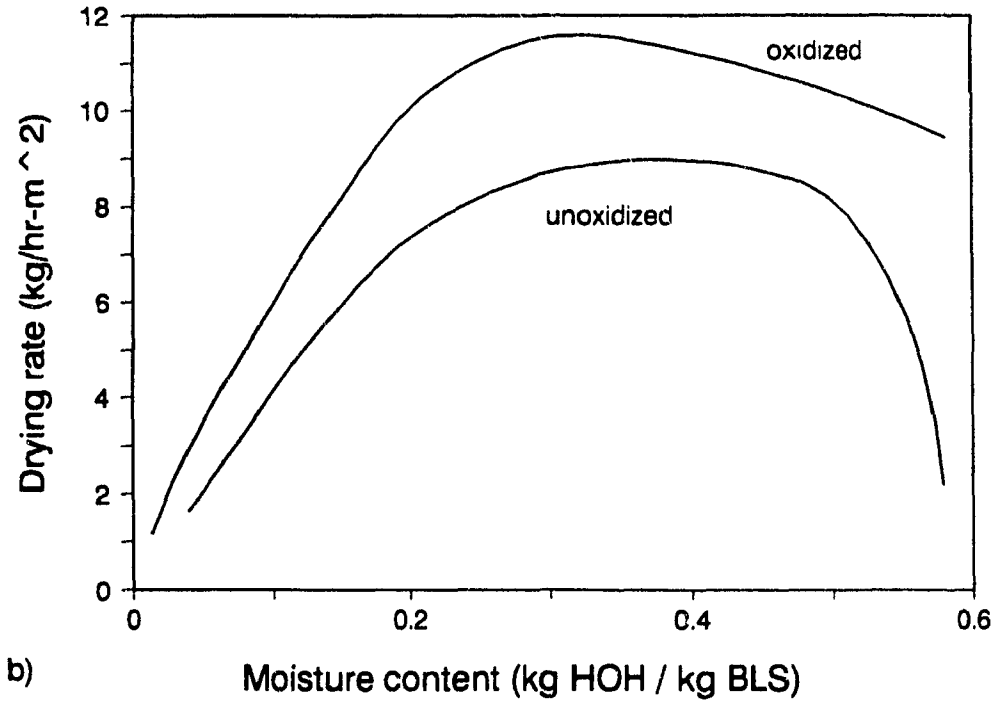

Fig 3.26 : Influence of oxidation on black liquor drying.
a) air, b) steam drying.

CHAPTER IV

MATHEMATICAL MODEL FOR SUPERHEATED STEAM DRYING

4.1 INTRODUCTION

The experimental results of drying black liquor were presented in Chapter III of this thesis The moisture contents reported there as a function of time represented the average values in the film of black liquor from which the drying rates were calculated. While in practical operation, the black liquor and the supporting surface will be preheated to the drying temperature, in the experiments the pan and black liquor were introduced into the drying chamber at room temperature This caused condensation of steam on the black liquor surface. In order to evaluate these equipment specific effects on the drying rates it was decided to simulate the experiments In addition, the simulation would also lead to a better understanding of the black liquor drying process.

The detailed numerical simulation of superheated steam drying of solutions has not been attempted before. Scientifically, the problem of superheated steam drying is interesting, since it presents sharp gradients in concentration and temperature, a moving boundary, a coupled boundary condition, and nonlinear physical properties which lead to coupling of the transport equations. The coupled boundary condition which sets the surface temperature at the boiling point rise temperature as determined by the solids level at the surface, is perhaps a unique feature of this study.

4.2 LITERATURE REVIEW

Numerical studies of superheated steam drying have been reported before. However most of these investigations pertained to evaporation where external heat transfer was the limiting factor.

Chow and Chung (1983 a,b) studied the evaporation of water from a flat plate into laminar and turbulent streams of air, humid air and superheated steam. They estimated the heat transfer coefficient on the surface from empirical correlations for flow over a flat plate. The correlations were corrected using Spalding's Couette flow approximation to account for the effect of cross flow due to evaporation. All the thermophysical properties of the gas phase were evaluated at a reference temperature, T_R, using the one third rule :

$$T_R = T_o + \frac{1}{3} (T_\infty - T_o) \qquad (4\text{-}1)$$

where T_o is the temperature of the water surface, and T_∞ is the bulk temperature of the drying gas. Good agreement with the experimental results was obtained including the prediction of an inversion temperature of about 190°C.

Hasan, Taleb and Mujumdar (1986,1987) performed a theoretical study of evaporation of liquids into their own vapors where the liquid surface was moving cocurrently with the vapor. They used parameters similar to those of Chow and Chung (1983 a) and got parallel results

Dolinsky and Ivanitsky (1988) studied the heat and mass transfer during evaporation of fluid drops in air and superheated vapor They erroneously concluded that the rate of evaporation of pure liquid drops in superheated vapor should always be lower than that in air because the temperature driving force is lower in vapor than in air at the same operating conditions Though they mention about the formation of a crust on the surface of the droplets and hence imply the presence of dissolved solids, they do not include a boiling point rise equations in their analysis. Further more they do not give the methodology used for solving the heat and mass balance equations

Moyne, Stemmelen and Degiovanni (1990) studied the evaporation of

water from an unsaturated porous medium using air and steam as the drying media They included three driving forces in their model the temperature gradient, the humidity gradient, and the total pressure gradient in the gas phase When modeling drying in superheated steam their boundary condition for the moisture flux at the gas solid interface became indeterminate To get around this problem, they included a small amount of noncondensables into the vapor stream.

A number of process modeling calculations also have been made dealing with the feasibility of the superheated steam drying process in terms of cost, and capacity (Cui and Mujumdar, 1985). However, these studies fall outside the scope of the present investigation.

4.3 ANALYSIS OF THE PROBLEM

The concentration of black liquor / solutions in an environment of superheated steam is fairly complicated in terms of the boundary conditions The physics of the problem will be briefly described and analyzed before presenting the relevant transport equations and boundary conditions

The problem is schematically described in Fig. 4.1. The thickness of the black liquor film is about 1 mm thick. The width of the film along the sample holder is about 6 cm radius, and in the case of the proposed industrial drier it will be even wider. Hence it is assumed that the problem is one dimensional with gradients only in the depth of the film.

The heat supplied by the impinging jets is used to a) evaporate water from the black liquor, and b) to raise the temperature of the black liquor film A certain amount of heat is lost from the bottom of the sample to the atmosphere due to radiation and natural convection.

As described in Chapter II, the sample is at room temperature when

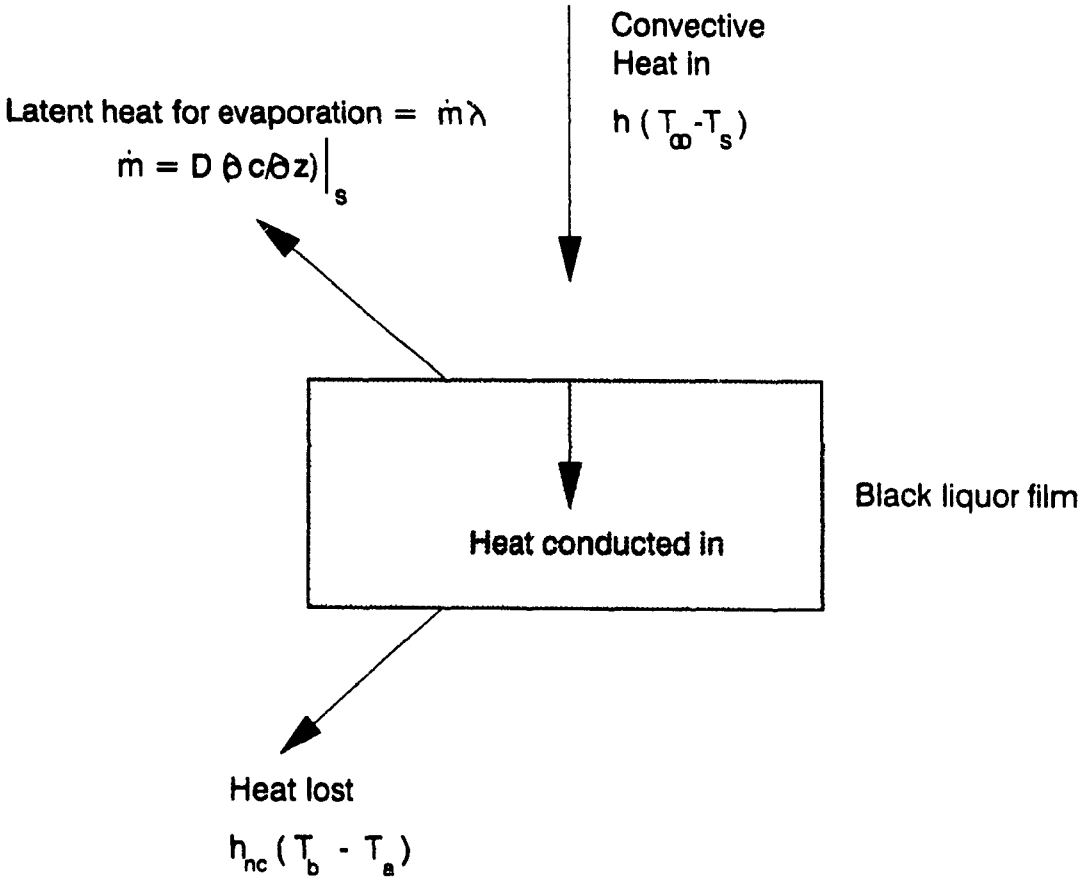

Fig. 4.1 : Schematic of heat and mass balance for the black liquor film.

inserted into the drying chamber. Hence when the steam impinges on the surface of the black liquor film a certain amount will condense on the surface. The rate of heat transfer,q, released during condensation is given by (Maa, 1970) :

$$q = \sqrt{\frac{R}{2 \pi M}} \quad \frac{dP}{dT} \quad (T_v^{3/2} - T_l^{3/2}) \qquad (4\text{-}2)$$

where T_v and T_l are the absolute temperature of the vapor and liquid, M is the molecular weight, R is the gas constant, and dP/dT is the slope of the vapor pressure curve. When experimental values of the heat transfer were substituted together with other quantities, the temperature difference across the interface was found to be very small and thus the heat transfer resistance was negligible *" In fact there is no limit to the rate at which pure steam will condense but the power of the surface to carry off the heat "* (Othmer 1929). Hence the amount of steam condensed corresponds to the difference between the amount of heat that can be conducted away and the amount of heat entering the film due to the heat transfer from the impinging jets, i.e.·

Heat released due to condensation	=	Heat that can be conducted into the black liquor film.	-	Convective heat transfer due to impinging jets.

or

$$\dot{m}_{cond} \lambda = k \, (\partial T/\partial z)\big|_{z = 0} - h \, (T_{inf} - T_s) \qquad (4\text{-}3)$$

where $\dot{m}_{cond}$ is the condensation rate, λ is the latent heat of vaporization at the surface temperature, k is the thermal conductivity of black liquor, z is the direction into the film (surface z = 0), "h" is the external heat transfer coefficient, T_{inf} is the jet temperature, and T_s is the surface temperature in equilibrium with the liquor solids content at the gas liquid interface. When condensation occurs, there will be an increase in the film thickness while the moisture content at the surface will also increase (solids concentration will decrease).

Once the ability of the black liquor film to carry away the heat becomes less than the convective heat supplied by the impinging jets, condensation will stop and evaporation will begin At this moment the moisture content at the surface will be higher than that inside Hence internal mass transfer will not be the rate limiting factor and the drying rate will be controlled by external heat transfer. This behavior is similar to that of the constant rate drying period However it is not a true constant rate period because the solute concentration increases, resulting in an increase in the film surface temperature as demanded by the boiling point rise Thus the driving force (T_{inf} - T_{surf}) will decrease monotonically, and the amount of water removed is given as

$$m_{evap} * \lambda = h (T_{inf} - T_s) - k (\partial T/\partial z)\big|_{Z=0} \qquad (4\text{-}4)$$

After some time the water concentration gradient at the surface becomes significantly large so that internal diffusion will be the limiting factor for water removal Hence in this case the evaporation rate is calculated from the product of the diffusivity and moisture gradient at the film surface and the heat flux entering the film is given by .

Heat flux conducted into the film = Heat entering in due to impinging jets - Heat for evaporation

$$k (\partial T/\partial z)\big|_{z=0} = h (T_{inf} - T_s) - m_{evap} \lambda \qquad (4\text{-}5)$$

Equation 4-5 is the same as equation 4-4, however it is rearranged to highlight the fact that in equation 4-4 the external heat transfer is the limiting factor, while in equation 4-5 internal mass transfer is the limiting factor for evaporation.

The drying behavior of black liquor in superheated steam is shown schematically in Fig. 4.2 (a - e) Initially the entire film is at a uniform temperature and moisture content as shown in Fig. 4.2 a As the film enters the drying chamber, there is a certain amount of condensation on the surface. This causes the surface temperature to increase to the boiling point Due to condensation on the surface, the solids content of the surface decreases and the thickness of the film increases. It should be noted that the sharp concentration gradient near the surface is a potential source of numerical instability.

As water evaporates from the surface, the concentration gradient at the surface changes sign and the surface concentration is lower than inside the film With further evaporation the surface moisture content progressively decreases and internal diffusion of moisture becomes the rate limiting factor (Fig. 4-2 d,e) The film thickness also decreases as the film dries

Hence it is apparent that the drying problem is a moving boundary problem with sharp gradients in temperature and moisture content. Further for most liquids/slurries, the thermal conductivity and mass diffusivity are very strong functions of moisture content (variations of two or three orders of magnitude) and temperature The physical picture given above presents a challenging problem in terms of numerical solution

4.4 MATHEMATICAL MODELING

The pertinent equations and boundary conditions which describe the problem will now be presented

The appropriate form of the unsteady one dimensional energy balance is .

$$\rho c_p \left(\frac{\partial T}{\partial t} \right) = \frac{\partial}{\partial z} \left(k \frac{\partial T}{\partial z} \right) \qquad (4\text{-}6)$$

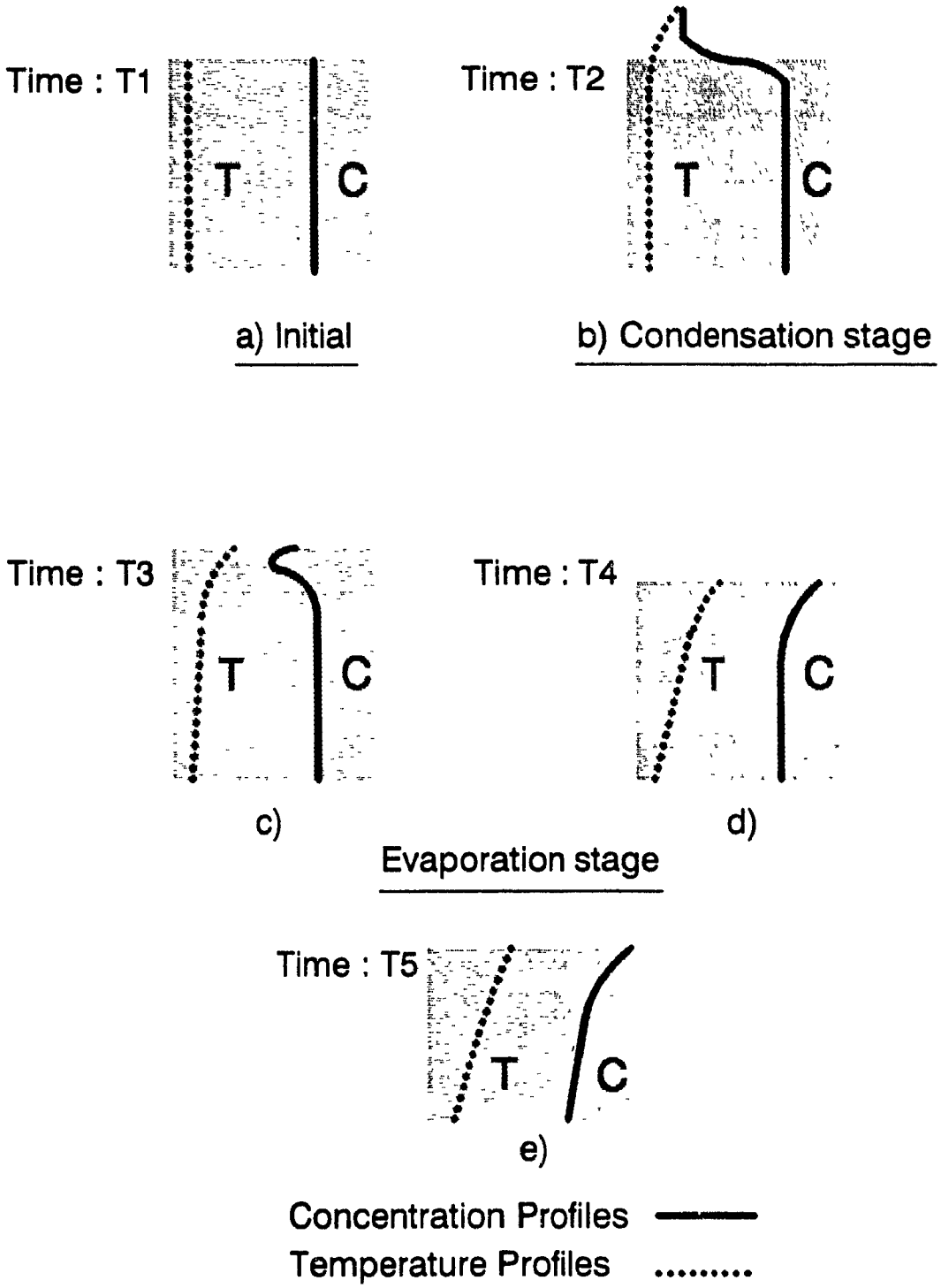

Fig.4.2 : Schematic of temperature and concentration profiles during condensation and evaporation in superheated steam drying.

and that for mass balance

$$\left(\frac{\partial \rho_s X}{\partial t} \right) = \frac{\partial}{\partial z} \left(\mathbb{D} \frac{\partial \rho_s X}{\partial z} \right) \qquad (4\text{-}7)$$

where ρ is the density of black liquor (kg of black liquor/m^3) and ρ_s is the density of black liquor solids (kg of BLS/m^3), c_p is the specific heat, t is the time and $\mathbb{D}$ is the diffusivity of water in black liquor.

The coordinate system is chosen such that the surface is z=0 and the bottom of the film is z = s(t) The location of the bottom of the film is a function of time because the thickness of the film changes due to condensation and evaporation. The problem described above is further complicated if the presence of the pan is taken into account. Since there is no transfer of mass in the region of the pan the diffusivity and concentration of water in the pan should be set to zero. This solution procedure leads to a discontinuity in the concentration profile at the node on the interface between the pan and the black liquor film. Attempts to solve this more realistic situation were unsuccessful and will not be reported here.

4.5 BOUNDARY CONDITIONS

The boundary conditions for the heat and mass balance equations are now presented. First the film bottom boundary conditions are described.

At the interface between the black liquor and the supporting surface there is no mass transfer so

$$[\mathbb{D} (\partial \rho_s X / \partial z)] = 0. \qquad (4\text{-}8)$$

There is a small heat thermal loss from the bottom surface due to natural convection and radiation. They are combined into a convective loss with a heat transfer coefficient of 10 W/m^2K (This was assumed to

be an order of magnitude suggested by Bird et al., (1960). This convective loss is essential because if this is not accounted, then the film temperature approaches the jet temperature very fast.

$$k \left.\frac{\partial T}{\partial z}\right|_{z = s(t)} = h \left(T_{s(t)} - T_{room} \right) \qquad (4\text{-}9)$$

where h_{nc} is the heat transfer coefficient and $T_{s(t)}$ is the temperature at the bottom of the black liquor film.

At the black liquor free surface, z = 0, the following boundary conditions are used :

The temperature and moisture concentration are linked by the boiling point rise equation (Robinson and Clay, 1986) :

$$\text{Moisture content (\%)} = 54.678 \; e^{-0.046\, T} \qquad (4\text{-}10)$$

where T is the superheat in degrees Celusius. Superheat is defined as the equilibrium temperature (film surface) - the boiling point of water (atmospheric pressure here).

The other boundary condition is obtained from a heat balance, linking the temperature and moisture gradients on the film surface. The balance is expressed in form of either equations 4-4 or 4-5.

$$\mathbb{D}\left(\frac{\partial \rho X}{\partial z}\right)\Big|_{z=0} * \lambda = \dot{m}_{evap} * \lambda = h \, (T_{inf} - T_s) - k \left(\partial T/\partial z \right)\Big|_{z=0} \qquad (4\text{-}4)$$

$$k \, (\partial T/\partial z)\Big|_{z=0} = h \, (T_{inf} - T_s) - \mathbb{D} \left(\frac{\partial \rho X}{\partial z} \right)\Big|_{z=0} * \lambda \qquad (4\text{-}5)$$

Equation 4-10 with the moisture content in explicit form is used together with equation 4-5. Equation 4-4, on the other hand, is used with the form of equation 4-10 whereby the temperature is explicit.

The choice of which pair of boundary conditions to use, depends on whether the drying process is external heat or internal mass transfer controlled. If the drying process is limited by external heat transfer, then the moisture gradient inside the black liquor film at the interface is small. In this case the temperature at the surface is calculated from the boiling point rise equation 4-10. The water mass flux and hence the moisture content at the surface are subsequently calculated from equation 4-4. In other words, in the iterative numerical procedure the film temperature is calculated first while the moisture content is determined next.

If the internal mass transfer is the rate limiting factor then the black liquor moisture gradient at the film surface is relatively large. In this situation the surface moisture content is calculated first using equation 4-10, and the film temperature is subsequently determined from equation 4-5.

It should be recognized that since the equations 4-4 and 4-5 are the same, the converged solution should be the same irrespective of the solution procedure. However, only by adopting the above described solution method a converged solution could be obtained in all cases.

The initial conditions are :

$$T\,(z,0) = 30^{\circ}C \qquad (4\text{-}11)$$

$$X\,(z,0) = 0.429 \text{ kg water / kg BLS} \qquad (4\text{-}12)$$

A flow sheet showing how the boundary conditions are incorporated

in the solution procedure is given in Fig 4.3.

The thickness of the black liquor film, s(t), is increasing or decreasing due to condensation or evaporation of water respectively. The rate of change of film thickness is determined by the water transfer rate as

$$\frac{d\,s(t)}{d\,t} = \dot{m}_{\substack{evap \\ cond}} / \rho_w \qquad (4\text{-}13)$$

$$s(0) = \text{constant} \qquad (4\text{-}14)$$

The density was assumed to be a constant for calculation of the moving boundary for each iteration by calculating the density from the previous iteration.

4.6 NUMERICAL PROCEDURE

The properties of the black liquor, namely, heat capacity and density, are taken from published data (Hough, 1986). The thermal conductivity was measured (Chapter V). A rough estimate of effective diffusivity was obtained using the drying data obtained at relatively low jet temperature where there was no boiling observed visually (described in Appendix IV).

$$\rho = 1007 - 0.495\,T + 600/(1+X) \qquad kg / m^3$$

$$c_p = 0.98 - 0.52 / (1+X) \qquad Kcal/kg^oC$$

$$k = 0.01\,[\,1.36 - 0.65/(1+X) + 0.003*T\,] \qquad Kcal/m\ s^oC$$

$$\mathbb{D} = 0.028 * \exp(-9500/(273+T)) * \exp(20.4 * X)$$

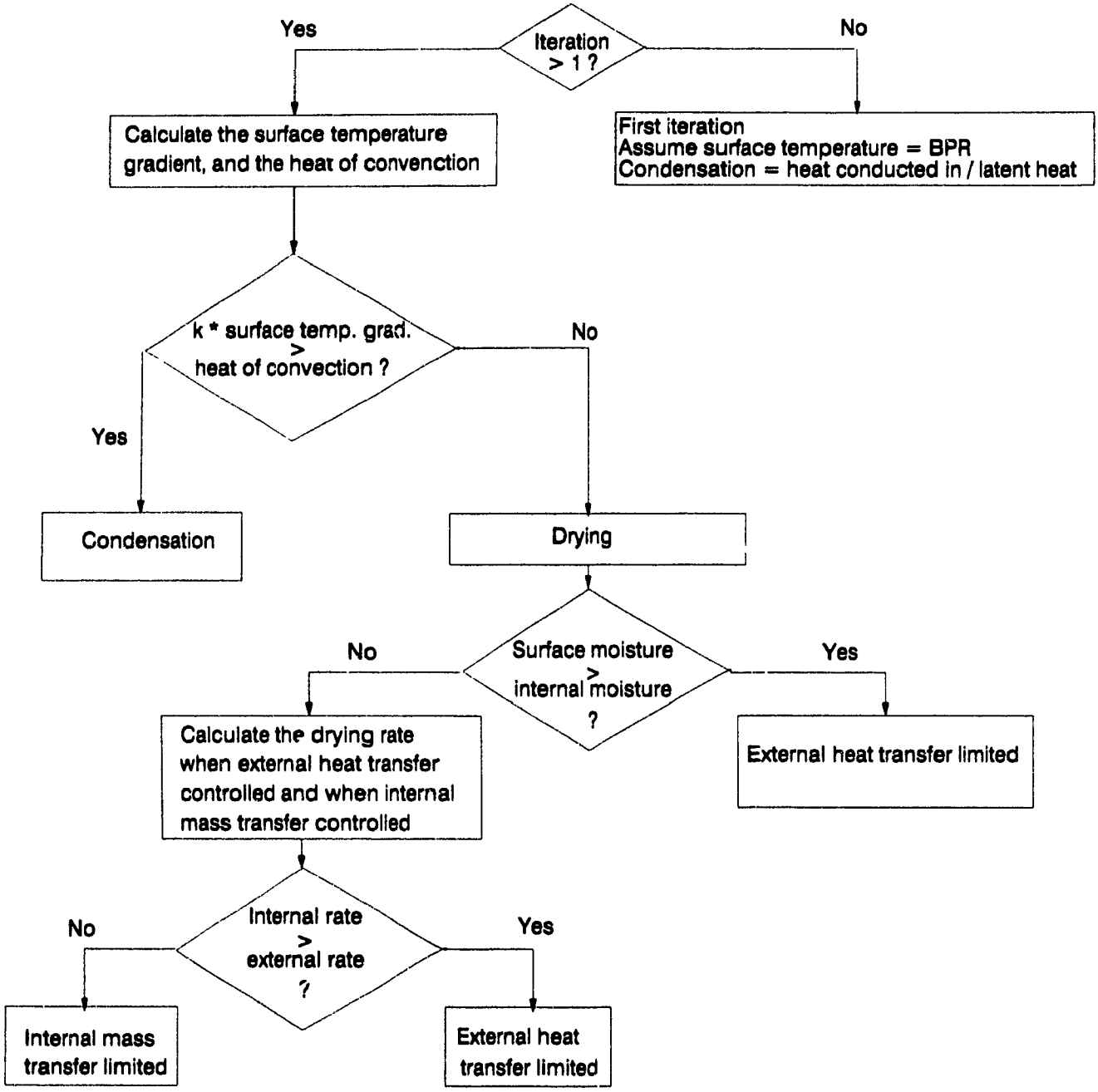

Fig. 4.3 : Flowsheet for selection of surface boundary condition calculation procedure.

The finite element method (FEM) was used as the numerical technique. FEM is a general technique of constructing approximate solution to boundary value problems. This method involves dividing the domain of solution into a finite number of simple elements, and using variational principles obtain an approximate solution over the region of interest. A Petrov-Galerkin (upwind finite element) method was used for the solution of the present problem. An adaptive mesh was implemented to capture the sharp concentration gradients. Details of the Galerkin FEM are given by Becker et al (1981) and Rey (1989).

The energy balance equation 4-6 will be taken to highlight the features of the numerical problem. A variational formulation of equation 4-6 is :

$$\text{Residual } \langle R, \phi^i \rangle = \int_0^{s(t)} \left[\rho c_p \frac{\partial T}{\partial t} - \frac{\partial}{\partial z} k \frac{\partial T}{\partial z} \right] \phi^i dz = 0 \qquad (4\text{-}15)$$

where ϕ^i is the weight function
and R is the residual.

The Galerkin method consists of seeking an approximate solution to the above formulation in a finite-dimensional subspace (elements) of the overall space 0 · s(t). This is done by approximating the actual solution with admissionable functions (in each element), rather than solving for the whole space by a single expression

Let T_a be the approximate solution and given as :

$$T_a = \sum T_j \phi^j(x) \qquad (4\text{-}16)$$

where T_j is the value at a particular node
and ϕ^j is the basis function.

The basis functions used in the Galerkin formulation are *chapeau* functions (linear basis function). The weight functions (ϕ^i) and the basis functions (ϕ^j) are taken to be equal in the Galerkin finite element formulation.

Equation 4-15 can be recast in the following form :

$\langle R, \phi^i \rangle$ = Forcing vector = **F** =

$$\int_0^1 \rho c_p \frac{\partial T}{\partial t} \phi^i dz - \left\{ \phi_z^i \, k \, \frac{\partial T}{\partial z}\Big|_0^{s(t)} - \int_0^1 k \frac{\partial T}{\partial z} \frac{\partial \phi^i}{\partial z} dz \right\} \tag{4-17}$$

It should be recognized that here the formulation is segmented to account for each element. However the boundary conditions apply only over the real space : i.e., the first and last element. The forcing vector (load vector) and the Jacobian matrix (stiffness matrix) are first assembled

The Jacobian matrix $\underline{\underline{J}}$ is obtained by taking the derivative of the forcing vector with respect to the dependent variable (T in this case).

$$\underline{\underline{J}} = \int_0^1 \rho c_p \frac{\phi^j \phi^i}{\Delta t} dz + \int_0^1 k \frac{\partial \phi^j}{\partial z} \frac{\partial \phi^i}{\partial z} dz \tag{4-18}$$

After assembling the forcing vector and the Jacobian matrix, the solution vector is obtained as

$$\mathbf{CT}^{k+1} = \mathbf{CT}^k + \underline{\underline{J}}^{-1} \mathbf{F} \tag{4-19}$$

$\| \underline{\underline{J}}^{-1} \mathbf{F} \|$ is measured as the error. At each time step the solution is assumed to be converged if $\| \underline{\underline{J}}^{-1} \mathbf{F} \|$ obtained is smaller than 10^{-4}. The time step was incremented depending on the difference of the solution

from the predicted solution (based on the norm of the difference between the predicted and the corrected value after iteration)

4.7 MESH GENERATION SCHEME

As mentioned earlier this problem is characterized by very sharp concentration gradients. One way to approach this problem is to use exceedingly small time steps and a fine mesh Both these methods were found to be unsuitable for the problem of superheated steam drying in preliminary trials. As a result an adaptive or moving grid design was used. The underlying principle of this method is to add additional nodes in places where there exists sharp concentration gradients, and fewer nodes in places where the concentration gradients are relatively small.

The ability of this method to accurately represent a function using relatively few grid nodes is illustrated in Fig 4 4. The function $f(x) = 5^* \exp[(x-21)^2/10]$ is plotted for $0 \le x \le 40$ using a total of 21 nodes. It is apparent that sharp gradients in f(x) only occur for $15 \le x \le 27$. Hence with most of the nodes in this area all the features of the function f(x) are well represented as shown in Fig 4.4 b, while a poor description is obtained with an uniform grid (Fig. 4 4 a) The algorithm used for the generation of a non-uniform grid is called Benner's Algorithm (Rey 1989). The algorithm is described in Appendix A-1.

4.8 MOVING BOUNDARY

The exposure of black liquor to an atmosphere of superheated steam leads initially to the condensation of steam followed by evaporation of water after the heating up of the black liquor. These two processes cause the thickness of the black liquor to increase initially and then decrease.

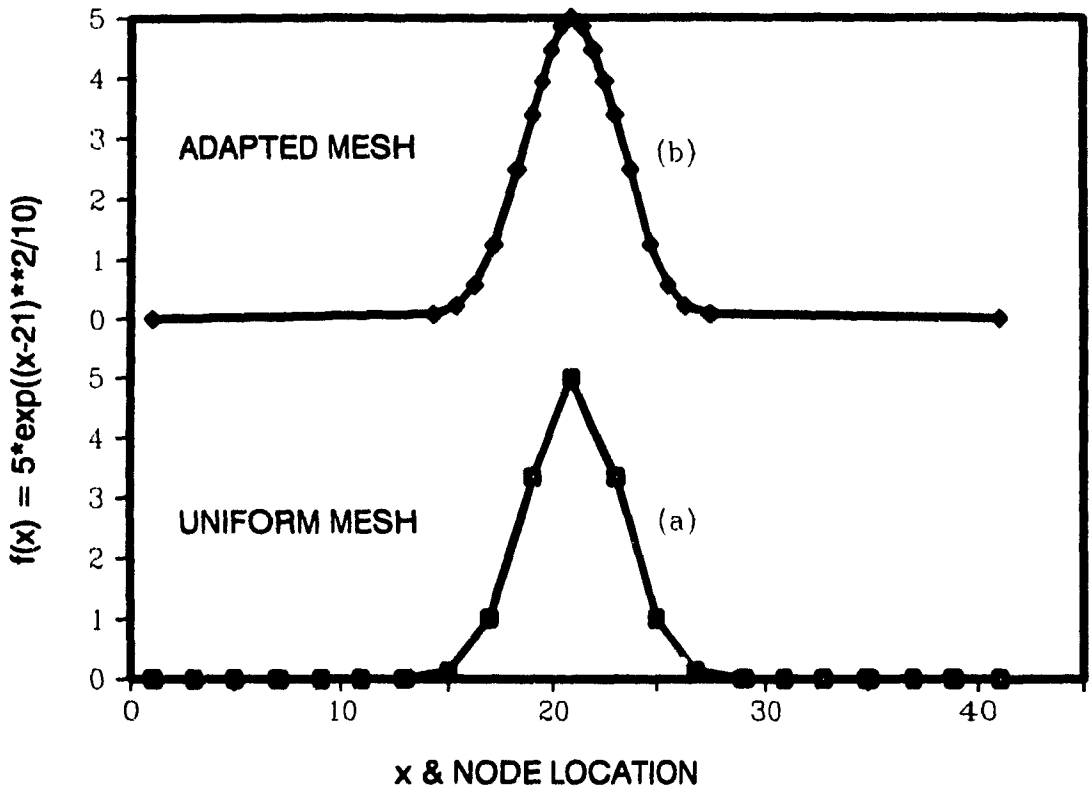

Fig. 4.4 : Illustration of adaptive remeshing scheme example

There have been a number of studies dealing with the numerical calculation of the location of a moving front (Bonnerot and Jamet, 1974,1980, Rolph and Bathe, 1982, Agaras et al., 1988, Crank, 1988, Murray and Carey, 1988). Crank (1988) has given an excellent review on the methods to solve free boundary problems The methods generally operate by :

a) coordinate transforms,
b) determining the presence of the boundary as to exist between two nodes
c) a combination of fixed coarse mesh and a moving fine mesh (Stanish et al., 1986)
d) tracing the location with a predictor-corrector formulation

The present method used to identify the location of the surface was similar to that proposed by Murray and Carey (1988) In this method the equations for moisture concentration and location, linked through the evaporation boundary condition, are iteratively uncoupled by alternately solving the moisture concentration/ temperature and boundary location equations The gradient of the moisture concentration required to estimate the boundary location is obtained from a previous converged solution of the concentration / temperature equation

A predictor-corrector method was used to integrate the boundary location equation (4-11). The calculation by the predictor is :

$$s_p^{n+1} = s^n + \Delta t\, \dot{m}/\rho_s \qquad (4\text{-}20)$$

where the superscript n refers to the previous time for which the solution was obtained, the superscript p indicates that this is the predictor step, and Δt is the time interval. This method utilizes the concentration at time t to predict the boundary location at time $t + \Delta t$ For the corrector step the concentration and temperature at both n and n+1 are used to compute the location of the surface. One approach for

the corrector predictor method is given by

$$s_c^{n+1} = s^n + \Delta t\ \dot{s}^{n+1/2} \qquad (4\text{-}21)$$

where s_c is the corrected location, and $\dot{s}^{n+1/2}$ is the average approximation of the boundary velocity at times n and n+1 :

$$\dot{s}^{n+1/2} = \frac{1}{2}\left(\dot{s}^n + \dot{s}^{n+1}\right) \qquad (4\text{-}22)$$

Given a computed $\dot{s}$ (predicted or corrected), a stretching or shrinking transformation moves all the nodes inside the domain by an amount proportional to the velocity of the moving boundary.

4.9 UPWINDING METHOD

The upwind finite element methods were developed for convection problems (Christie et al. 1976). However it can also be incorporated for problems with sharp gradients The underlying principle is that if the Peclet number is large, i.e. the convective transport is large compared to the diffusive transport, then the influence of a variable in the "upwind" direction (region of higher pressure) is felt mostly in the "downwind" region In fact if the Peclet number is higher than 10, it can be assumed that the concentration upwind effectively acts at the control volume face (in finite differences). In finite elements, the upwind effect is incorporated by modifying the basis functions to be biased towards the upwind side.

In a diffusion problem, one must be very careful to implement an upwind scheme, as it results in false diffusion. It has been suggested to use a mild upwinding scheme (for example upwinding factor = 0.1 : if factor is 1.0 represents complete upwind formulation) to remove the presence of oscillations near sharp gradients (Carey and Oden 1983).

4.10 VERIFICATION OF NUMERICAL SCHEME

Before presenting the numerical result for black liquor drying, the numerical program will be tested on a related problem for which a solution is available in literature. The test problem is that of unsteady one dimensional diffusion with chemical reaction at the receding interface between the unreacted and reacted phases

The schematic of the problem is shown in Fig 4-4. It represents a (well mixed) phase on the left hand side which contains species A. The species diffuses to the right over a distance s(t) through a layer of reaction product C to the interface with layer B At the interface A reacts rapidly with B forming the reaction product C. Because B is consumed, the interface between C and B moves to the right with time The component B is impervious to the diffusing species A.

The test problem is described by tow coupled time-dependent differential equations. The diffusion equation for species A through the product layer with reaction at the boundary z = s(t)

$$\frac{\partial u}{\partial t} - \mathbb{D} \frac{\partial^2 u}{\partial z^2} = 0 \qquad (4\text{-}23)$$

for $0 < z < s(t)$, where u is the concentration of species A and $\mathbb{D}$ is the diffusivity of A,

The following boundary condition apply :

the mass balance at the reacting interface :

$$- \mathbb{D} \left.\frac{\partial u}{\partial z}\right|_{s(t)} = \kappa\, r(u(s(t),t)) = \kappa\, u^n \qquad (4\text{-}24)$$

where κ is the reaction rate constant, and r is a kinetic expression and n the order of the reaction, and at the interface between A and C :

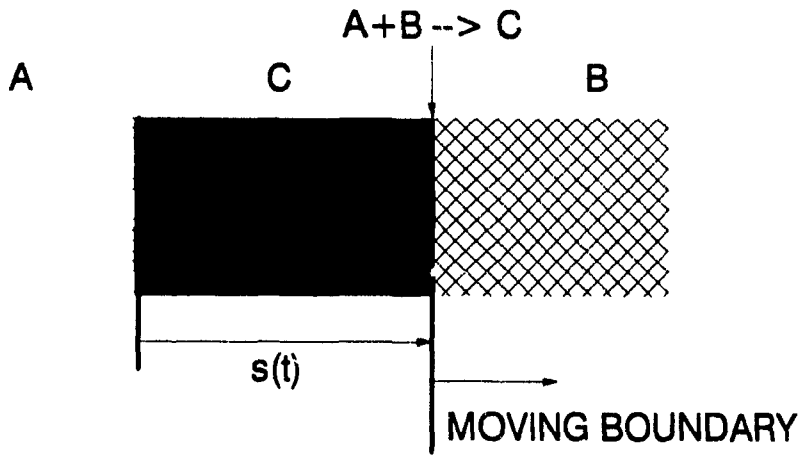

Fig.4.5 : Schematic of test problem.

and the concentration at the surface (z = 0)

$$u(0,t) = f(t) \qquad t \geq 0 \tag{4-25}$$

where f(t) can be any function. However in the present case f(t) will be a constant.

The initial condition is given by

$$u(z,0) = \phi(z) \qquad 0 \leq z \leq b = s(0) \tag{4-26}$$

where $\phi(z)$ is some initial distribution of reactant A in the product layer.

The ordinary differential equation characterizing the motion of the boundary is :

$$N\,\dot{s}(t) = \kappa\, r(u(s(t),t)) \qquad 0 \leq t \tag{4-27}$$

and the initial thickness of the of the product layer, s(0) is given by

$$s(0) = b \text{ (constant)} \tag{4-28}$$

The dimensionless quantities are now defined :

$$u^* = \frac{u}{\bar{u}} \; ; \qquad z^* = \frac{z}{l} \; ; \qquad t^* = \frac{t}{\bar{t}} \; ; \qquad s^* = \frac{s}{l}$$

where $\bar{u}$, l and $\bar{t}$ are a characteristic concentration, length and time respectively.

Introducing the following quantities in equations 4-23 to 4-28 gives the following non-dimensional expression :

$$\alpha \frac{\partial u^*}{\partial t^*} - \frac{\partial^2 u^*}{\partial z^{*2}} = 0 \qquad 0 < z^* < s^*(t),\ t^* \geq 0 \qquad (4\text{-}29)$$

$$u^*(0,t) = f(t)/\bar{u} \qquad t^* \geq 0 \qquad (4\text{-}30)$$

$$-\frac{\partial u^*}{\partial t^*}(s^*(t),t^*) = Da\ r(u^*(s^*(t),t^*)) = \beta\, \dot{s}(t) \qquad t^* \leq 0 \qquad (4\text{-}31)$$

$$u^*(z^*,0) = \phi(z^*)/\bar{u} \qquad 0 \leq z^* \leq b/l \qquad (4\text{-}32)$$

where "α" = $l^2/\mathbb{D}\bar{t}$, Da = $\kappa\, l u^{n-1}/\mathbb{D}$, β = $N\, l^2/\bar{u}\, \mathbb{D}\, \bar{t}$.

Numerical calculations were performed for the test problem described by equations 4-29 to 4-32 with a first or second order reaction (n = 1 or 2 respectively), $f(t)/\bar{u} = 1$, $\phi(z)/\bar{u} = 0$, and b/l=1. The model parameters were $\alpha = 1$, Da = 1, and $\beta = 1$. The results for a first and second order reaction are given in Fig. 4-6 and Fig. 4-7. Fig 4-6 shows the concentration of A at the reaction interface and Fig. 4-7 shows the location s(t) of the reaction interface function of time. As can be seen from these figures, the results agree exactly with those published by Murray and Carey (1988), thereby validating a number of key aspects of the present code.

For a zero initial concentration of A in the product layer, the differential equation for s(t) is very stiff at short times. During this time the boundary concentration increases rapidly until it begins to deplete slowly due to reaction as shown in Fig. 4-6. The effect of the diffusion process is to raise the concentration of A to that of the bulk, while the reaction leads to depletion of A at the boundary. The combined effect of the two processes produce an unstable (numerically)region for short times This behavior requires the use of very small time steps. Since Murray and Carey used uniform time steps the total number of time steps was very large. However, in the present study the time step was also adaptive and hence the initial time steps were small but increased later in the process.

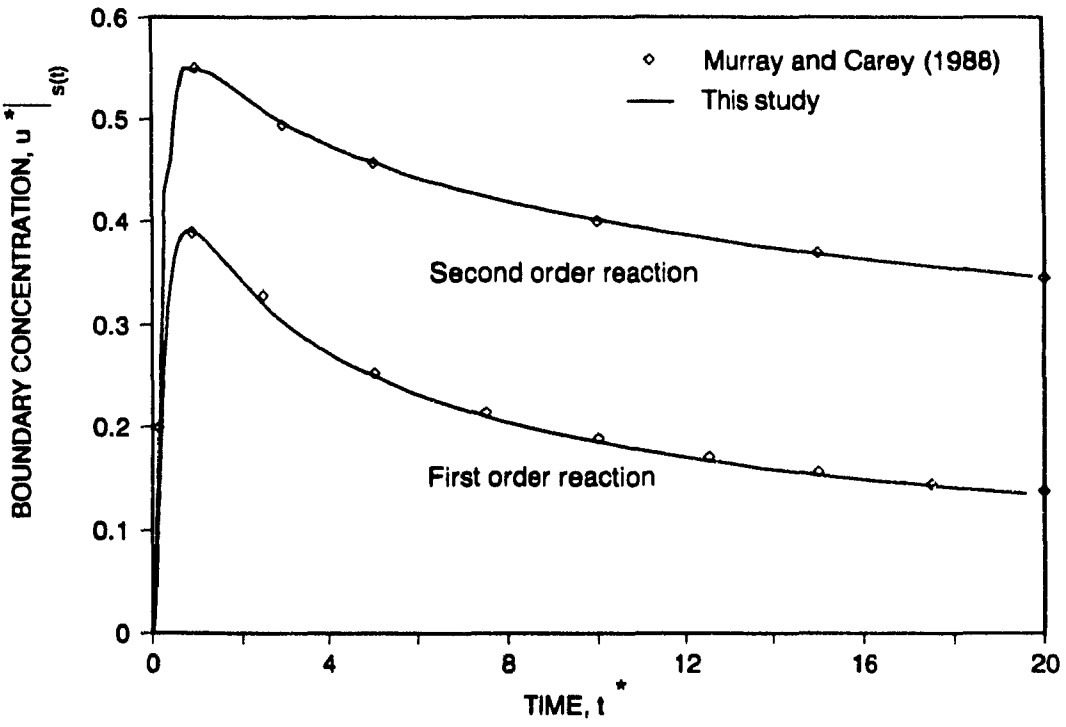

Fig. 4.6 : Concentration of A at the reaction interface, s(t)

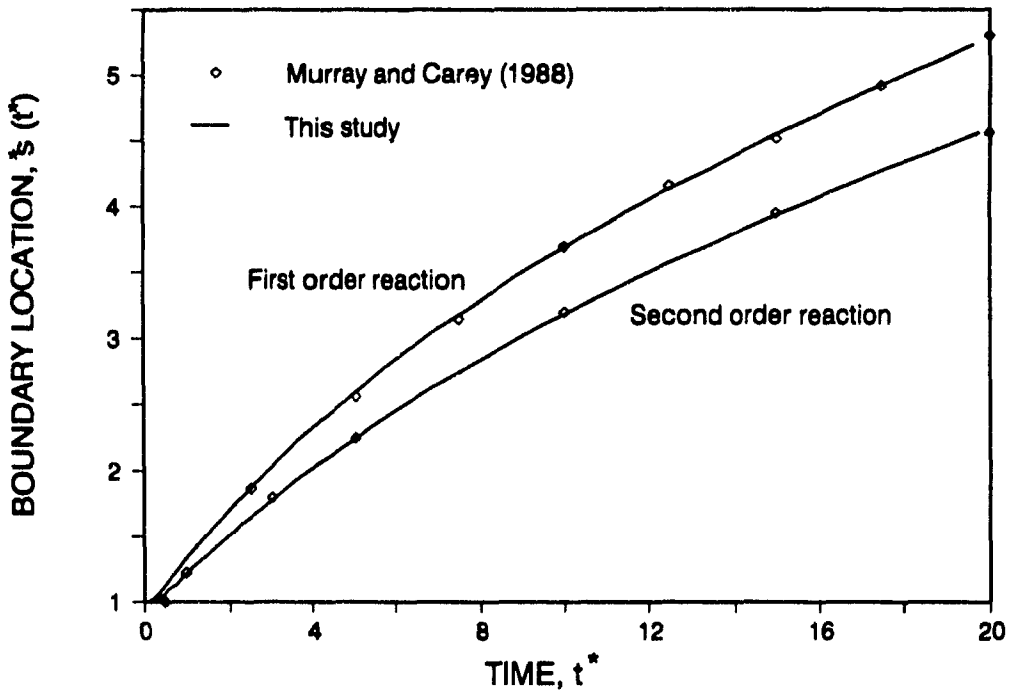

Fig. 4.7 : Location of the reacting interface, s(t) as a function of time.

4.11 NUMERICAL RESULTS FOR BLACK LIQUOR DRYING

The numerical results of drying a black liquor film without the presence of the sample pan and pan holder as outlined in section 4.4 are presented in this section.

Fig. 4-8 shows the calculated moisture content of a 1.0 mm film of 42.9 % initial moisture content as a function of time The boundary condition for the external heat transfer rate is a heat transfer coefficient of 300 W/m^2K and a jet temperature of 160°C. Also shown in the Fig 4.7 are the experimental results obtained under the same conditions. As is evident from the comparison figure, the agreement between the measurements and the predictions of the time required to achieve a particular solids level is very poor This is expected because in the experiment a significant amount of steam is condensed in order to heat up the sample pan and the pan holder As a result the experiments show an initial increase in moisture content from 0 429 to 0.66 kg HOH/ kg BLS, while in the numerical predictions the black liquor moisture content increases only from 0.429 to 0 44 kg HOH/kg BLS

Fig. 4-9, compares the drying rates versus moisture content of the data in Fig. 4-8. Contrary to Figure 4.8, the results in Fig. 4 9 show that at the same average moisture content the predicted drying rates agree very well with the experimental rates, especially if one considers that the mass diffusivity of water used represents only a crude estimate. The difference between the the predicted and experimental drying rate is most significant at a moisture content of around 0.4 The explanation for this is that because the moisture level and thus diffusivity is much higher at the surface in the numerical simulation than in the experiments. In the latter case the surface moisture content is low because the drying process has been ongoing for some time when the average moisture content reaches a value of about 0.4. Fig. 4.10 a,b show the development of the moisture and temperature profiles in the film. They are numbered for comparison at same times.

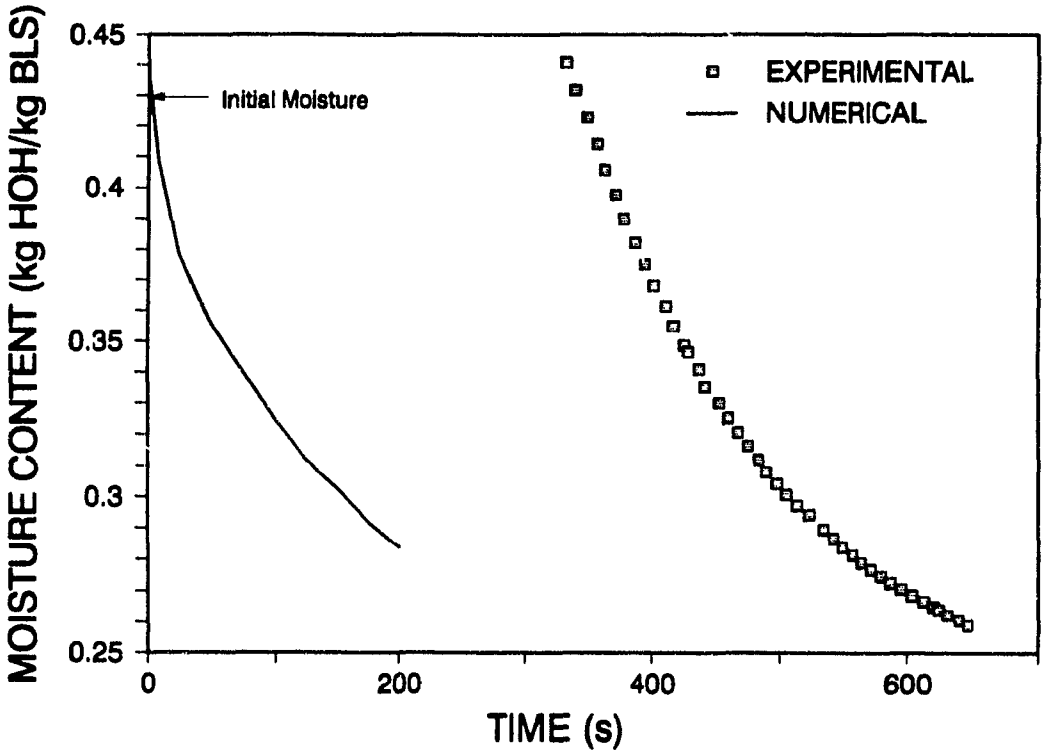

Fig. 4.8 : Comparison of experimental and numerical moisture content - time curves.

Conditions : Initial moisture content = 0.429 (70 % BLS)
Steam temperature = 160 °C
Film thickness = 0.8 mm

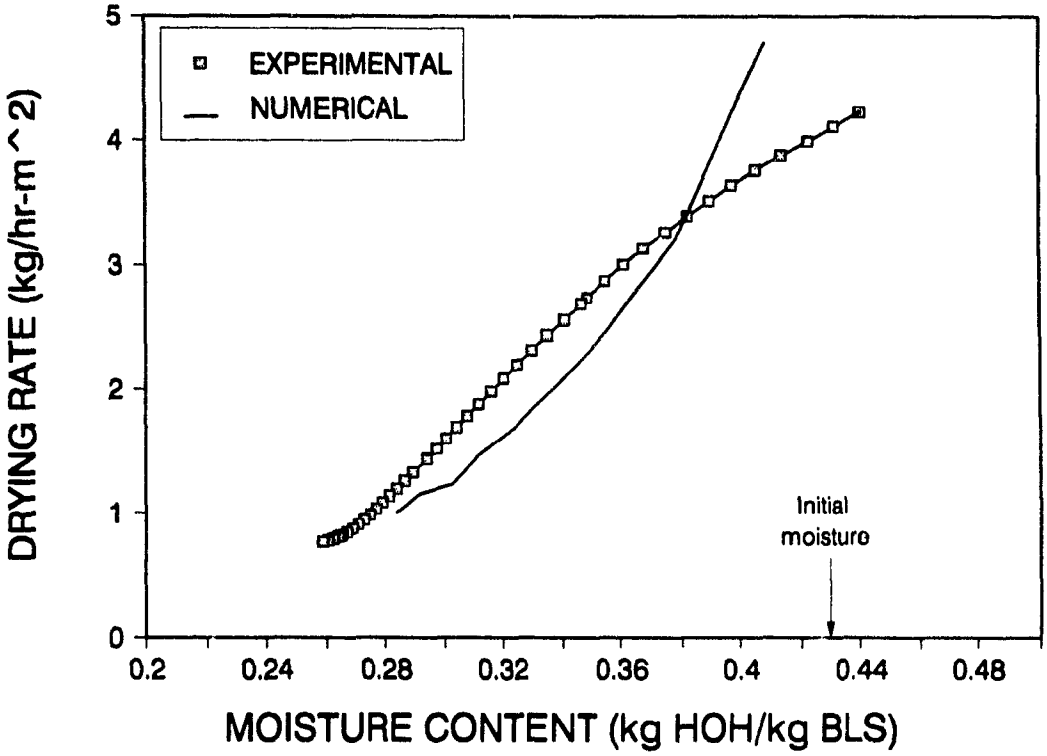

Fig. 4.9 : Comparison of experimental and numerical drying rate - moisture content curves (of the data in Fig. 4.7).

Conditions : Initial moisture content = 0.429 (70 % BLS)
Steam temperature = 160 °C
Film thickness = 0.8 mm

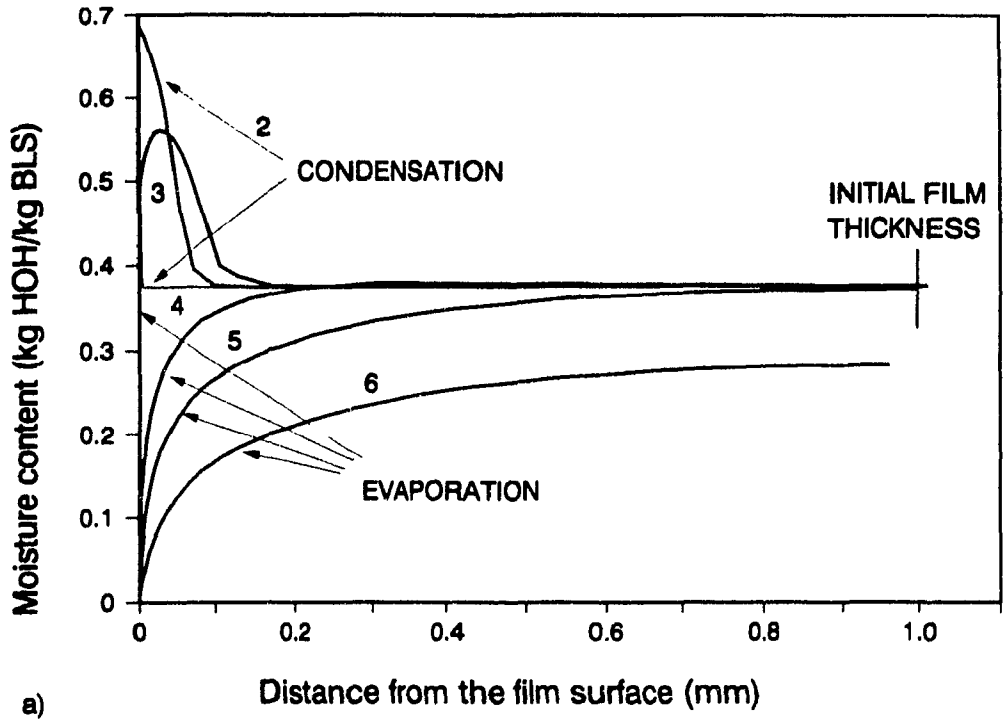

a)

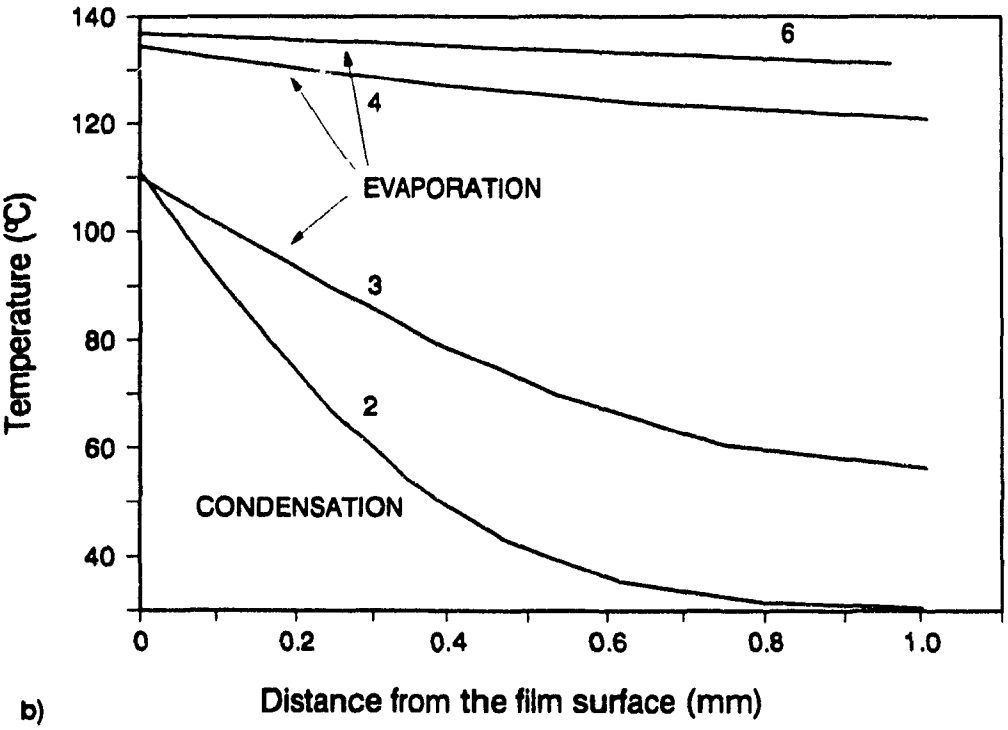

b)

Fig 4.10 : a) Moisture and b) temperature profiles in the black liquor film.

Fig. 4 11, shows the influence of film thickness on the drying rate. As is evident a decrease in film thickness resu.ts in an increase in the drying rate at a given moisture content This was also observed experimentally (Chapter III at low temperatures) Film thickness is an important operating variable when drying films of black liquor since it determines the distance the solvent has to diffuse before it can be removed form the solution. Hence a decreased film thickness will lead to an increased drying rate. It should be noted however that thin films are only advantageous when the drying rate is limited by internal mass diffusion. In the case of higher temperatures of impinging jets when boiling takes place inside the film the optimum film thickness must be determined experimentally

Fig. 4.12 shows the influence of initial moisture content on the black liquor drying rates. As can be seen from the figure, at relatively high moisture content of about 0 36 kg HOH/kg BLS there is a substantial difference in the drying rates between the two liquors with different initial moisture contents (0 429 and 0 375 kg HOH/kg BLS) However this difference disappears below 0 31 kg HOH/kg BLS This is attributed to the fact that the moisture content profiles are substantially different between the two films when one is still in the initial phase of drying. This is clearly seen in Fig. 4 13 which compares the profiles at an average moisture content of 0 36 kg HOH/kg BLS. However, the moisture profiles are the same at a low average moisture content as shown in Fig 4.13 b Thus the differences in Fig 4.13 a can be attributed to the fact that the moisture profile for the liquor with high initial moisture content is already well established while that of the liquor with the relatively low moisture content is still influence by the condensed steam and initial conditions

The black liquor drying rate is a strong function of the diffusivity of water. Since the diffusivity of water used in the program was only a rough estimate (Appendix IV), the sensitivity of the numerical solution towards the value of diffusivity was determined.

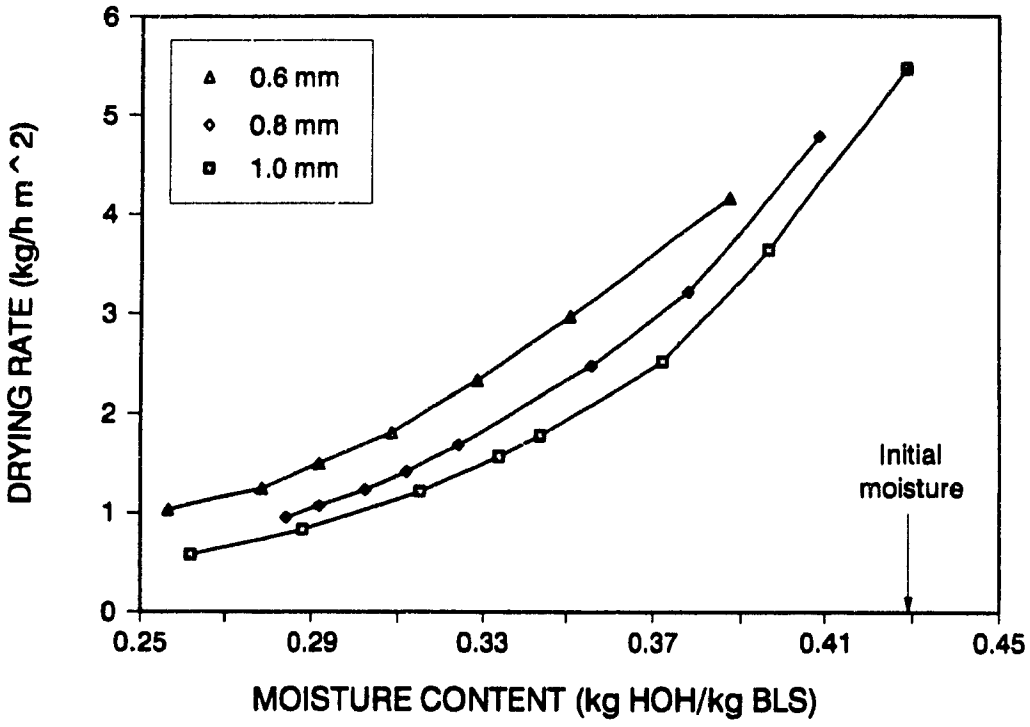

Fig. 4.11 : Influence of film thickness on drying rate

Conditions : Initial moisture content = 0.429 kg HOH/kg BLS
Steam temperature = 160 °C

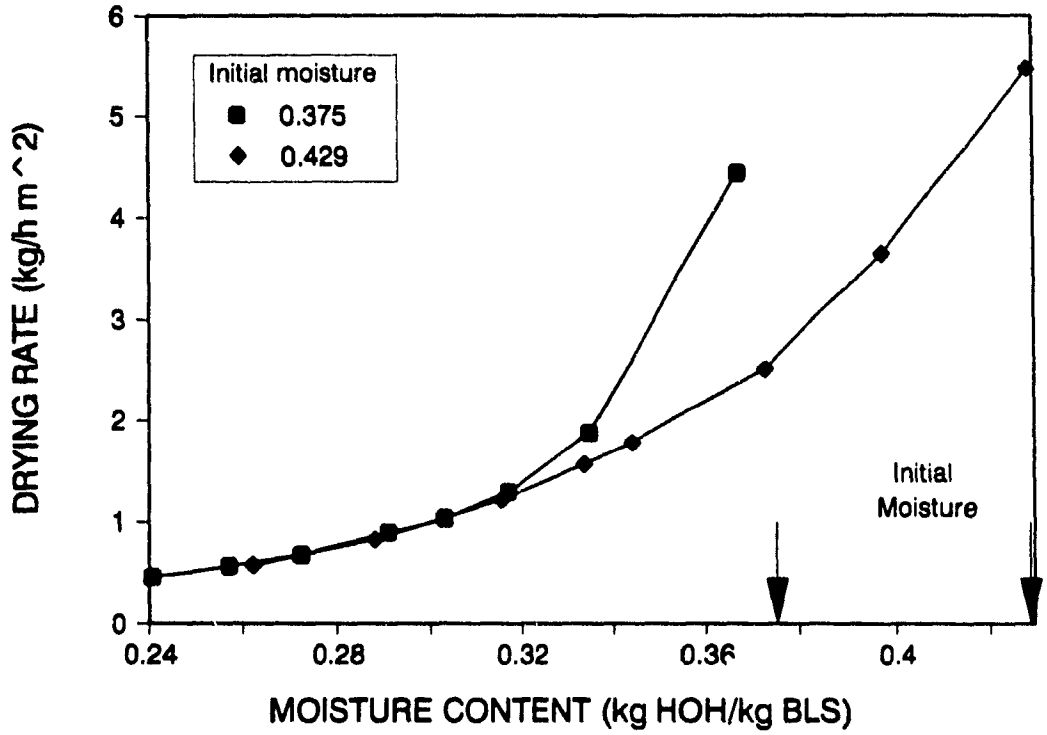

Fig. 4.12 : Influence of initial moisture content on drying rates.

Conditions : Film thickness : 0.8 mm
Steam temperature : 160 °C

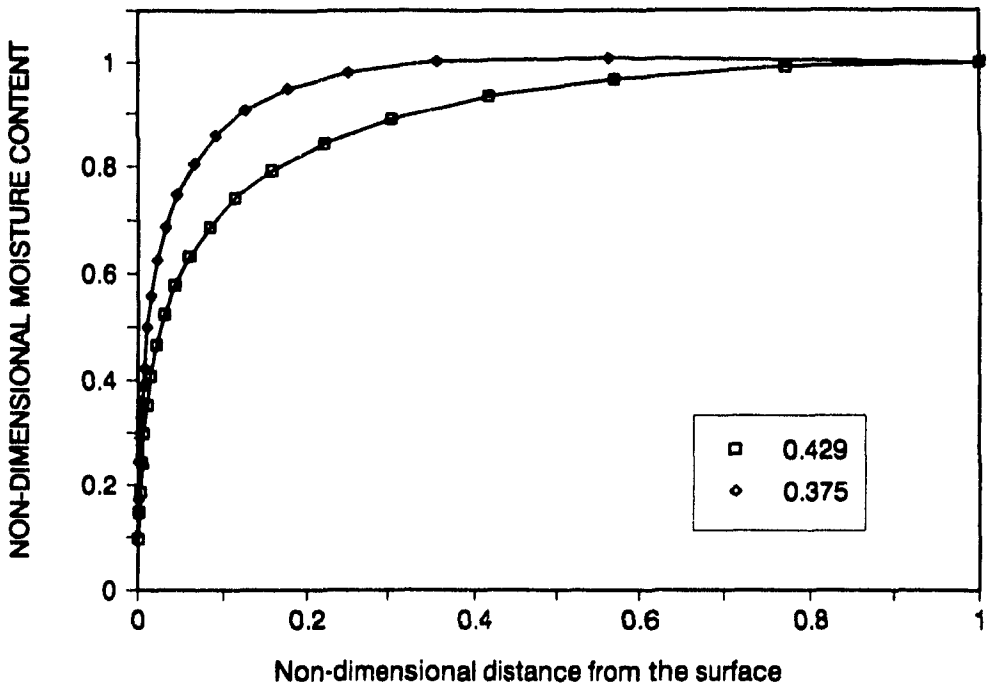

Fig. 4.13 a) : Moisture profiles at ≈ 0.36 kg HOH/kg BLS from Fig. 4.10

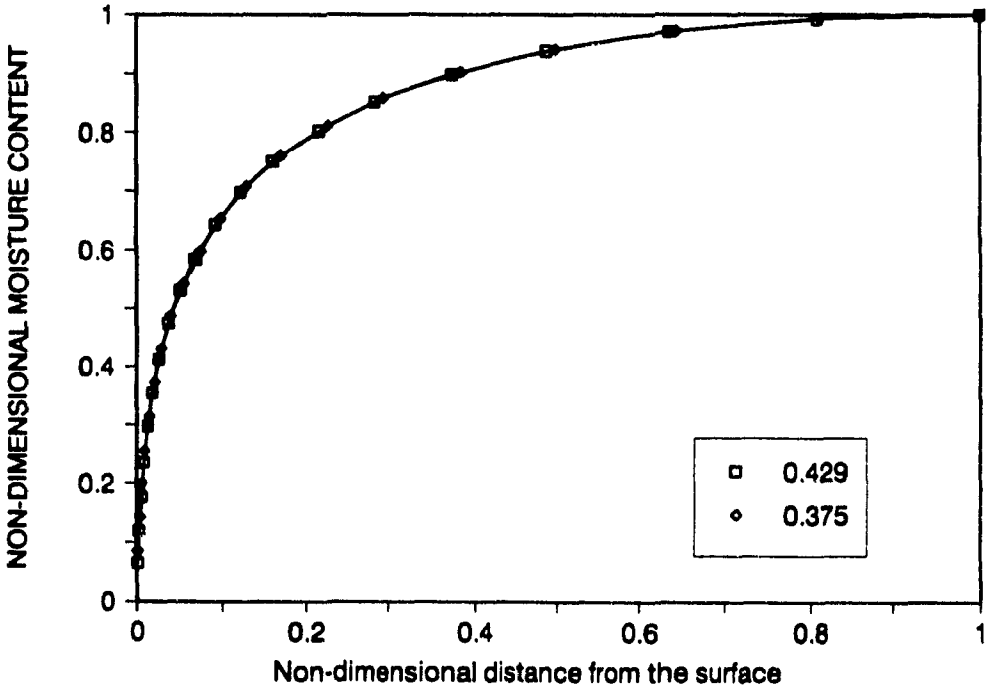

Fig. 4.13 b) : Moisture profiles at ≈ 0.30 kg HOH/kg BLS from Fig. 4.10

Fig. 4-14 shows the effect of the diffusivity of water on the drying rate - moisture content curves for different diffusivities. This result shows that the diffusivity has a profound influence on the prediction of the drying rate, and thus emphasizes the need for accurate and independent water diffusivity data in order to predict the drying rate of films of black liquor by superheated steam

The effect of increasing the inlet steam temperature on the drying rate - moisture content is shown in Fig. 4-15. As expected it shows that the numerical results are not much influenced by the steam temperature because in the present system the drying rate is controlled by diffusion of water inside the black liquor film, and not by the external heat transfer It is surprising that an increase in the steam temperature leads to a slight decrease in the drying rate with increase in the steam temperature This can be explained that at higher temperatures the equilibrium temperature that can be achieved by steam is higher than at lower temperatures This will result in a lower moisture content on the surface While this is advantageous in terms of increasing the concentration gradient, it is disadvantageous since it reduces the diffusivity (by increasing the solids level) Between these two opposing effects, the effect of decreasing the diffusivity is predominant since it decays exponentially, thus a decrease in the drying rate. Contrary to the numerical results, the experimental drying rates in Fig. 4-13 increase substantially with increasing steam temperature This is due to the fact that in the experiments boiling occurs for steam temperatures above 160°C, while the convective transport of water in the film was neglected in the numerical simulation

4.12 SUMMARY

A program has been developed which for the first time solves the coupled transport equations and boundary conditions describing the drying process of aqueous suspensions. The numerical analysis of superheated steam drying of black liquor films indicates that the drying

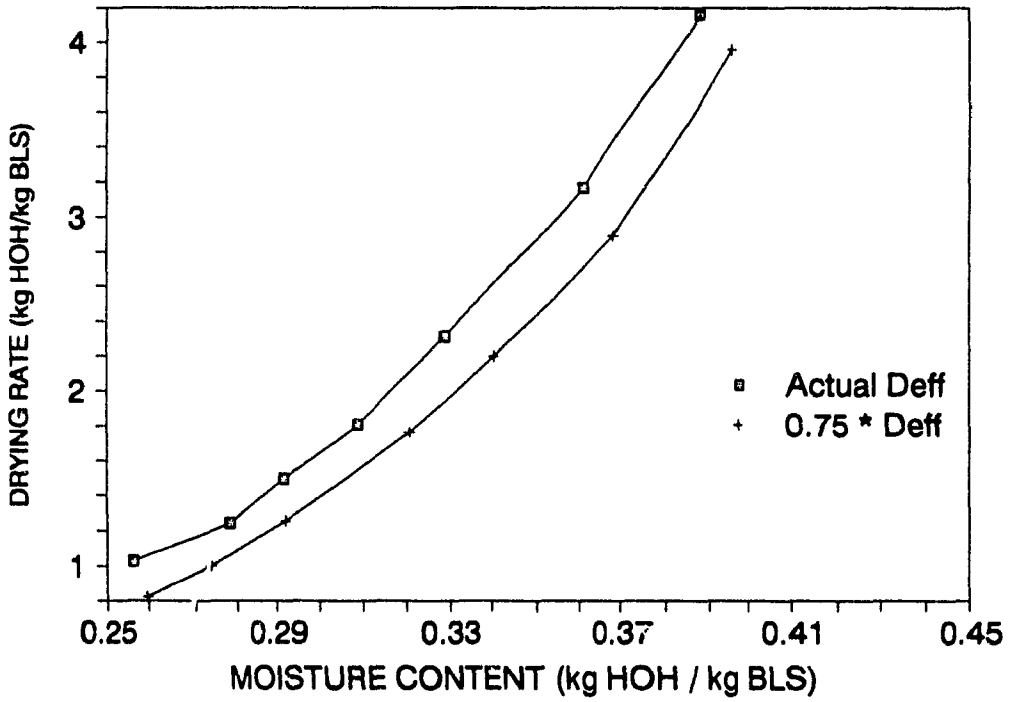

Fig. 4.14 : Influence of Black liquor diffusivity on moisture content.
Steam temperature : 160°C.
Initial moisture content : 0.429.

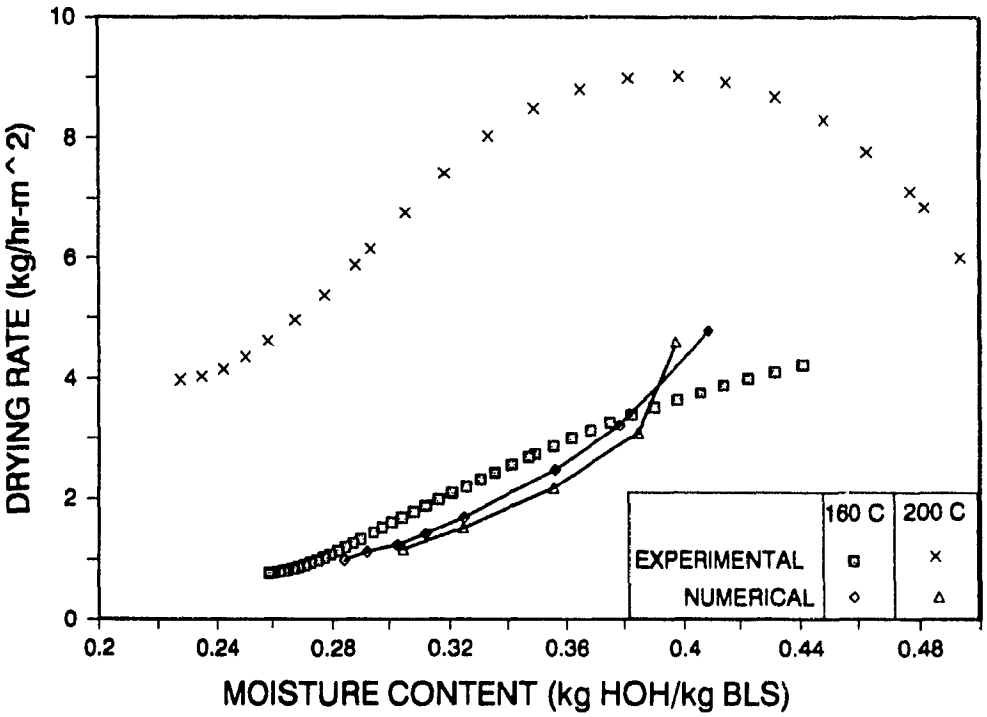

Fig. 4.15 : Influence of jet temperature on drying rates.
Initial film thickness : 0.8 mm
Initial moisture content : 0.429.

rates predicted by the present program when the process is controlled by diffusion of water in the film to the free surface. It cannot predict the drying rate when boiling in the film occurs. Another deficiency of the present program is that the condensation of steam due to the thermal inertia of the sample holder is not taken into account. Since diffusion is assumed to be the rate controlling process, the accuracy of the present results depend on the availability and quality of water diffusivity data and whether actual black liquor drying is limited by diffusion of water in the film.

4.13 NOMENCLATURE

b	:	Initial product layer thickness
c	:	Concentration (kg/m^3)
c_p	:	Specific heat (kJ/kg K)
$\mathbf{CT}$	:	Solution vector
$\mathbb{D}$	:	Mass diffusivity (m^2/s)
$\mathbf{F}$	:	Forcing vector
h	:	Heat transfer coefficient (W/m^2K)
h_{nc}	:	Natural convection heat transfer coefficient (W/m^2K)
$\underline{\underline{J}}$	:	Jacobian matrix
k	:	Thermal conductivity (W/m K)
κ	:	Reaction rate constant
M	:	Molecular weight
$\dot{m}$	:	Mass flux (kg/m^2s)
N	:	Mass of reaction
P	:	Pressure
q	:	Heat flux (W/m^2)
R	:	Universal gas constant
$\mathbb{R}$	:	Residual in GFEM
$s(t)$	:	Location of the bottom of pan wrt the surface of black liquor (m)
t	:	Time (s)
T	:	Temperature

T_a : Approximate solution

$T_b, T_{s(t)}$: Pan bottom temperature (K)

T_l : Temperature of liquid

T_o, T_s : Surface Temperature (K)

T_{room} : Ambient temperature (room temperature) (K)

T_R : Reference Temperature ($1/3^{rd}$ rule) (K)

T_v : Temperature of vapor

T_{inf}, T_∞ : Bulk temperature of drying medium (K)

u : Concentration of reactant A

X : Moisture content (kg H0ϕ/kg BLS)

z : Direction into the film (m)

Superscripts :

* : Non-dimensionalized value

Greek Letters :

λ : Latent heat of vaporization (kJ/kg)

ρ : Density (kg/m^3)

ϕ^i : Weight functions

ϕ^j : Basis functions

4.14 CITED REFERENCES

Agras, H., R.J. Aguerre, J.F. Gabitto : "Solution of moving boundary problems by coordinate transformation". Int. Comm Heat Mass Tr. 15, pp 41-50 (1988).

Becker, E.B., G.F. Carey, J.T. Oden : "Finite Elements" vol 1-4 Prentice Hall, Inc, (1981).

Bird, R.B, W.E. Stewart, W E., E.N Lightfoot "Transport Phenomena" John Wiley & Sons, pp 393 (1960).

Bonnerot, R., P. Jamet : "A second order finite element method for the one dimensional Stefan problem". Int. J for Numerical Meth in Eng 8, pp 811-820 (1974).

Bonnerot, R., P. Jamet : "A conservative finite element method for one-dimensional Stefan problems with appearing and disappearing phases". J. of Comp. Phy. pp 357-388 (1982)

Chow, L.C., J.N. Chung : "Evaporation of water into a laminar stream of

air and superheated steam". Int. J. Heat Mass Transfer 26(3), pp 373-380 (1983 a).

Chow, L C., J.N. Chung · "Water evaporation into a turbulent steam of air, humid air or superheated steam". 21st ASME/AIChE National Heat Transfer Conference, Seattle, WA, ASME Paper No. 83-HT-2 (1983 b)

Christie, I., D F Griffiths, A R. Mitchell, O.C. Zienkiewicz : "Finite element methods for second order differential equations with significant first derivatives". Int. J. for Numerical Meth. Eng., 10, pp 1389-1396, (1976).

Crank, J : "Moving Boundary Problems", Permagon press. (1988).

Dolinsky, A A, G.K. Ivanitsky · "Heat and mass transfer on the interface at evaporation of fluid drops in air and superheated vapor". Proceeding of Int. Drying Sym., Versailles PC 51-58 (1988).

Hasan, M., A S Mujumdar, M Al-Taleb : "Laminar evaporation from flat surfaces into unsaturated and superheated vapor". Proceedings of the 5th Int. Drying Symposium, Aug. 1986, pp 604-616

Hough, G "Chemical Recovery in the Alkaline Pulping Processes", TAPPI, pp 15-85, (1985)

Lapidus, L , N R Amundson . "Chemical Reactor Theory A Review". Prenctice Hall Inc. pp 269-313 (1977)

Moyne, C., D. Stemmelen, A Degiovanni . "Asymmetric drying of porous materials at high temperature. Theoretical analysis and experiments" Int Chem Eng. 30(4), pp 654-671 (1990)

Murray, P., G F. Carey : "Finite Element Analysis of Diffusion with Reaction at a Moving Boundary". J of Comp. Phy 74, pp 440-455 (1988)

Othmer, D.F · "The Condensation of Steam". I&E C, 21(6), pp 576-583 (1929).

Rey, A.D · "Class notes on Computational methods in Chemical Engineering" (1989).

Rolph, W.D., K-J Bathe : "An efficient algorithm for analysis of nonlinear heat transfer with phase changes" Int. J. for Numerical Meth. in Eng. 18, pp 119-134 (1982)

Stanish, M.A , G.S. Schajer, F Kayihan : "A mathematical model of drying for hygroscopic porous media". AIChE J, 32(8), pp 1301-1311, (1986).

Taleb, M.A, M. Hasan, A.S. Mujumdar : "Evaporation of liquids from a wet stretching surface into air, unsaturated air and superheated solvents". Proceedings of 6th Int. Drying Symposium, pp 261-269 (1987).

CHAPTER V

VISCOSITY AND THERMAL CONDUCTIVITY OF HIGH SOLIDS BLACK LIQUOR

5.1 INTRODUCTION

The viscosity and thermal conductivity of black liquor play a crucial role in the operation of a kraft recovery plant. The fluid viscosity determines the power requirement of the pumps, the heat transfer coefficient in the evaporators, the sprayability and droplet size distribution of the liquor when introduced in the furnace, etc. Thermal conductivity is critical to estimate the rate of heat transfer in the black liquor evaporators, and for the drying of droplets in the furnace. However, with the continuous trend of evaporation towards higher solids concentration there is a need for accurate physical property data of high solids black liquor. In this chapter a simple modified technique is presented for viscosity measurement of high solids black liquor The thermal conductivity of black liquor is measured for the first time at solids level above 53 %.The hygroscopic nature of black liquor is mentioned in the literature, however no quantitative data on the absorption of water has been reported. This property is very important for future processes which require the handling black liquor dry solids.

5.2 VISCOSITY OF BLACK LIQUOR

In recent years the measurement of black liquor viscosity has received considerable attention (Kim et al., 1981, Soderhjelm, 1986). Researchers have very carefully studied the influence of temperature and solids content on viscosity using various instruments, most of which can operate under pressure. However all instruments discussed are prohibitively expensive and fragile for routine mill measurements.

The objective of this study is to present a simple technique to measure the viscosity of black liquor at high solids content and temperatures using a common rotating spindle type (Brookfield) viscometer (Instruction manual). This is a ubiquitous and rugged viscometer. One of the features which has prevented acceptance of this type of viscometers for black liquor viscosity measurements is the exposure of liquor to atmosphere which leads to crust formation on the free surface. Since the crust sticks to the spindle, erroneously high readings are obtained for the viscosity.

Boger and Ramamurthy (1969) studied the influence of evaporation on a Weissenberg rheogoniometer. They prevented evaporation by covering the surface by a very thin film of nonvolatile fluid This procedure is also suggested by the supplier of the viscometer used in this study (Brookfield Eng Lab. Inc). The same method was adopted here for black liquor.

5.2-1 THEORY

A schematic of the viscometer is shown in Fig 5 1 The torque required to rotate a disc or cylinder in the fluid is measured and converted to viscosity readings assuming the fluid to be Newtonian. The torque increases with the radius, R, and height, h, of the disc/cylinder. The torque to rotate a thin disc in an infinite medium is proportional to the fourth power of the radius (Schlichting, 1955) :

$$\text{Torque} \propto \rho\, R^4\, \omega \sqrt{\nu\, \omega} \qquad (5\text{-}1)$$

and the torque to rotate a long cylinder in an infinite medium is given by (Schlichting, 1955) :

$$\text{Torque} \propto \mu\, h\, R^2\, \omega \qquad (5\text{-}2)$$

where ρ : density of the fluid

R : radius of spindle (disc or cylinder)

ω : angular velocity

ν : kinematic viscosity (μ/ρ)

μ : absolute viscosity

h : height of cylinder.

The proportionality constants in equations (5-1) and (5-2) for a Newtonian fluid, laminar flow, and no end effects can be evaluated exactly as 0.616π and 4π respectively. The shear stress is calculated as

$$\text{Shear stress} = \text{Torque} / (\text{area} * \text{arm}) \qquad (5\text{-}3)$$

All the above expressions have to be modified to account for end effects. These are provided by the manufacturer and the shear rates are also specified in the manuals. The torque is exerted to rotate the spindle according to equations (5-1) or (5-2). The shear stress is calculated using the area and arm of the spindle in equation (5-3). The viscosity is calculated as the ratio of shear stress to shear rate and is read from the dial of the viscometer with a suitable scaling factor (depending on the spindle and the shear rate).

5.2-2 EXPERIMENTAL PROCEDURES

Black liquor was obtained from a local pulp mill (hardwood). The solids level of the black liquor was 67.7%. The black liquor was homogenized by stirring and maintained at a desired temperature in a thermostat. The Brookfield viscosities were measured at 20 rpm. When a silicone film (on the surface of black liquor) was used, a thin film (about 1 mm) of silicone oil was poured on the black liquor surface. The silicone oil was immiscible with black liquor and had a low specific gravity (about 0.87 gm/cc versus 1.38 gm/cc for black liquor). The oil had a very low viscosity (2.3 mPa s at 20 °C) so that the contribution of the silicone oil to the drag on the spindle can be neglected.

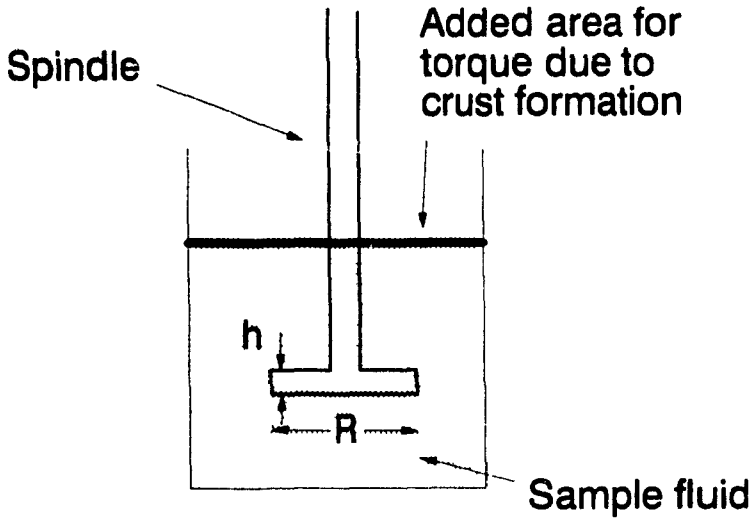

Fig. 5.1 : Schematic of Brookfield viscometer

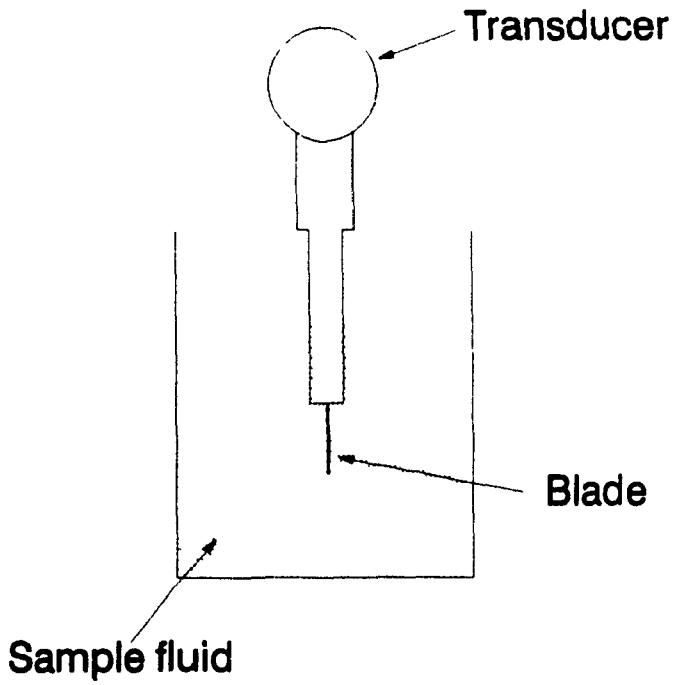

Fig. 5.2 : Schematic of vibrating blade viscometer.

Two viscometers were used for comparison. One was a Bendix 1800 ultrasonic viscometer. The sensor consisted of a magnetrostrictive transducer with a blade vibrating at a frequency of 28 kHz (Fig. 5-2). When the blade was immersed in a fluid, the vibrations are dampened according to the properties of the fluid. The change in pulse frequency is proportional to the square root of the product of viscosity and density. This product is measured by the viscometer and then corrected for density to obtain the viscosity. The other viscometer used for comparison was a coaxial cylinder viscometer.

5.2-3 RESULTS

Fig. 5.3 shows the influence of the presence of the silicone film on the viscosity measurement. It is apparent that the addition of silicone oil reduces the measured viscosity. In order to verify the fact that the reduction in viscosity is not due to mixing of silicone oil in black liquor, the experiment was repeated with oil films of different thicknesses. Since there was no influence of film thickness on viscosity, these results indicated that the decrease in viscosity was solely due to prevention of evaporation at the black liquor free surface.

Fig. 5.3 also shows the viscosity measured with the other viscometers. The data with the coaxial cylinder viscometer was measured on the same liquor at the University of Florida, Gainesville, Florida by the group of Professor A.L. Fricke. As can be seen the viscosity readings above 60°C are similar for the vibrating blade viscometer, the coaxial cylinder viscometer and the Brookfield viscometer with a silicone oil film. Below 50°C the difference in readings could be due to the non-Newtonian behavior of black liquor, which is pronounced at low temperatures and high solids.

A crust of approximately the same area is formed with the strong

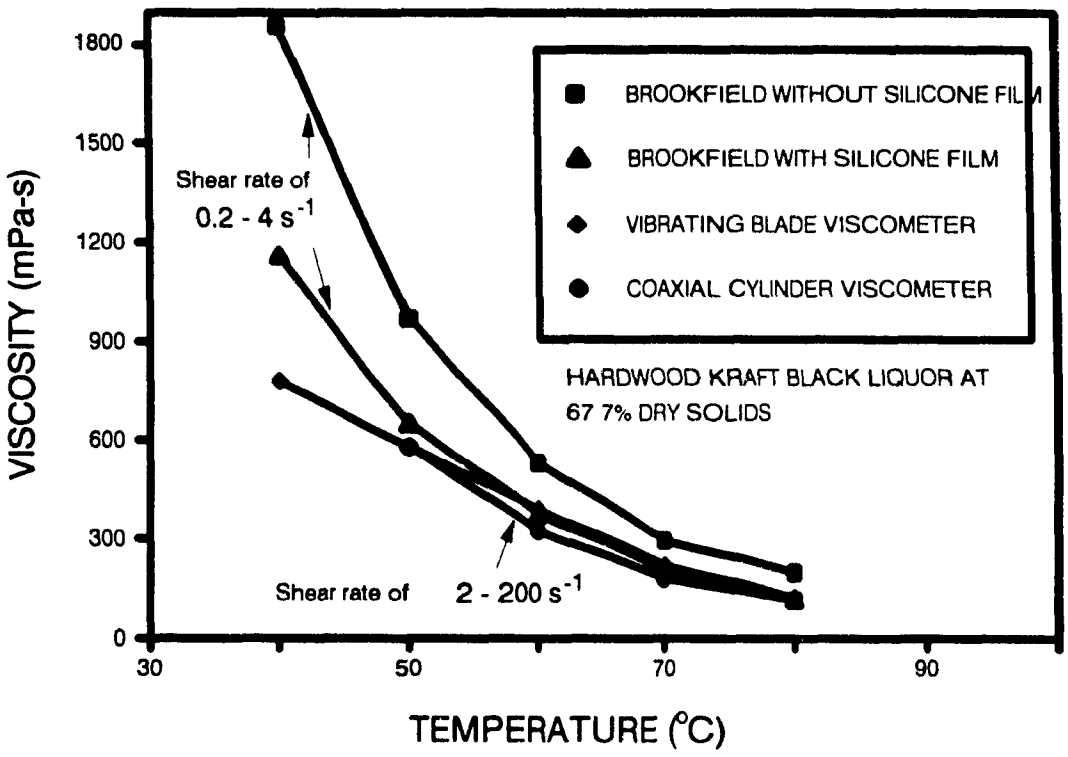

Fig. 5.3 : Comparison of viscosities measured by different viscometer.

black liquor irrespective of the temperature of viscosity measurement. Hence, the ratio of the measured viscosities with and without crust formation is expected to be independent of temperature of operation of the Brookfield viscometer. This is seen in Fig. 5.4., where the Brookfield viscosity without silicone oil film divided by the viscosity measured by other techniques are plotted against temperature. The constant viscosity ratio of about 1.5 implies that the exposed surface creates an error of about 50 %.

Also included in Fig. 5.4 is data of Stenuf and Agarwal (1981) who compared the viscosity measured with a Brookfield viscometer to that obtained with a flow tube viscometer. The higher ratios obtained by Stenuf and Agarwal could be due to different liquors used, surface areas and shear rates used.

The precautions to be taken when using the suggested method, i.e., the Brookfield viscometer with silicone oil film are :

1] Care must be taken to ensure that the temperature of the spindle is in equilibrium before recording the viscosity. If the temperature of the spindle is lower, then the viscosity of the fluid near the spindle will be relatively high and erroneous readings will be recorded. Allowing the spindle to turn for about 20 revolutions is sufficient to assure equilibrium. With an exposed surface, this equilibration time is generally sufficient for a crust to form

2] The spindle must be carefully inserted into the black liquor so that the silicone oil is not trapped under the spindle disk. This can be avoided easily by inserting the spindle at an angle into the liquor sample.

5.2-4 CONCLUSION

For routine measurement of black liquor viscosity in a pulp mill

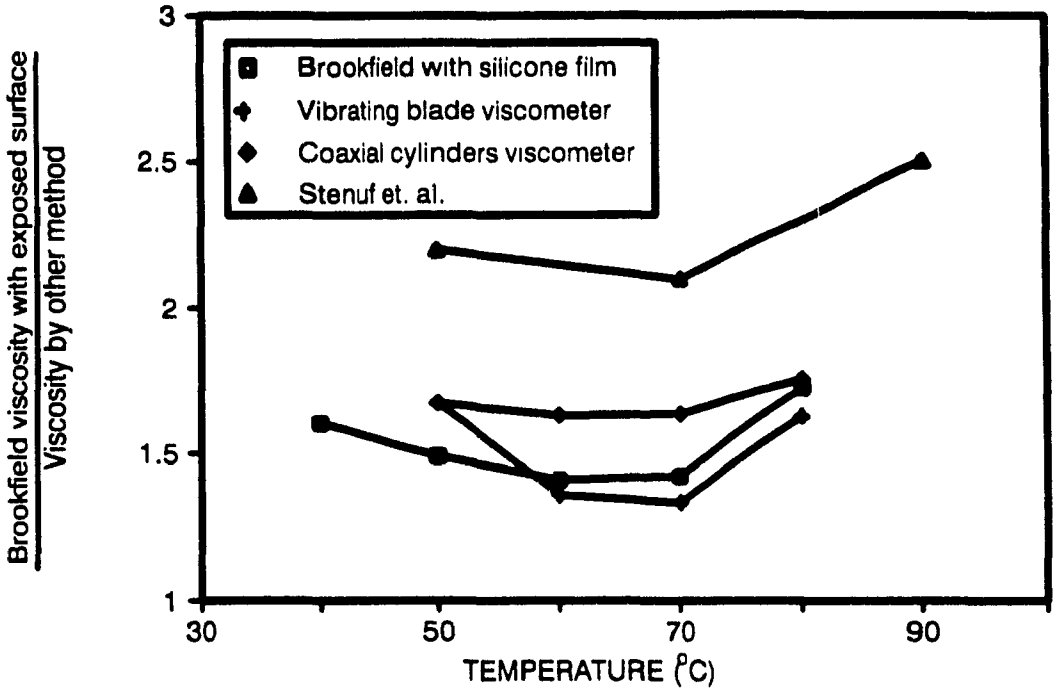

Fig. 5.4 : Ratio of conventional Brookfield viscosity to other methods.

the rotating spindle viscometer can be used when the free surface open to atmosphere is covered with a thin layer of silicone oil. With this modification the simple, cheap and rugged Brookfield viscometer gives reproducible and reasonably accurate results

5.3 THERMAL CONDUCTIVITY OF BLACK LIQUOR

In 1956 Harvin and Brown (1956) presented an excellent paper on the thermal conductivity of black liquor at solid concentration upto 53%. Since then no more data has been published of the conductivity of black liquor even though the present industrial standard is to fire liquor at a solids level of 68 - 72 % (see Fig. 1.1). Also, as the thermal conductivity of high solids black liquor could be of importance in alternative processes such as drum drying or spray drying, it was the objective of this study to measure the thermal conductivity of black liquor with a simple technique called the "*line source method or probe method*"

5.3-1 THEORY

In the line source method the thermal conductivity of a material is determined from the thermal response of a heated long cylindrical probe of small diameter The schematic of the set and the probe are shown in Fig. 5.5 a,b, is similar to that described by Lobo and Cohen (1990). The 11 cm long and 0.2 cm diameter probe contains a heater element (Constantan, 0.01 cm diameter) and a J-type thermocouple which measures the surface temperature midway along the length of the probe. The heat flux of typical 0 6 W, supplied to the probe is measured. A tape heater wound around the sample is used to bring the fluid and the probe to a uniform temperature From the temperature-time history during heating the thermal conductivity can be calculated Tye (1969) has given an excellent description of the apparatus and the errors involved in this method.

Ideally the set up should be that of an infinitely long thin heat source placed in an infinite homogeneous medium of uniform temperature. The solution of the Fourier equation leads to a transient temperature rise, T, a distance, r, from the heat source (Tye, 1969) .

$$T = -\frac{\mathbb{Q}}{4\pi\lambda}\,\mathbb{Z}\left(-\frac{r^2}{4\alpha t}\right) \qquad (5.4)$$

where $\mathbb{Q}$ is the heat input per unit length (W/m), λ is the thermal conductivity of the medium, $\mathbb{Z}$ represents an exponential integral, α is the thermal diffusivity, and t is the heating time.

For small values of ($r^2/4\alpha t$) equation 5.4 can be approximated as :

$$T = \frac{\mathbb{Q}}{4\pi\lambda}\left(\ln t + \ln\left[\frac{4\alpha}{r^2}\right] - \gamma\right) \qquad (5.5)$$

where γ is the Eulers constant, 0.5772156. From the equation 5.5 it follows that over a time interval, $t - t_0$, the rise in temperature at a point in the medium is given by

$$T - T_0 = \frac{\mathbb{Q}}{4\pi\lambda}\ln\left(t/t_0\right) \qquad (5.6)$$

Since equation 5.6 is valid anywhere in the fluid, and thus also at the interface between the fluid and the probe, the heating of the probe surface can also be described by equation 5.6 after an initial transient. In order to account for the deviations from ideality equation 5.6 was modified as

$$T - T_0 = \frac{C\,\mathbb{Q}}{4\pi\lambda}\ln\left(t/t_0\right) \qquad (5.7a)$$

or

$$T = \frac{C\,\mathbb{Q}}{4\pi\lambda}\ln\left(t\right) + \text{constant} \qquad (5.7b)$$

where C is the so called probe constant. The probe constant was determined as 0.82 by calibrating the probe in glycerol, a material for which the thermal conductivity is accurately known. With this constant,

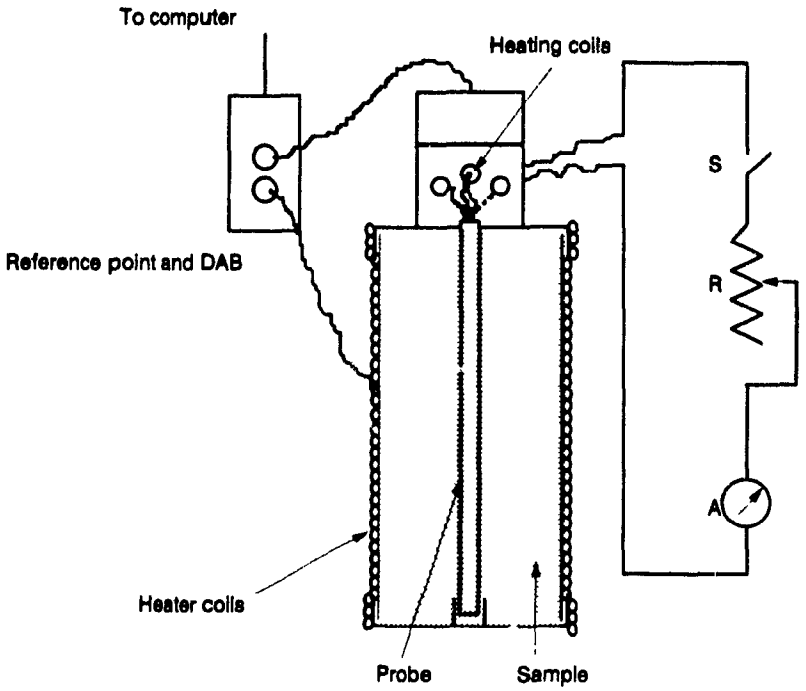

Fig. 5 5 a : Experimental setup for measurement of thermal conductivity.

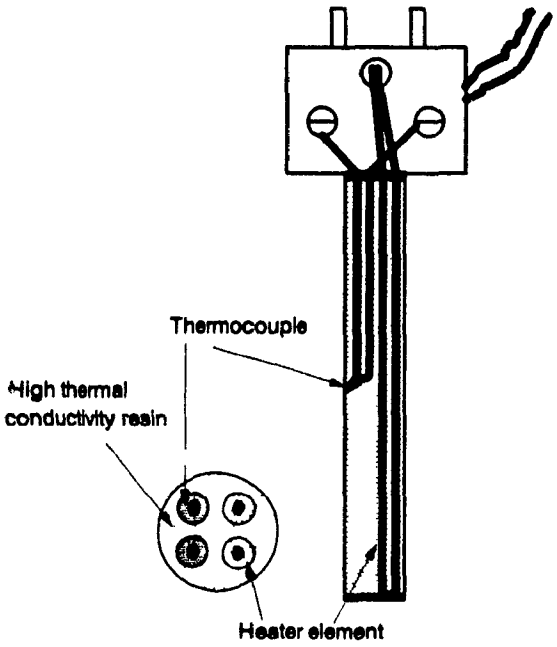

Fig. 5.5 b : Probe construction for measurement of thermal conductivity.

the thermal conductivity of water was determined as 0.63 W/m K at 38°C and 0.658 W/m K at 65°C both of which are within 2 % of the value published by Green and Perry (1985). The above analysis is only valid if natural convection effects can be neglected The natural convection effects are generally neglected when the Grashoff number is ≤ 10^4 The Grashoff number of the present system was typically between 10^{-2} and 10^2 based on the temperature rise of the probe of about 3°C and viscosities between 0.8 - 1000 mPa s.

5.3-2 RESULTS

Fig. 5.6 a shows the temperature rise of the probe, T, during the heating period of about 40 seconds. The same data is replotted in Fig 5.6 b against the natural logarithm of time.

The thermal conductivity is calculated from the slope of the straight line through the data in Fig 5 6b calculated by linear regression analysis. The thermal conductivity of black liquor was determined as a function of solids level at two temperatures and plotted in Fig. 5.7 It is seen that the present data agree well with that of Harvin and Brown (1956) who used a measurement technique based on steady state heat transfer through a slab The present results show that Harvin and Brown's thermal conductivity date can be extrapolated to higher solids evel to predict the thermal conductivity

5.3-3 CONCLUSIONS

A cylindrical heater/probe technique was successfully used to measure the thermal conductivity of black liquor from 0 to 83% solids, over a temperature range from 24 to 68 °C The results show that the present thermal conductivity data are well described by the correlations of Harvey and Brown who used liquors with a solids concentration of ≤ 53 %. It should be noted that the agreement was obtained despite the fact that different liquors were used in the two studies.

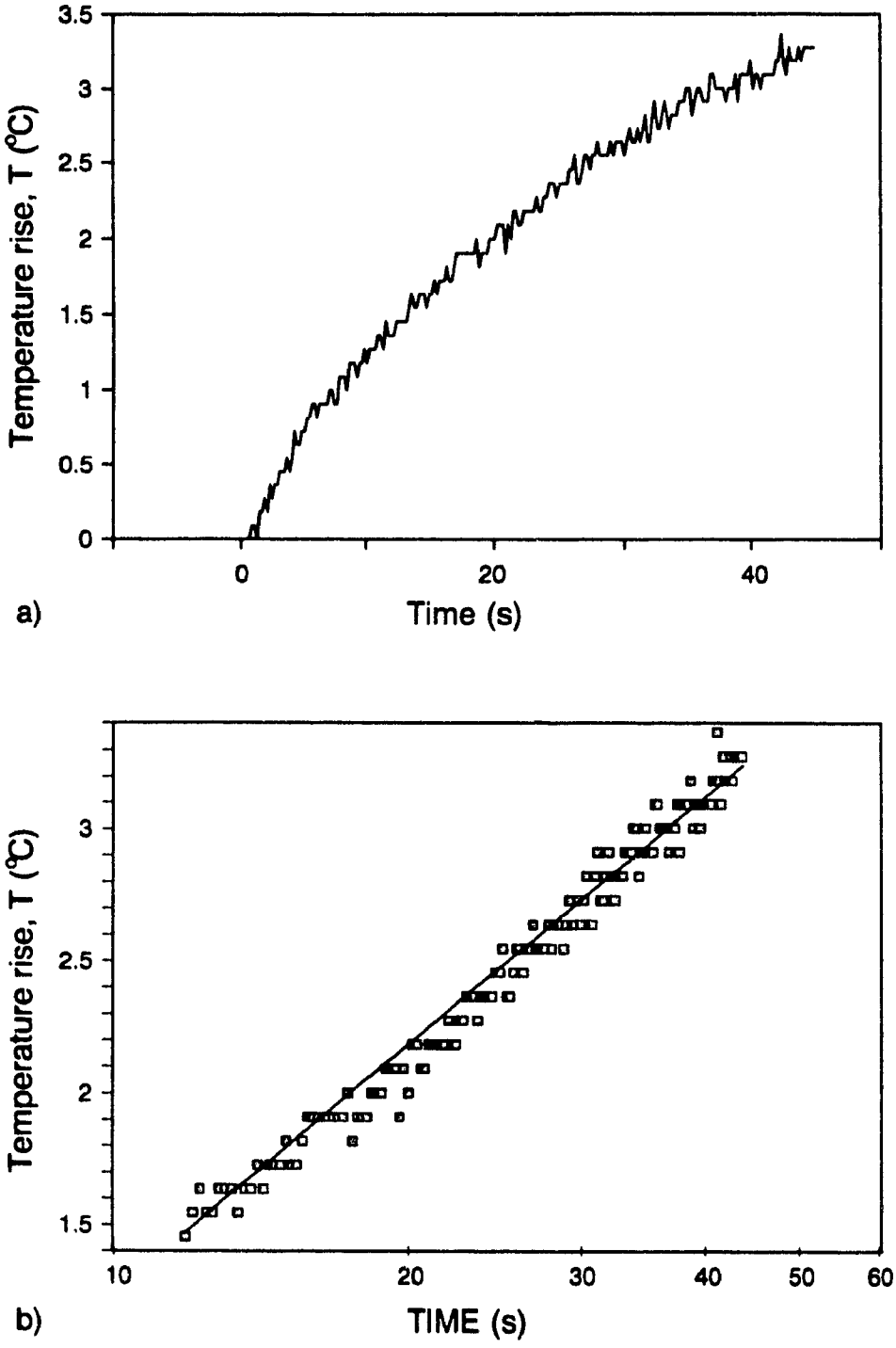

Fig. 5.6 : Typical temperature rise of the probe during heating.

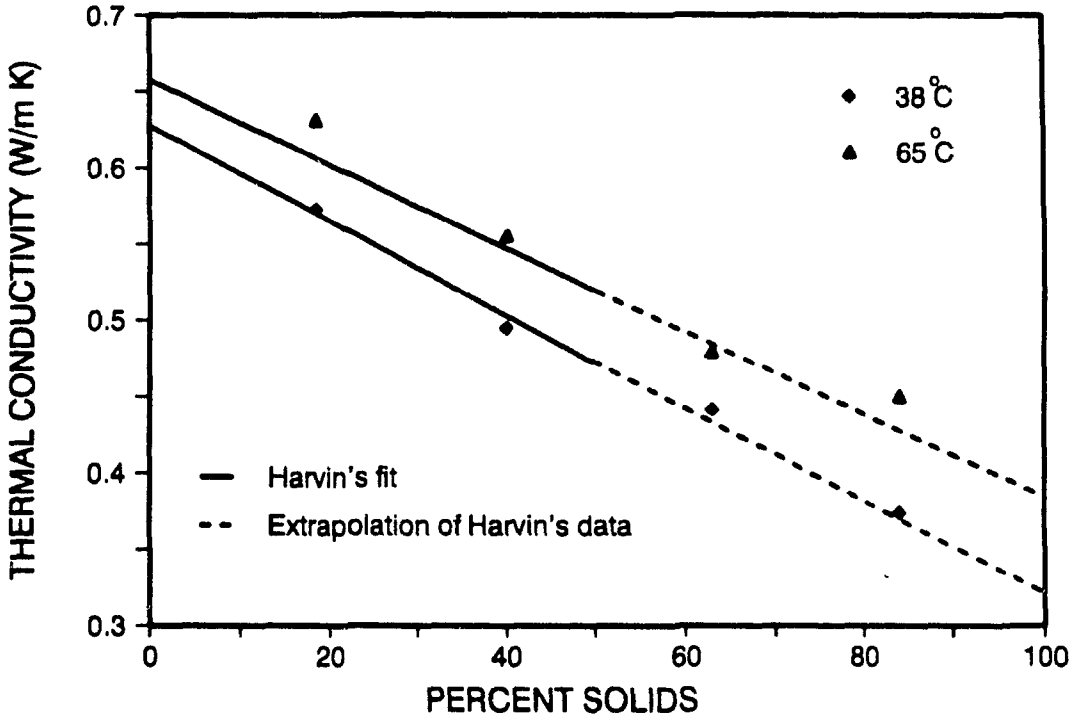

Fig. 5.7 : Thermal conductivity of black liquor as a function of solids level at 38 and 65°C.

5.4 NOMENCLATURE

h	:	Height of cylinder
Q	:	Heat input per unit length (W/m)
r	:	radius of temperature measurement (m)
R	:	Radius of spindle (disc or cylinder)
t_1, t_2	:	Times for calculating the slope in eqn 5.7 (s)
T	:	Temperature (^oC)

Greek letters

α	:	Thermal diffusivity (m^2/s)
λ	:	Thermal conductivity (W/m K)
μ	:	Absolute viscosity (mPa s)
ρ	:	Density of fluid (kg/m^3)
ν	:	Kinematic viscosity (μ/ρ)
ω	:	angular velocity (rad/s)

5.5 CITED REFERENCES

Boger, D.V , and Ramamurthy, A V. Transaction of the Society of Rheology, 13 (3), 405 (1969).

Brookfield Synchro-lectric Viscometer : Instruction Manual. pp 20.

Robinson, M.L. and D T. Clay "Equilibrium behavior of Kraft Black liquor in Superheated Steam" Chem. Eng. Commun. 43, pp 225-235 (1986).

Kim, H.-Y , Co, A., and Fricke, A.L.: AIChE Symposium Series No. 205, Vol. 77, 2(1981)

Lobo, H., Claude, C . "Measurement of Thermal Conductivity of Polymer Melts by the Line-Source Method". Poly. Sc & Eng. 30(2), pp 65-70, (1990).

Perry, R H , Green, D.W.: "Perry's Chemical Engineers' Handbook". Sixth Edition, McGraw-Hill Book Company. pp 20-11 to 20-14 (1984).

Schlichting, H. "Boundary layer Theory", 6th Ed. McGraw Hill, pp 81,97 (1955).

Solderhejlm, L.: Paperi Ja Puu, 9, 62 (1986).

Solutions to Sticky Problems, Brookfield Eng. Lab. Inc. pp 2.

Stenuf, T.J., Agarwal, M.L.: AIChE Symposium Series No. 207, Vol. 77, 13 (1981).

Tye, R.P. : "Thermal Conductivity", Academic Press, pp 376-380 (1969).

CHAPTER VI

CONCLUSIONS

6.1 GENERAL SUMMARY

The present work is the first detailed study on drying of black liquor films. Impinging jets of hot air and superheated steam were used as the drying media. The film thickness varied from 0.8 to 1.2 mm and the drying medium temperatures ranged from 180 to 250°C. Other operating parameters investigated were the initial liquor solids level (60-74%) solids, and drying medium mass flow rate (0.8 to 1.0 kg/s m^2).

The black liquor drying rates were higher in superheated steam than in air at jet temperatures above 200 °C. Four major differences between air and steam drying of black liquor can be identified :

1] Because the sample is introduced at room temperature into the drying chamber there is an initial condensation of steam on the black liquor film with steam as the drying medium.

2] The rising rate period in air drying occurs over a larger range of solids level than in steam.

3] The drying rate during the final stages of drying is higher in superheated steam than in air.

4] The film temperature in steam drying approaches the boiling point very rapidly. However, when air is used as drying medium the film temperature approached the boiling point only very slowly.

The behavior of black liquor films of varying film thickness of black liquor provided significant information about the drying characteristics in air and in steam. In air drying these experiments

revealed the importance of the mass transfer resistance of a crust formed on the free surface. Since the surface temperature in air drying is below the boiling point it is believed that the lignin and other polymers form a "skin" on the black liquor surface When water below the crust evaporates due to heating by the impinging jets, the vapor formed below the crust expands and extensive swelling behavior is observed. In steam drying it is seen that at low temperatures, an increase in film thickness causes a decrease in the drying rate as predicted by Fick's law of diffusion However at high temperatures, it is seen that the influence of the film thickness is not significant. This has been attributed to the fact that there is extensive boiling at high temperature causing the film thickness to be less important, since molecular diffusion was not the limiting phenomenon

The influence of increasing jet temperature, solids content, and impingement medium mass flow rates did not indicate any anomalies. Drying of lignin exhibited extensive swelling and is perceived as the material which offers the plasticity for black liquor to swell Oxidation of black liquor resulted in an increase in the steam drying rate and is attributed to the decrease in boiling point rise due to oxidation.

The viscosity of black liquor up to a high solids level of 75% was successfully measured using a modified Brookfield method The modification was to prevent evaporation of water from the surface of the black liquor and hence the formation of the crust by using a thin film ($\approx$ 1 mm) of silicone oil on the black liquor surface The results obtained with this method are comparable to those obtained with vibrating blade and coaxial cylinders viscometers A line source method was used to measure the thermal conductivity of black liquor up to 83 % solids. There was good agreement between the thermal conductivity measured and those published before Dry black liquor was found to absorb moisture extremely rapidly from the atmosphere causing the solids level to fall down to 70%. This would cause significant problems in

storing the black liquor.

A finite element analysis of the condensation-drying problem was performed. It was seen that the analysis performed well for low temperature drying, and even that for the drying rate estimation only. Since, the thermal inertia of the sample holder, and the window was neglected the estimation of the condensation amounts was significantly in error. Since boiling was not accounted for in this study, the correspondence to high temperature drying was poor.

The bottom line of this thesis is that **the advantage of steam over air** as a drying medium is **not significant enough** to outweigh the problems of steam handling and insulation (mass and thermal) of the apparatus. The use of steam would become advantageous only if very efficient cycles were available for obtaining the energy of spent steam by condensation / recirculation.

6.2 CONTRIBUTIONS

1] A simple thermodynamic analysis of the superheated steam drying process was presented.

2] The drying of black liquor films were studied. The influences of a range of parameters were investigated. The physics of the problem was related to drying of black liquor.

3] A numerical analysis was performed to solve a moving boundary, moving front problem with coupled partial differential equations (due to parameters) and coupled at a boundary condition (due to the equilibrium between solids level and temperature through the boiling point rise at the surface).

4] A simple technique for the measurement of viscosity was established.

5] Thermal conductivity data was obtained for high solids black liquor using a line source method.

6.3 SUGGESTIONS FOR FURTHER STUDY

Fundamental work is needed to obtain the drying rates of black liquor in air and steam with :

a] The liquor inlet temperature close to the boiling point.

b] Heat supplied from the drum side of black liquor by condensing steam.

The ease of removal of the "dry black liquor" from the drum surface in a continuous process should be investigated. The mass diffusivity of water in black liquor should be measured accurately

APPENDIX I

Benner's algorithm for adaptive meshing :

A brief methodology of the adaptive meshing process is presented here since it was obtained from an internal report (Rey, 1989). The principle of this process is to locate the nodes over the area of interest so that errors are equal in size for the individual elements. This is schematically shown in Fig. A.1.1.

The error in the FEM representation of the k^{th} derivative is :

$$e_i^{(k)} \leq \Delta x_i^{m-k} \int_{x_i}^{x_{i+1}} \left| \frac{d^m y}{dx^m} \right| dx \qquad \text{(A-1.1)}$$

where k : order of the derivative of y

m-1: order of the polynomial basis function.

Considering k = 1 (first order derivative), and m = 2 (linear basis functions), the error is expressed as :

$$e_i^1 \leq \Delta x_i \int_{x_i}^{x_{i+1}} \left| \frac{d^2 y}{dx^2} \right| dx \qquad i = 1,2,\ldots N-1 \quad \text{(A-1.2)}$$

N = # of nodes.

The residual of the errors is given by :

$$R_i^{\#} = e_o - e_i^1$$

A residual is a function that describes the difference between the exact solution and the approximate (numerical) solution.

$$R_i^{\#} = e_o - \Delta x_i \int_{x_i}^{x_{i+1}} \left| \frac{d^2 y}{dx^2} \right| dx \qquad i = 1,2,\ldots N-1 \quad \text{(A-1.3)}$$

Hence,

$$R_i^{\#} = e_o - \Delta x_i [\, |M_{i+1} - M_i| + |M_i - M_{i-1}| \,] \qquad (A\text{-}1\ 4)$$

where

$$M_i = \frac{\Delta y_i}{\Delta x_i} \text{ (slope of y(x) on the ith element)} \qquad (A\text{-}1.5)$$

Hence the algorithm is given as :

1] Find the error in each element (second RHS term in equation A-1 4).

2] Find the square root of each error $\|e^1\|_2 = \sqrt{e_i^{(1)2}}$

3] Find the average.

4] If some elements have errors above some upper bound set the errors in these elements to upper bound ($e_{upper} = 5\ e_{avg}$). Conversely, if some elements have errors less than a lower bound set error in these elements to e_{lower}.

5] Find the new average.

6] Compute the integral of the error (cumulative error).

7] Find the size of the new elements by requiring that the interpolating local errors be the same size on each element. This was done using a cubic interpolation technique.

8] Interpolate the values of the variables at the new nodes, and return to the FEM code.

Cited Reference

Rey, A.D. : "Class notes - Computational methods in Chemical Engineering, 302-664A", McGill University, (1989)

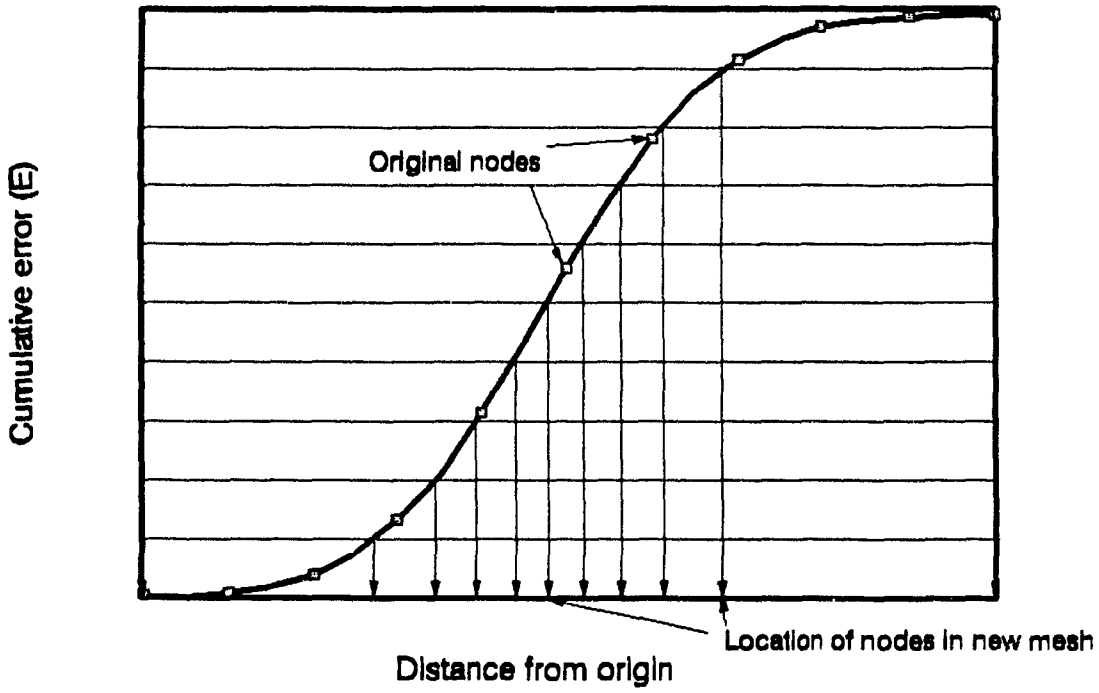

Fig. A-1.1 : Schematic of cumulative error distribution over element in a finite element scheme.

APPENDIX II

Errors in various measurements.

Table A-1 gives the errors in the various measurements made. The errors were measured by repeating the experiment at a pivotal point / few points and the standard deviations were calculated. The primary sources of error are also included for further improvement. This table indicates the precision of the various measurements.

Table A-1.

Property or variable	Standard deviation	Source
Local mass transfer coeff. [m/s]	0.005	depth
Overall mass transfer coeff [m/s]	0.001	mass
Water loss (air & steam) [g] Aluminum oxide slurry	0.01	mass
Water loss (air) [g] Black liquor	0.01	mass
Water loss (steam) [g] Black liquor	0.02	mass condensation
Drying rate (air) [kg/h m^2] Black liquor	0.09	mass gradients
Drying rate (steam) [kg/h m^2] Black liquor	0.22	mass condensation gradients
Viscosity (without film) [mPa s]	3.1	crust equipment
Viscosity (with film) [mPa s]	0.9	equipment
Thermal conductivity [W/m K]	0.02	gradient

APPENDIX III

Estimation of water diffusivity in black liquor.

It was essential to obtain an order of magnitude and approximate behavior of water diffusivity in black liquor as a function of moisture content and temperature for use in the numerical model.

While it was depicted in Fig. 3.8, there exists high levels of boiling during black liquor drying in SHS, it is believed that this data would be of use in a fluidized bed boiler, film drying in rotating kilns, etc

To date there is no estimate of the magnitude and influence of physical parameters such as solids level and temperature, on the diffusivity of water in black liquor. This can be attributed to the fact that only in the last decade has the industry been considering drying of black liquor a potential unit operation.

Theory

A brief review of the literature indicates that there are two commonly mentioned methods to determine the diffusivity during the drying or desorption process. One is an empirical procedure proposed by Schoeber and Thijssen (1985). The other is a well established method and compares the non-dimensional weight loss versus Fourier number data (Perry and Green, 1984). The latter approach is taken here.

One dimensional diffusion-controlled mass transfer is described by Fick's law .

$$\partial c / \partial t = \mathbb{D} (\partial^2 c / \partial x^2) \qquad (A\text{-}1)$$

where c is the concentration of the component, t is the diffusion time,

x is the direction of diffusion, and $\mathbb{D}$ is the binary diffusivity. The solution of equation (5-4) for a slab when one exposed surface is dry or at an equilibrium moisture content and the initial moisture distribution is uniform is (Perry and Green, 1984) :

$$\frac{W - W_e}{W_c - W_e} = \frac{8}{\pi} \left[\sum_{n=0}^{n=\infty} \frac{1}{(2n+1)} e^{-(2n+1)^2 \mathbb{D} t (\pi/2d)^2} \right] \qquad (A-2)$$

where W is the average moisture content (dry basis) at any time, W_c is the initial moisture content, and W_e is the moisture content in equilibrium with the environment, $\mathbb{D}$ is the diffusivity and d is the film thickness.

For long drying times the equation 5-9 simplifies to a limiting form of the diffusion equation as

$$\frac{W - W_e}{W_c - W_e} = \frac{8}{\pi^2} \left[e^{-\mathbb{D} t (\pi/2d)^2} \right] \qquad (A-3)$$

At a given value of $(W - W_e)/(W_c - W_e)$ the corresponding value of mass Fourier Number $(\mathbb{D}t/d^2)_{theoretical}$ obtained from published graphs (Perry and Green, 1984), and the experimental diffusivity $\mathbb{D}_{avg}$ (m/s^2) is calculated as

$$\mathbb{D}_{avg} = \frac{(\mathbb{D} t / d^2)_{theoretical}}{(t / d^2)_{experimental}} \qquad (A-4)$$

The above analysis is straight forward for materials which are rigid whose equilibrium moisture contents are known All the published diffusivity data obtained by the above method was generated using air as the drying medium. The advantage of using is that the equilibrium moisture content can be taken to be zero over a range of temperatures. However, as shown in Fig 3 8, when

air is used as drying medium, extensive swelling of black liquor and crust formation occurs, thus preventing its use for the determination of D_{avg} with equation 5-11. Since superheated steam drying of black liquor at steam temperatures between 140 and 160°C did not exhibit any swelling or boiling in the film this data was used in the above analysis.

The equilibrium moisture content for superheated steam drying of black liquor was calculated from the measured surface temperature of the film, the boiling point rise data published by Robinson and Clay (1986) and the assumption that at the surface, the temperature and moisture content are at equilibrium with each other.

Results

The experiments were conducted in the experimental apparatus described in Chapter II The weight loss and temperature data were assimilated as described.

The weight loss (after smoothing using the extended spline fit technique described in Chapter II) is plotted as a function of time in Fig. A-2. From the temperature data (after smoothing again) the equilibrium moisture content is also plotted in Fig A-2 From the analysis described in section 5 3-1, the diffusivities are calculated and are plotted in Fig. A-3 The process was repeated at 140, 150 and 160°C to obtain the three curves presented in Fig A-3 It should be noted that the temperature of the film gradually increases as a function of time Hence, the diffusivity curves obtained are not isothermal (constant temperature) ones

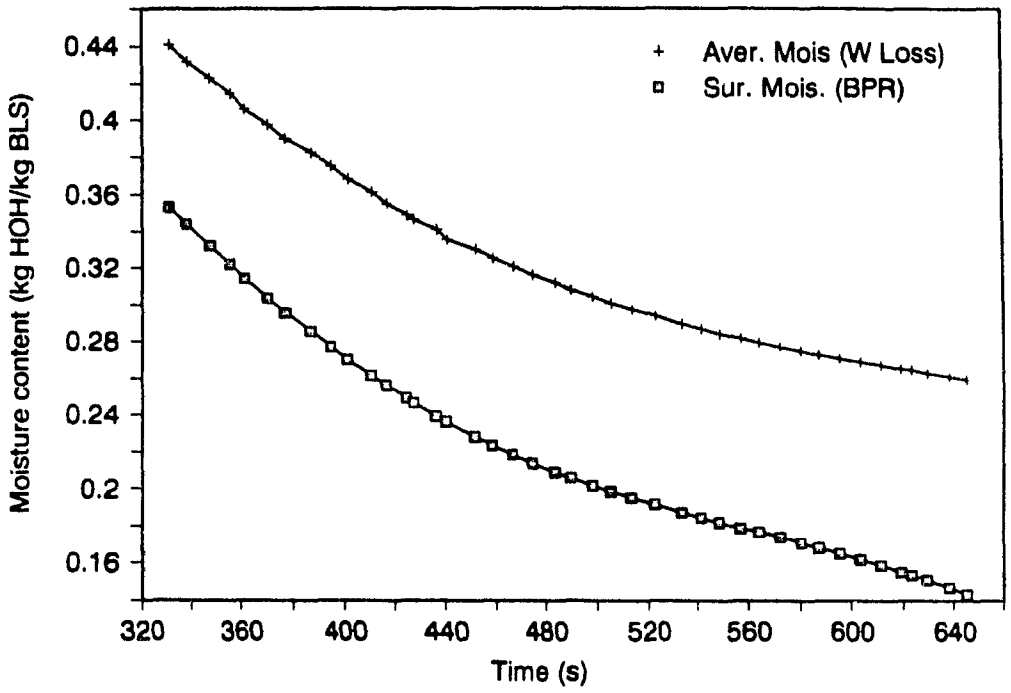

Fig A-3.1 : Average (from weight loss data) and surface (from BPR data) versus time. Steam temperature = 150°C.

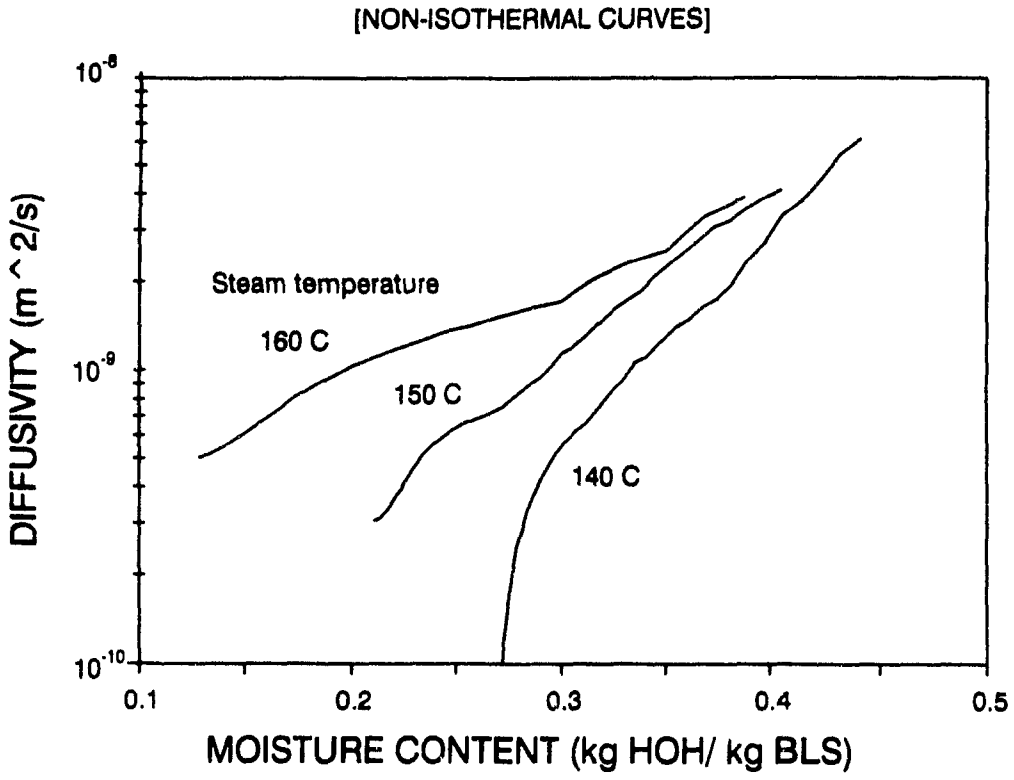

Fig A-3.2 : Diffusivity as a function of moisture content : non isothermal curves.

A multiple linear regression analysis of the diffusivity - temperature - moisture content expresses diffusivity as :

$$\mathbb{D} = 0.028\, e^{-\frac{9500}{T}}\, e^{20.4\,X} \qquad \text{(A-4)}$$

where T is the temperature in Kelvin, and X is the moisture content (kg HOH/kg BLS).

A plot of the predicted value of diffusivity versus the measure value of diffusivity is plotted in Fig. A-3.3.

The limitation of this estimation of diffusivity are :

1] In the derivation of equation A-2 to A-3, the diffusivity is assumed to be a constant (which is not as shown in Fig A-3 3),
2] The equations are also valid only if W_e is a constant (which is not the case as shown in Fig. A-2),
3] The starting moisture content was arbitrarily chosen to be 0 429 (the initial moisture content before putting the sample in the dryer),
4] The film thickness was assumed to be a constant, (the film thickness decreases with water removal),
5] No account has been made for any convective currents (boiling or natural) which could be present though not seen.

Cited references :

Green, D.W, Perry, R.H : :Perry's Chemical Engineers' Handbook". Sixth Edition. McGraw Hill Book Company, pp 20-11 to 20-14 (1984)

Schoeber, W.J.A.H, Thijssen, H A.C : "A short cut method for the calculation of drying rates for slabs with concentration dependent diffusion coefficients". AIChE Symposium Series 73 (163), pp 12-24 (1977).

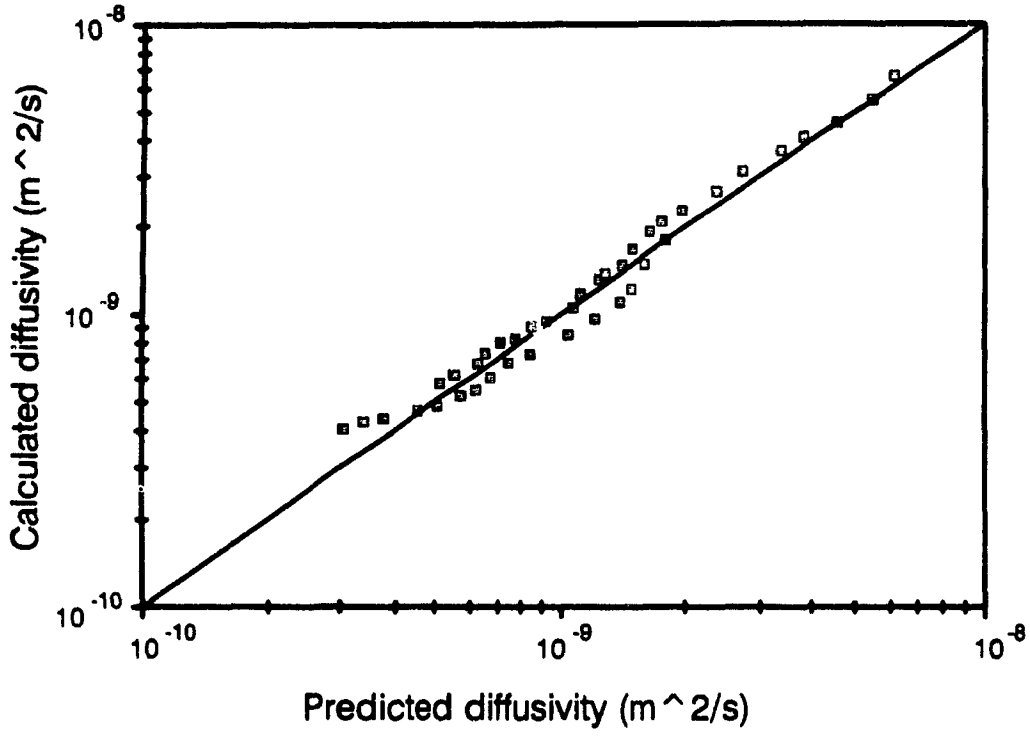

Fig. A-3.3 : Measured versus predicted mass diffusivities.

APPENDIX IV

This appendix contains the listing of the program used in the numerical simulations.

```
$DEBUG
C
C!!!!!!!!!!!!!!!!!!!!!!!!!!!!!!!!!!!!!!!!!!!!!!!!!!!!!!!!!!!!!!!!!!!!!!!!!!!
C
C       THE PROBLEM CONSIDERS A FILM OF SLURRY LIKE MATERIAL
C       WHICH HAS TO BE DRIED.  THE MATERIAL IS ASSUMED TO ENTER
C       THE DRYER AT BELOW THE BOILING POINT AND IS DRIED USING
C       SUPERHEATED STEAM AS THE ENVIRONMENT
C
C       THERE OCCURS AN INITIAL CONDENSATION TILL THE SURFACE
C       REACHES THE REQUIRED TEMPERATURE (CONDENSATION TEMP)
C       FOLLOWED BY THE CONVENTIONAL DRYING PERIOD.
C
C!!!!!!!!!!!!!!!!!!!!!!!!!!!!!!!!!!!!!!!!!!!!!!!!!!!!!!!!!!!!!!!!!!!!!!!!!!!
C
C
C       DEFINING THE VARIABLES AND ARRAYS
C
        IMPLICIT REAL *8 (A-H,O-Z)
        IMPLICIT INTEGER (I-N)
        REAL *8 CT(42),CTO(42),CTOO(42),CTP(42),RLOCAX(42),DELTAX(42)
        REAL *8 SF(42),SJ(42,42),SJINV(42,42),SC(42),CATP(42),CX(42)
        REAL *8 GP(3),WG(3),DI(42),PHI(2),PHIZ(2),RTIM(10000),
     &    RNTI(10000),REX(42),CATY(42),CATX(42),CATZ(42),CATPZ(42),
     &    CATTY(42),CATTZ(42),CATTPY(42),CATTPZ(42)
        REAL RWKSP(10938)
        COMMON /WORKSP/ RWKSP
        CALL IWKIN(10938)
C
C       GAUSS POINTS AND WEIGHTS
C
        GP(1)=0 11270166540
        GP(2)=0.5D+00
        GP(3)=0 88729833460
        WG(1)=0.27777777778
        WG(2)=0.44444444444
        WG(3)=0 27777777778
C
C
C       FLUID PROPERTIES
C
C
C       DEFEC : EFFECTIVE DIFFUSIVITY (D*RHO -- KG/M-SEC)
C       RHO   : DENSITY (KG/M^3)
C       RHOW  : DENSITY OF WATER (KG/M^3)
C       SPHT  : SPECIFIC HEAT (KCAL/KG-C)
C       AKAY  : THERMAL CONDUCTIVITY (KCAL/M-SEC-C)
```

```
C       HTRCOEFF : HEAT TRANSFER COEFFICIENT (KCAL/M^2-SEC-C)
C       AMBDA : LATENT HEAT OF CONDENSATION/EVAPORATION (KCAL/KG)
C       TINF  : INFINITE TEMPERATURE
C
C
        HTRCOEF=0.07D+00
        AMBDA=540D+00
        TINF = 433.00
        RHOW = 1000.0D+00
C
C       DEFINING AND INITIALIZING VARIABLES
C
        IC=0
        ICHEK = 1
        I9=10
        CRIT = 0.0005
C
C       NRC   · NEWTON RAPHSON COUNTER
C       DT,DTO: INITIAL TIME STEP
C       NE    : NUMBER OF ELEMETS
C       NEQ   : NUMBER OF EQUATIONS
C       NODES . NUMBER OF NODES
C       NNE   : EFFECTIVE NUMBER OF ELEMENTS
C       NNODES. EFFECTIVE NUMBER OF NODES
C       ESP   : EPSILON
C       EN    : THICKNESS OF THE FILM TO BE STUDIED.
C       IPRN  . PRINTER COUNTER = PRINT EVERY "X" TIMES
C       ITER  · TO CHANGE THE BOUNDARY CONDITION FOR THE FIRST
C               ITERATION.
C
        NRC=0
        DTO=0 05D+00
        DT=0.05D+00
        NE=20
        NEQ=2
        NODES=NE+1
        NNE=NE*NEQ
        NNODES=NODES*NEQ
        ANEW=0 001
        AOLD=0.001
        ANNEW=0 001
        TIME = 0 5D+00
        ESP=0.005
        IPRN=0
        ITER=1
        OWATFLUX=0.0D+00
        OPEN (7,FILE='LPT1')
        WRITE (7,*) 'THIS IS AN ATTEMPT TO SOLVE THE SHS'
C
C       INITIALIZING THE CT (SOLUTION)VECTOR
C
        DO 23 J = 1,NNODES,2
           J1=J+1
           CT(J)=0.429D+00
           CTO(J)=0.429D+00
```

```
            CTOO(J)=0.429D+00
            CTP(J)=0.429D+00
            CT(J1)=303.0D+00
            CTO(J1)=303.0D+00
            CTOO(J1)=303.0D+00
            CTP(J1)=303.0D+00
23        CONTINUE
            TMAX = CT(2)
C
C         WRITING OPERATION PARAMETERS.
C
          WRITE (7,*)
          WRITE (7,*) 'THE HEAT TRANSFER COEFFICENT IS  ',HTRCOEF
          WRITE (7,*) 'THE INITIAL SOLIDS LEVEL IS      ',CT(1)
          WRITE (7,*) 'THE INITIAL TEMPERATURE IS       ',CT(2)
          WRITE (7,*) 'THE JET TEMPERATURE IS           ',TINF
C
C
C         MESHING UP THE DOMAIN
C
C
C         RLOCAX    : LOCATION OF THE NODES
C         DELTAX    : ELEMENT DIMENSION
C
          CALL MESHUP(NNODES,NE,RLOCAX,DELTAX)
C
C
          GOTO 8004
C
C
C         CHECKING TO SEE WHETHER THE FILM THICKNESS PREDICTED IS THE
C         SAME AS THAT DONE BEFORE
C
C
8001      ANNEW=AOLD+DT*(OWATFLUX+WATFLUX)/2.0D+00/RHOW
C
C         ESTIMATING THE CHANGE IN THE THICKNESS
C
          CHA = (ANNEW-ANEW)/ANEW
C
C         INCREASING THE ITERATION TO "2" SO THAT THE SECOND BOUNDARY
C         CONDITION IS NOW INTRODUCED.
C
          IF(ITER.EQ.1) THEN
            ITER = 2
          ENDIF
C
C
C         CHECKING IF ONE IS IN THE CONSTANT RATE PERIOD OR IS IN THE
C         FALLING RATE PERIOD
C
C
          IF (ITER.NE.3.AND.CT(1).LT.CT(3)) THEN
            ITER = 3
          ENDIF
```

```
C
C       CHECKING THE PREDICTED AND CALCULATED FILM THICKNESS
C
        IF (ABS(CHA).GT.0.01) THEN
         ANEW=ANNEW
         GOTO 8112
        ELSE
         COLD = AOLD
         AOLD=ANEW
        END IF
C
C
C       CALCULATING THE NORMS FOR PREDICTING A NEW TIME STEP
C
C
        DNORM1=0.0D+00
        DNORM2=0.0D+00
        IF (ITER.EQ.3) THEN
          CT(1) = 54.67*DEXP(-0.064*(CT(2)-373))/100.0D+00
        ENDIF
        DO 2509 I = 3,NNODES-3,2
            IF(CT(I).LT.CT(I+2).AND.CT(I).LT.CT(I-2)) THEN
               CT(I) = (CT(I+2)+CT(I-2))/2.0D+00
            ENDIF
2509    CONTINUE
        DO 2508 I = 4,NNODES-2,2
            IF(CT(I).GT.CT(I+2).AND.CT(I).GT.CT(I-2)) THEN
               CT(I) = (CT(I+2)+CT(I-2))/2.0D+00
            ENDIF
2508    CONTINUE
        DO 2501 K=1,NNODES
          DI(K)=(CT(K)-CTP(K))/2.0D+00
2501    CONTINUE
        DO 2502 L=1,NNODES,2
          DNORM1=DNORM1+DI(L)**2
          DNORM2=DNORM2+DI(L+1)**2
2502    CONTINUE
C
C       CALCULATE CMAX AND TMAX
C
        CMAX=0 0D+00
        TMAX=0.0D+00
        DO 2503 I = 1,NNODES,2
         I1=I+1
         IF(CT(I).GE.CMAX) THEN
           CMAX=CT(I)
         ENDIF
         IF(CT(I1).GE.TMAX) THEN
           TMAX=CT(I1)
         ENDIF
2503    CONTINUE
C
C       CALCULATING THE NORM
C
        DNORM=DSQRT(DNORM1/(21.0D+00*CMAX**2)+DNORM2/(21.0D+00*
```

```
     &                                                TMAX**2))
C
C       CALCULATING THE NEW TIME STEP
C
        DTN=DT*DSQRT(ESP/DNORM)
C
C       UPDATE OLD TIME AND CURRENT TIME
C
        DTO=DT
        DT=DTN
C
C       WHAT TIME IS IT NOW ?
C
        TIME=TIME+DTO
        IC=IC+1
        RNTI(IC)=DTO
        RTIM(IC)=TIME
C
C       PRINT THE RESULTS FOR THE PREVIOUSLY CONVERGED SOLUTION
C
        IF (TIME.GT.90) THEN
          CRIT = 0.001
        ENDIF
C
C       PRINTING THE RESULTS FOR EVERY I9 ITERATIONS
C
        IPRN=IPRN+1
        IF(TIME.GT.10.0) THEN
          I9=5
        ENDIF
        IPN=I9*INT(IPRN/I9)
        IF (IPRN.EQ.IPN) THEN
          WRITE (7,*)
          WRITE (7,*) 'THE TIME IS    ',TIME
          WRITE (7,*)
          WRITE (7,*) 'THE MASS FLUX IS  ',WATFLUX
          WRITE (7,*)
         DO 2550 I = 1,NNODES,2
          WRITE(7,2602) RLOCAX(I),CT(I),CT(I+1)
2602      FORMAT(2X,F10.6,3X,F10.5,3X,F10.5)
2550     CONTINUE
        ENDIF
C
C       THIS STEP HAS ALSO GOT TO BE MODIFIED
C
        IF(TIME.GT.2100) THEN
          GOTO 11101
        ENDIF
C
C       CALCULATING THE PREDICTED VALUES USING FE METHOD
C
        DO 3501 I = 1,NNODES
          CTP(I)=CT(I)+DT*(CT(I)-CTO(I))/DTO
3501    CONTINUE
C
```

```
C       STORING THE CURRENT SOLUTION AND PREVIOUS SOLUTION IF
C       WE HAVE TO GIVE A NEW PREDICTION
C
        DO 3502 J = 1,NNODES
          CTOO(J)=CTO(J)
          CTO(J)=CT(J)
          CT(J)=CTP(J)
3502    CONTINUE
C
C       CALCULATING THE GRADIENT OF TEMPERATURE AND MASS
C
        FIRC = (2.0*RLOCAX(1)-RLOCAX(3)-RLOCAX(5))/
     &            ((RLOCAX(1)-RLOCAX(3))*(RLOCAX(1)-RLOCAX(5)))
        SECC = (RLOCAX(1)-RLOCAX(5))/((RLOCAX(3)-RLOCAX(1))*
     &            (RLOCAX(3)-RLOCAX(5)))
        THIC = (RLOCAX(1)-RLOCAX(3))/((RLOCAX(5)-RLOCAX(1))*
     &            (RLOCAX(5)-RLOCAX(3)))
        FIRCM= (2.0*RLOCAX(3)-RLOCAX(5)-RLOCAX(7))/
     &            ((RLOCAX(3)-RLOCAX(5))*(RLOCAX(3)-RLOCAX(7)))
        SECCM= (RLOCAX(3)-RLOCAX(7))/((RLOCAX(5)-RLOCAX(3))*
     &            (RLOCAX(5)-RLOCAX(7)))
        THICM= (RLOCAX(3)-RLOCAX(5))/((RLOCAX(7)-RLOCAX(3))*
     &            (RLOCAX(7)-RLOCAX(5)))
C
C       k * dT/dz
C
        AKA = (1.06-0 65*(1.0/(1.0+CT(1)))+0.003*(CT(2)-273 0))*0.01
        SURDOTE = -AKA*(CT(2)*FIRC+CT(4)*SECC+CT(6)*THIC)
        WRITE (6,*) SURDOTE
C
C       dX/dz
C
        IF (ITER.EQ.3.AND.CT(3).LT.CT(5)) THEN
          SURDOME = (CT(3)*FIRCM+CT(5)*SECCM+CT(7)*THICM)
          IF (SURDOME.LT.0.0D+00) THEN
            SURDOME = (CT(3)-CT(1))/(RLOCAX(3)-RLOCAX(1))
          ENDIF
        ENDIF
C
C
C       PREDICTING THE NEW FILM THICKNESS BY THE METHOD OF
C       BONNEROT AND JAMET
C
        ANEW=COLD+DTO*WATFLUX/RHOW
        OWATFLUX=WATFLUX
C
C       REMESHING THE FILM TO CORRESPOND TO THE NEW THICKNESS BY
C       FIRST CHANGING THE DELTAX'S PROPORTIONATELY.
C
8112    WRITE (6,*) 'ANEW IS  ',ANEW,'  AND AOLD IS ',AOLD
        WRITE (6,*)
        WRITE (6,*) 'THE TIME IS  ',TIME,'  AND FLUX IS  ',WATFLUX
        DO 5454 II = 3,NNODES,2
           DELTAX(II)=DELTAX(II)*ANEW/AOLD
           REX(II)=RLOCAX(II)
```

```
            RLOCAX(II)=RLOCAX(II-2)+DELTAX(II)
5454      CONTINUE
          REX(1)=RLOCAX(1)
          REX(NNODES-1)=RLOCAX(NNODES-1)
C
C         REMESH THE DOMAIN SO THAT THE NODES ARE NOW DISTRIBUTED
C         ACCORDING TO THE CONCENTRATION
C
           CALL REMESH (NNODES,RLOCAX,DELTAX,CT)
           DO 7824 I = 1,NNODES
              CTP(I) = CT(I)
7824       CONTINUE
C
C         CORRECTING OF THE CTO AT THE NEW LOCATIONS
C
          KP = NNODES/2
          DO 7285 K = 1,KP
             CATX(K) = REX(2*K-1)
             CATY(K) = CTO(2*K-1)
             CATZ(K) = CTOO(2*K-1)
            CATTY(K) = CTO(2*K)
            CATTZ(K) = CTOO(2*K)
7285      CONTINUE
          DO 7288 I = 2,KP-1
            CX(I) = RLOCAX(2*I-1)
7288      CONTINUE
           CALL IPOL (KP,CATX,CATY,CX,CATP)
           CALL IPOL (KP,CATX,CATZ,CX,CATPZ)
           CALL IPOL (KP,CATX,CATTY,CX,CATTPY)
           CALL IPOL (KP,CATX,CATTZ,CX,CATTPZ)
           DO 7286 K = 2,KP-1
              CTO(2*K-1) = CATP(K)
              CTOO(2*K-1)= CATPZ(K)
              CTO(2*K) = CATTPY(K)
              CTOO(2*K)= CATTPZ(K)
7286      CONTINUE
C
C
C         SETTING THE NEWTON RAPHSON COUNTERS TO ZERO
C
          NRC=0
C
C         UPDATING NEWTON RAPHSON COUNTER
C
8004      NRC=NRC+1
C
C         ASSEMBLING THE F VECTOR AND THE  JACOBIAN MATRIX
C
C         EMPTYING THE VECTOR AND MATRIX FOR EACH SOLUTION
C
          DO 211 J = 1,NNODES
            SF(J)=0.0D+00
            SC(J)=0.0D+00
            DO 211 K = 1,NNODES
              SJ(J,K)=0 0D+00
```

```
                SJ(L3,M3)=SJ(L3,M3)+WG(J)*DX*SQJ11
              SQJ12=0.00
                SJ(L3,M4)=SJ(L3,M4)+0.0
              SQJ21=0.00
                SJ(L4,M3)=SJ(L4,M3)+0.0
              SQJ22=RHO*SPHT*PHI(L)*PHI(M)/DT+AKAY*PHIZ(L)*PHIZ(M)
                SJ(L4,M4)=SJ(L4,M4)+WG(J)*DX*SQJ22
100         CONTINUE
C
C         BOUNDARY CONDITIONS
C
C         IF THE ITERATION NUMBER IS ONE THEN WE CALCULATE THE HEAT FLUX
C         ASSUMINC THAT THE TEMPERATURE OF THE FILM SURFACE REACHES HUNDRED
C         IMMEDIATELY.  THE HEAT FLUX AND HENCE THE MASS FLUX INTO THE
C         SURFACE IS CALCULATED BY USING THE FORMULA GIVEN IN BSL FOR
C         STEP CHANGE IN INLET TEMPERATURE
C
          IF (ITER.EQ.1) THEN
            SF(2)=0.0D+00
            DO 3832 K = 1,NODES
              SJ(2,K) = 0.0D+00
3832        CONTINUE
            SJ(2,2) = 1.0D+00
            PI = 3.14D+00
C           TSURF = 373.0D+00 - DLOG(CT(1)*100.0D+00)/0.046
            TSURF = 373.0D+00
            WATFLUX = AKAY*(TSURF-CT(4))/(AMBDA*DSQRT(0.5*RHO*SPHT/
     &                                          AKAY*PI))
            SF(1) = SF(1) + WATFLUX
            CT(2) = TSURF
          ENDIF
C
C         FROM THE SECOND STEP ON THE TEMPERATURE AT THE SURFACE IS
C         ASSUMED TO BE AT EQUILIBRIUM CORRESPONDING TO THE SURFACE SOLIDS
C         CONCENTRATION.
C
C
C       TEMPERATURE GRADIENT AT THE SURFACE :
C
          IF(SURDOTE.LT.0.0D+00) THEN
            SURDOTE = 0.0D+00
          ENDIF
C
C       HEAT COMING IN IS  :     H (TINF - TSURF)
C
          TSURF = 373.00D+00+7.0D+00/CT(3)
          HEATIN = HTRCOEF*(TINF-CTO(2))
C
C         THIS IS THE BOUNDARY CONDITION FOR THE PERIOD WHERE HEAT
C         TRANSFER (EXTERNAL) IS THE LIMITING FACTOR
C
          IF (CT(3).GT.CT(5).OR.ITER.EQ.2) THEN
            SF(2)=0.0D+00
            DO 3833 K = 1,NNODES
              SJ(2,K) = 0.0D+00
```

```
            DO 3833 K = 1,NNODES
               SJ(2,K) = 0.0D+00
3833        CONTINUE
            SJ(2,2) = 1.0D+00
            WATFLUX = (SURDOTE-HEATIN)/AMBDA
            IF(WATFLUX.GT.0.8D+00) THEN
               WATFLUX = 0.8D+00
            ENDIF
            SF(1) = SF(1) + WATFLUX
            CT(2) = 373.0D+00 + 7.0D+00/CT(1)
         ENDIF
C
C        THIS IS THE BOUNDARY CONDITION FOR THE FALLING RATE
C        PERIOD.
C
         IF (CT(3).LT.CT(5).AND.ITER.EQ.3) THEN
            SF(1) = 0.0D+00
            DO 3834 K = 1,NNODES
              SJ(1,K) = 0.0D+00
3834        CONTINUE
            SJ(1,1) = 1.0D+00
            ANUM = 13.3776D+00*(CT(1)+CT(3))/2.0D+00-24.6299
            IF (ANUM.GT.-6.0) THEN
              ANUM = -6.0
            ENDIF
            ADEFEC = 1400.0D+00*DEXP(ANUM)
            DIFC = ADEFEC*SURDOME
            WATFLUX = DIFC
            IF (DIFC.GT.0.0D+00) THEN
               DIFC = 0.0D+00
            ENDIF
            HEATFLUX = HEATIN + DIFC*AMBDA
            HEATC = HEATIN/AMBDA
            IF (HEATC.LT.DIFC) THEN
             HEATFLUX = 0.0D+00
            ENDIF
            SF(2) = SF(2) + HEATFLUX
            HEATLOSS = 0.005D+00*(CT(NNODES)-303)
            SF(NNODES) = SF(NNODES)-HEATLOSS
             IF (CT(2).GT.TINF) THEN
                CT(2) = TINF
             ENDIF
            CT(1) = 54.67*DEXP(-0.064*(CT(2)-373))/100.0D+00
         ENDIF
C
C        THE JACOBIAN MATRIX IS INVERTED AND THEN MULTIPLIED WITH THE
C        F-VECTOR TO FIND THE INCREMENTS.
C
         CALL DLSGRR(NNODES,NNODES,SJ,NNODES,TOL,IRANK,SJINV,NNODES)
         CALL DMURRV(NNODES,NNODES,SJINV,NNODES,NNODES,SF,1,NNODES,SC)
C
C        CALCULATING THE ERROR FOR THE NEWTON RAPHSON
C
         ERR=0.0D+00
         DO 40 I =1,NNODES,2
```

```
      DO 41 I = 2,NNODES,2
       ERR = ERR +(SC(I)/TMAX)**2
41    CONTINUE
      ERRO=DSQRT(ERR)
C
C     ESTIMATING THE NEW VALUE OF CT VECTOR
C
      DO 30 I = 1,NNODES,2
         CT(I)=CT(I)+SC(I)
         CT(I+1) = CT(I+1)+SC(I+1)
       IF (CT(I+1).LT.303) THEN
          CT(I+1) = 303.0D+00
      ENDIF
30    CONTINUE
C
C     LIMITING THE NUMBER OF NEWTON RAPHSON ITERATIONS
C
      IF(ERRO.LT.CRIT) THEN
       GOTO 8001
      ELSEIF(NRC.GT.50) THEN
       GOTO 8002
      ELSEIF(NRC.GT.5) THEN
       GOTO 8003
      ELSE
       GOTO 8004
      ENDIF
C
C     UPDATING THE INITIAL GUESS IF THE TIME TAKEN IS VERY HIGH
C
8003  DT=DT/2.0
      DO 8100 I = 1,NNODES
       CTP(I)=CTO(I)+DT*(CTO(I)-CTOO(I))/DTO
       CT(I)=CTP(I)
8100  CONTINUE
      NRC = 1
      GOTO 8004
8002  WRITE(6,8601) NRC
8601  FORMAT(2X,'THE NUMBER OF NEWTON RAPHSON ITERATION IS ',I3)
      GOTO 11111
C
C     WRITING THE FINAL RESULTS WHEN THE SURFACES REACHES
C     AT THE END OF THE COMPLETION
C
11101 DO 1102 I = 1,NNODES,2
      WRITE (7,11502) TIME,RLOCAX(I),CT(I),CT(I+1)
11502 FORMAT (2X,F10.5,3X,F10.5,3X,F10.5,3X,F10.5)
1102  CONTINUE
11111 STOP
      END
C
C
C     SUBROUTINE TO CALL THE BASIS FUNCTIONS
C
C
      SUBROUTINE TFUNCT(GP1,DX,W,PHI,PHIZ)
```

```
      REAL *8 GP1,DX,APHI(2),APHIZ(2),PHI(2),PHIZ(2),W
      REAL *8 WPP,DWPP
C
C     WEIGHT FOR THE UPWINDING EFFECT
C
        APHI(1)=1-GP1
        APHI(2)=GP1
        APHIZ(1)=-1.0/DX
        APHIZ(2)=1.0/DX
C
C     BASIS FUNCTIONS AND DERIVATIVES DUE TO UPWINDING.
C
       WPP = W*APHI(1)*APHI(2)
       PHI(1)=APHI(1)-WPP
       PHI(2)=APHI(2)+WPP
       DWPP=W*(APHI(2)*APHIZ(1)+APHI(1)*APHIZ(2))
       PHIZ(1)=APHIZ(1)-DWPP
       PHIZ(2)=APHIZ(2)+DWPP
      RETURN
      END
C
C
C     SUBROUTINE MESHUP (START WITH A NON-UNIFORM MESH)
C
C
      SUBROUTINE MESHUP(NNODES,NE,RLOCAX,DELTAX)
      REAL *8 RLOCAX(42),BETA,RLOCALX,DELTAX(42)
      INTEGER NE,NNODES
      ALPHA = 1.0D+00
      BETA=0.0D+00
      DO 10050 M = 1,NNODES,2
        RLOCALX=BETA**3
        RLOCAX(M)=(RLOCALX/FLOAT(NE)**3)*0.001
        BETA=BETA+1.0
10050 CONTINUE
      DO 10051 N = 3,NNODES,2
       DELTAX(N) = RLOCAX(N)-RLOCAX(N-2)
10051 CONTINUE
      RETURN
      END
C
C
C     REMESHING WITH THE BENNER'S ALGORITHM AS DESCRIBED IN
C     APPENDIX A-1.1.
C
C
      SUBROUTINE REMESH (NNODES,RLOCAX,DELTAX,CT)
C
      IMPLICIT REAL *8 (A-H,O-Z)
      REAL *8 RLOCAX(42),DELTAX(42),CT(42),X(21),Y(21),DLX(21),
     &        PYI(21),PXI(21),Z(21),EM(21),E(21),YY(21),
     &        PXXI(21),PYYI(21),PZZI(21)
C
      NP= NNODES/2
      DO 6241 I = 1,NP
```

```
            X(I) = RLOCAX(2*I-1)
            Y(I) = CT (2*I-1)
            Z(I) = CT (2*I)
6241      CONTINUE
          DO 6242 I = 1,NP-1
            DLX(I) = DELTAX(2*I+1)
6242      CONTINUE
          DO 6243 I = 1,NP-1
            EM(I)=(Y(I+1)-Y(I))/DLX(I)
6243      CONTINUE
          DO 6244 I = 2,NP-2
            E(I)=DLX(I)*(DABS(EM(I+1)-EM(I))+DABS(EM(I)-EM(I-1)))
6244      CONTINUE
          E(1)=2*DLX(1)*DABS(EM(2)-EM(1))
          E(NP-1)=2*DLX(NP-1)*DABS(EM(NP-1)-EM(NP-2))
          SUM=0.0D+00
          DO 6245 I = 1,NP-1
            SUM=SUM+E(I)
6245      CONTINUE
          AVG = SUM/FLOAT(NP-1)
          ELAVG = AVG/1.05D+00
          EUAVG = AVG*1.05D+00
          SUM = 0.0D+00
          DO 6246 I = 1,NP-1
            IF (E(I).LT.ELAVG) THEN
              E(I)=ELAVG
            ELSEIF (E(I).GT.EUAVG) THEN
              E(I)=EUAVG
            ENDIF
            SUM = SUM+E(I)
6246      CONTINUE
          ANAVG=SUM/FLOAT(NP-1)
          YY(1)=0.0D+00
          DO 1650 I = 2,NP
           YY(I) = YY(I-1)+E(I-1)
1650      CONTINUE
          DO 1651 J = 2,NP-1
            PXI(J) = (J-1)*ANAVG
1651      CONTINUE
          CALL IPOL (NP,YY,X,PXI,PYI)
          PXXI(1) = 0.0D+00
          DO 1652 I = 2,NP-1
            DEXA = PYI(I) - PXXI(I-1)
              IF (DEXA.LT.0.000001) THEN
                 DEXA = 0.000001
              ENDIF
              PXXI(I) = PXXI(I-1)+DEXA
1652      CONTINUE
          CALL IPOL (NP,X,Y,PXXI,PYYI)
          CALL IPOL (NP,X,Z,PXXI,PZZI)
          DO 1653 I = 2,NP-1
            RLOCAX(2*I-1) = PXXI(I)
            CT(2*I-1) = PYYI(I)
            CT(2*I) = PZZI(I)
1653      CONTINUE
```

```
      DO 1654 I = 3,NNODES-1
        DELTAX(I) = RLOCAX(I)-RLOCAX(I-2)
1654  CONTINUE
      RETURN
      END
C
C
C     SUBROUTINE WHICH DETERMINES THE LOCATION FOR EACH ITERATION
C     USING A CUBIC SPLINE METHOD TO INTERPOLATE THE ERRORS AND
C     TO OBTAIN THE NEW NODES.
C
C
      SUBROUTINE IPOL (N,AX,AY,APX,APY)
      IMPLICIT REAL*8 (A-H,O-Z)
      REAL *8 AX(42),AY(42),APX(42),APY(42),BREAK(42),CSCOEF(4,42)
      EXTERNAL DCSVAL,DCSAKM
      CALL DCSAKM(N,AX,AY,BREAK,CSCOEF)
      NINTV = N-1
      DO 8991 J = 2,N-1
         APY(J) = DCSVAL(APX(J),NINTV,BREAK,CSCOEF)
8991  CONTINUE
      RETURN
      END
```

APPENDIX V

Hygroscopic nature of black liquor

It has long been recognized that dry black liquor is very hygroscopic. However, no quantitative data is available on the rate of moisture uptake if exposed to humid air.

The hygroscopic nature of black liquor was characterized by exposing (about 7mg) dry black liquor (oven dried) to 20°C air with a relative humidity of 65 % and measuring the weight gain as a function of time. The weight gain data was then transformed into solids level and the result is plotted in Fig. A-5 Black Spruce wood was used as a reference material since moisture absorption by wood has been investigated in great detail

It can be seen that black liquor is indeed very hygroscopic and under present conditions no equilibrium has been established when solids level of 70% is reached after about 1 5 hours The results in Fig A-5 also show that oxidized black liquor is less hygroscopic than unoxidized black liquor. This is attributed to the fact that the sodium sulfide is more hygroscopic than sodium sulfate in black liquor It is also seen clearly that black liquor is much more hygroscopic than wood

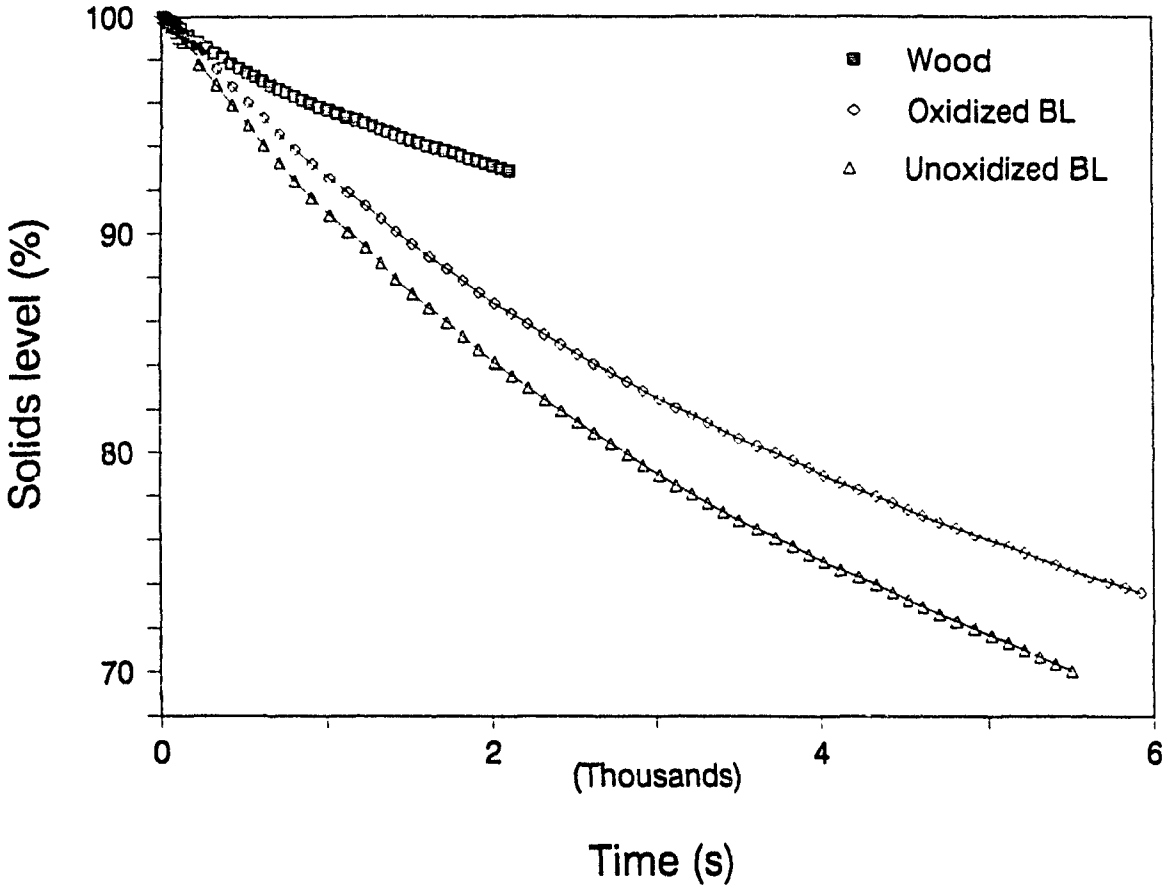

Fig. A-5.1 : Hygroscopic nature of black liquor.

APPENDIX VI

Typical heat and mass balance for drying black liquor.

Let "f" be the fraction of the surface area where boiling occurs and hence complete mixing.

Mass balance :

$$\dot{m} = \frac{h\,(T_\infty - T_s)}{\lambda}\, f + \mathbb{D}\left.\frac{\partial\, \rho X}{\partial z}\right|_0 (1-f) \qquad (A\text{-}6\ 1)$$

where

$\dot{m}$: overall evaporation rate ($\simeq$ 10 kg/hr m^2)

h : heat transfer coefficient ($\simeq$ 300 W/m^2K)

T_∞ : Jet temperature (225°C)

T_s : Surface temperature (150°C)

λ : Latent heat of vaporisation (2250 kJ/kg)

$\mathbb{D}\left.\frac{\partial\, \rho X}{\partial z}\right|_0$: Diffusion limited drying rate from numerical calcuation ($\simeq$ 3 kg/hr m^2)

Substituting the above values in (A-6.1) **f = 0.2121.**

Heat balance :

$$h\,(T_\infty - T_s) = \dot{m}\,\lambda + m\,c_p\,\frac{\partial T}{\partial t} \qquad (A\text{-}6\ 2)$$

where

m : Mass of sample and sample holder offering thermal interia which has to be overcome to raise the surface temperature of the black liquor film.

c_p : approx. specific heat of the above $\simeq$ 2250 J/kg

$\frac{\partial T}{\partial t}$: rate of temperature rise of film ($\simeq$ 0 5 °C/s)

Substituting the values in (A-6.2) **m = 40.82 g/pan area.**

In experiments the sample was $\simeq$ 4 g and sample holder was $\simeq$ 30 g Thus the theoretical mass to be raised to the desired temperature compares well with the actual mass of the sample and sample holder

APPENDIX VII

The typical composition of kraft black liquor is given in Table A.7 (Hough, 1985) :

Table A.7 : Composition of black liquor.

Component	% of dry solids.
Lignin	30
Hemicellulose & sugars	0 5
Extractives	2
Acetic acid	2
Formic acid	3
Other organic acids	2
Unknown organics	30
Inorganic salts	20
Organically combined Na	10
Unknown inorganics	0.5

Reference :

Hough, G. : "Chemical Recovery in the Alkaline Pulping Processes". TAPPI Press. pp 25, 1985.